Mobilization of Komatiite-Associated Ni-Cu-(PGE) Mineralization in the Southern Manneville Fault Zone, Southern Abitibi Subprovince, Quebec

by

Danielle Shirriff

A thesis submitted in partial fulfillment
of the requirements for the degree of
Master of Science (MSc) in Geology

The Faculty of Graduate Studies
Laurentian University
Sudbury, Ontario, Canada

THESIS DEFENCE COMMITTEE/COMITÉ DE SOUTENANCE DE THÈSE
Laurentian Université/Université Laurentienne
Faculty of Graduate Studies/Faculté des études supérieures

Title of Thesis Titre de la thèse	Mobilization of Komatiite-Associated Ni-Cu-(PGE) Mineralization in the Southern Manneville Fault Zone, Southern Abitibi Subprovince, Quebec
Name of Candidate Nom du candidat	Shiriff, Danielle
Degree Diplôme	Master of Science
Department/Program Département/Programme	Geology
Date of Defence Date de la soutenance	March 25, 2020

APPROVED/APPROUVÉ

Thesis Examiners/Examinateurs de thèse:

Dr. Michael Lesher
(Co-Supervisor/Co-directeur de thèse)

Dr. Bruno Lafrance
(Co-Supervisor/Co-directeur de thèse)

Dr. Xiaohui Zhou
(Committee member/Membre du comité)

Dr. Benoit-Michel Saumur
(External Examiner/Examinateur externe)

Approved for the Faculty of Graduate Studies
Approuvé pour la Faculté des études supérieures
Dr. David Lesbarrères
Monsieur David Lesbarrères
Dean, Faculty of Graduate Studies
Doyen, Faculté des études supérieures

ACCESSIBILITY CLAUSE AND PERMISSION TO USE

1 Abstract

The Cubric showing and Marbridge deposit occur in the 2714 ± 2 Ma La Motte-Vassan Formation, 20-25 km north of Malartic, Québec. Mineralization at the Cubric showing is hosted by a silicate-magnetite facies iron formation as well as gabbro, but the high Ni/Cu and Ir/Pd ratios of the mineralization suggest that it formed from a komatiitic magma, similar to the mineralization at the historic Marbridge deposit. Normal abundances of most metals in the mineralization in the gabbro suggest that it was mechanically mobilized into the gabbro as a high-temperature monosulfide solid solution, whereas low abundances of Cr and Ir-Ru-Rh in the mineralization in the iron formation suggest that Ni-Cu-Pt-Pd-Au and other metals were mobilized into the iron formation by metamorphic-hydrothermal fluids. The host rocks and country rocks have experienced two phases of deformation during regional metamorphism, and it is likely that the mineralization was mobilized from unexposed/eroded mineralized cumulate komatiites during this deformation and metamorphism, which occurred after emplacement of the younger 2680 ± 1.5 Ma gabbro.

2 Keywords

Komatiite, Ni-Cu-(PGE), magmatic ore deposits, Archean, Abitibi greenstone belt, sulfide mobilization, Destor-Porcupine-Manneville fault

3 Co-Authorship Statement

This manuscript has multiple authors. Below are the specific contributions made by each author:

1) The candidate performed all of the fieldwork, sample collection, sample preparation, petrographic work, and SEM analyses, and wrote the first draft of the manuscript.
2) Prof. Michael Lesher and Prof. Bruno Lafrance helped focus the research problem; visited the field site with the candidate and reviewed the mapping; guided the core logging, sampling, sample preparation, petrographic work, and geochemical interpretations; and reviewed several drafts of the manuscript.
3) Dr. Xiaohui Zhou provided numerous discussions and support that helped put the project area into a regional context.
4) Dr. Michael Hamilton carried out the single-zircon U-Pb ID-TIMS analysis and provided the Concordia diagram used in the thesis.

4 Acknowledgments

I want to thank everyone who has supported me over the past two years while I completed my thesis. Michael Lesher, Bruno Lafrance, and Xiaohui Zhou provided invaluable guidance, wisdom, and patience. Mike Hamilton from the University of Toronto performed the geochronological analysis and interpretation. E.M. Ripley from Indiana University supervised the S isotope analyses. Pierre Pilote (Ministère de l'Énergie et des Ressources Naturelles du Québec) and Réal Daigneault (UQAC) provided information about the regional and local geology in the Val d'Or area and showed us key outcrops in the surrounding area. Michael Houlé (GSC) provided numerous discussions and two additional samples from the Cubric mineralized zone. Globex Mining Enterprises Inc., Quebec Precious Metals Corporation, and Sphinx Enterprises Ltd. provided access to the Cubric Ni showing and Marbridge deposit site, drill core, and company data. I am grateful for receiving funding from Metal Earth, the Mineral

Exploration Research Centre, and the Canada First Research Excellence Fund to carry out this research.

I would additionally like to thank Amos-Malartic transect undergraduate field assistants Luc Roy, Naomi Welt, Sam Battey, Kevin Kotylak, Mouche Jacques, and Jeremy Rivest for their positive attitudes and enthusiasm even on the rainiest of days; the Metal Earth and Harquail School of Earth Sciences staff, especially Courtney Folz, Kipp Grose, Natalie Lafleur-Roy, and Roxane Mehes for helping me with navigating all my administrative and technological blunders; Brendon Sampson for literally and figuratively pulling me out of the mud; my best friend Will McNeice for all his support over the past three years me and helping troubleshoot problems even when he felt out of his depth; my sister Katherine Shirriff for always pushing me out of my comfort zone; and finally my parents Doug and Karen Shirriff for all their love, support, and enthusiasm whenever I bring rocks home.

5 Table of Contents

6 List of Figures

Figure 5 Photographs of sulfide textures as the Cubric showing. A) and B) gabbro-hosted semi-massive Fe-Ni-(Cu) sulfide breccia zone in chlorite-altered gabbro. C) and D) banded Fe-(Cu)-(Ni) mineralization in silicate-magnetite facies iron formation.

Figure 6 Photographs and photomicrographs of gabbro host and country rocks at the Cubric showing. A) Gabbro containing a pegmatitic pod (center of the photo). B) Gabbro (sample ME-AM19-DES0279AG07B) in plane-polarized light. C) The same area in crossed polarized light. D) Talc-altered ultramafic rock. E) Talc-altered ultramafic rock (sample ME-AM18-DES0279BG01B) in crossed polarized light. F) The same area in reflected light.

Figure 7 Outcrop-scale map of Marbridge Zone 1 showing mafic sills running parallel to the mineralized zone. Modified from LaFrance (2015) to include the sills and update the lithologies based on new geochemical data.

Figure 8 Photo of Marbridge mineralized Zone 1 mineralized zone transgressed by a mafic sill with a thin chilled margin. The scale card is 8.5 cm.

Figure 9 A D_2-D_3 interference fold pattern in the La Motte - Vassan formation near the Cubric showing. The scale card is 15 cm long.

Figure 10 Lower hemisphere (Schmidt projection) stereonets are showing the distribution of strikes and dips in the Cubric area. A) Contoured distribution of poles to the S2 foliation; black is high density and white is low density. B) Poles to the S3 cleavage.

Figure 11 Photomicrographs of deformed iron formation (sample ME-AM-18DES279CG10) in A) plane-polarized transmitted light and B) plane-polarized reflected light, showing folded magnetite-silicate bands and sulfide-rich pyrite-magnetite-chalcopyrite bands. Millerite and pentlandite occur along the margins of pyrite grains. Violarite locally replaces pentlandite. Chalcopyrite occurs along the margins and in the cores of pyrite grains. There are minor chalcopyrite, pyrite, and pentlandite grains in the magnetite-silicate layers.

Figure 12 Photomicrographs of the gabbro-hosted semi-massive sulfide breccia zone. Sample ME-AM18-DES0279EG22 in A) reflected light and B) plane-polarized light showing chlorite

concentrated around sulfides. Sample ME-AM18-DESEG23. A gabbro in reflected light showing weathering of pentlandite to violarite and chalcopyrite within pyrite. D) gabbro-hosted semi-massive sulfide breccia zone sample ME-AM18-DES279EG04B in reflected light showing sharp boundaries, polygonal shapes, and 120º grain boundaries between chalcopyrite and pyrite.

Figure 13 MgO vs. major oxide/element (SiO_2, TiO_2, Al_2O_3, Fe_2O_3, CaO, Na_2O, Cr_2O_3, Ni) plots for all barren lithologies in the La Motte-Vassan formation. All data recalculated volatile free.

Figure 14 Primitive mantle-normalized (McDonough and Sun, 1995) extended trace element diagram for the unmineralized gabbro in the Cubric outcrop. LLD is outlined but applies only to samples collected for this study.

Figure 15 MgO vs. Al_2O_3/TiO_2 plot of komatiite rocks from the La Motte-Vassan formation. The komatiites are Al-undepleted. All data recalculated volatile free to 100%. Spinifex Ridge data from Champagne (2005); Marbridge data from Lafrance (2014); Cubric data from this study.

Figure 16 Primitive mantle-normalized (McDonough and Sun, 1995) extended trace element diagram for the komatiite rocks in the La Motte-Vassan formation. Cubric komatiites are talc-carbonate altered and contain trace-1% disseminated sulfide. Ranges for Spinifex Ridge and Marbridge komatiites are plotted for comparison. LLD is outlined but applies only to samples collected for this study.

Figure 17 Metals vs. S in the sulfide-bearing rocks (iron formation and brecciated gabbro) at the Cubric showing and Marbridge Zone 1.

Figure 18 S-Fe-Ni plot showing the compositions of Cubric sulfides and mineral assemblages at 100-135°C (from Naldrett, 2004). Data for Marbridge Zone 3 and 4 from Graterol and Naldrett (1971). Fe corrected for Fe in silicate and magnetite.

Figure 19 Base and precious metals in 100% sulfides vs. Cu in 100% sulfides in the sulfide-bearing rocks (iron formation and brecciated gabbro) at the Cubric showing and Marbridge Zone 1.

Figure 20 Metals in 100% sulfide normalized to the primitive mantle (McDonough and Sun, 1995) and plotted in increasing order of compatibility from left to right (modified from Lesher and Keays, 2002). Kambalda Type I mineralization and Kambalda, Langmuir, and Thompson Type IV mineralization are plotted for comparison. The sulfides in Cubric iron formation are depleted in Ir, similar to Type IV mineralization. Brecciated sulfides in Cubric gabbro are similar to Type I mineralization but are slightly enriched in IPGE. The average values for each lithology are plotted with the blue and red lines showing the ranges for each element.

Figure 21 $^{206}Pb/^{238}U$ vs. $^{207}Pb/^{235}U$ Concordia plot showing ID-TIMS analyses of single zircons extracted from gabbro (sample ME-AM17-DES0147AG08) at the Cubric showing. The 2680.1 ± 1.5 Ma age constrains the maximum timing of deformation and mobilization of sulfides.

Figure 22 $\delta^{34}S$ ‰ data for sulfide-bearing lithologies in the Marbridge and Cubric areas, including 1) isotopically lighter Cubric komatiite, mineralized Cubric facies iron formation, and barren pyrite-bearing argillite; 2) intermediate Cubric gabbro-hosted mineralization; and 3) isotopically heavier Marbridge Zone 1 net-textured mineralization.

Figure 23 Summary of how metal fractionation/mobilization processes may change sulfide metal proportions. A) Segregation of Cr-Ni-Cu-IPGE-Zn-Mo-Bi-Te-Sb-Co-Fe-As-Se-rich MSS and Ag-Pb-Zn-Au-PPGE-rich residual sulfide liquid. B) Hydrothermal mobilization, leaving a Cr-IPGE-rich residue and, depending on ligands and temperature gradient, producing a precipitate that may be zoned with respect to Fe-Au-Pd-Pt-Zn-Cu. C) Low-T (<500°C) tectonic mobilization resulting in the mechanical separation of more ductile Zn ± Pb-bearing Ccp from less ductile Po-Pn-PGMs. D) High-T (>500°C) tectonic mobilization where most elements are housed in MSS.

Figure 24 Schematic model for the formation and mobilization of the Ni-(Cu)-(PGE) mineralization at the Cubric showing.

7 List of Tables

Chapter 1: Thesis Introduction

1 Introduction

The ca. 2800-2600 Ma Abitibi greenstone belt hosts one large, low-grade komatiite associated Ni-Cu-platinum group element (PGE) deposit (Dumont), several small, high-grade deposits (e.g., Alexo-Dundonald, Langmuir-Redstone, Texmont, Alexo, Marbridge), and numerous showings (**Fig 1**) (Houlé and Lesher, 2011). Although several of the deposits on the Ontario side of the Abitibi greenstone belt have been studied in detail, others – particularly on the Quebec side – are less well understood. The Amos-Malartic area in Quebec hosts two major komatiite-associated deposits (Marbridge and Dumont) and several showings (Cubric, Quebec Moly, Caminco Nickel, Ataman, and La Motte La Blanc). The undeveloped Dumont deposit is located between Launay and Trécesson Townships 27 km east of Amos QC and contains 1665.6 Mt of ore grading 0.26% Ni (Staples et al., 2019). It has been studied by Eckstrand (1975), Duke (1986), Brügmann et al. (1990), and Sciortino et al. (2015). The Marbridge deposit is located in La Motte Township 24 km north of Malartic QC and was mined between 1962 and 1968, producing 774 227 tonnes of ore with an average grade of 2.28% Ni and 0.1% Cu (Giovenazzo, 2000; Sphinx Enterprises Ltd., 2015). It has been studied by Graterol and Naldrett (1971), Giovenazzo (2000), and Lafrance (2015). The Cubric showing is located in La Motte Township 3 km southeast of the Marbridge deposit and has an average grade of 2.5% Ni and 0.1% Cu (19 grab samples). Although its high Ni: Cu ratio is consistent with mineralization formed from an ultramafic magma, it is hosted by iron formation and gabbro and was likely mobilized from an ultramafic body.

The goal of this project is to determine the relative roles of tectonic mobilization and metamorphic-hydrothermal mobilization in the genesis of the mineralization at the Cubric Showing. Although many komatiite-associated Ni-Cu-PGE deposits have been modified to varying degrees by magmatic diffusion, deformation, metamorphism, and metamorphic-

hydrothermal processes (e.g., Green and Langmuir, 1981; Lesher and Keays, 1984; Paterson et al., 1984; During et al., 2007, 2010; Layton-Matthews et al., 2007, 2011; Houlé and Lesher, 2011; see reviews by Lesher, 1989; Lesher and Keays, 2002; Barnes, 2006; Lesher and Barnes, 2009), few of these deposits have complete geochemical datasets that can be used to differentiate between different mobilization processes, so the data collected for this study will help fill this knowledge gap.

Research methods included outcrop mapping, interpretation of a high resolution airborne magnetic survey, re-logging of available diamond drill cores, and petrographic examination of 81 samples (64 from outcrop, 17 from drill core). Of these, 64 were examined in polished thin section, 81 were analyzed for whole-rock geochemistry, 14 were analyzed for platinum-group elements and Au, and 15 were analyzed for mineral compositions. Four zircons from a gabbro sample were dated using U-Pb single-zircon ID-TIMS methods. Sample preparation and analytical details are described in Chapter 2.

2 Structure of the Thesis

This thesis comprises two chapters. Chapter 1 (this chapter) includes an introduction to the thesis and a description of the structure of the thesis. Chapter 2 is a scientific journal article with several co-authors to be submitted to *Mineralium Deposita*. The text, figures, and reference style comply with *Mineralium Deposita* guidelines.

There are three appendices attached to this manuscript. Appendix A is the supplementary data including the detailed method for acquiring the geochronological results, and the background lithology descriptions, Appendix B includes two Summary of Field Work and Other Activities papers published as open file reports by the Ontario Geological Survey. Appendix C includes the raw whole-rock data collected in this study.

Chapter 2: Mobilization of komatiite-associated Ni-Cu-(PGE) mineralization the Southern Manneville fault zone, southern Abitibi Subprovince, Québec

D. Shirriff[1], C.M. Lesher[1], B. Lafrance[1], X. Zhou[1], and M. Hamilton[2]

[1] Mineral Exploration Research Center and Harquail School of Earth Sciences, Laurentian University, 935 Ramsey Lake Road, Sudbury, ON P3E 2C6, Canada

[2] Department of Earth Sciences, University of Toronto, 22 Russell Street, Toronto, ON M5S 3B1, Canada

1 Abstract

The ca. 2800-2600 Ma Abitibi greenstone belt hosts eight small but significant komatiite associated Ni-Cu-PGE deposits, eleven undeveloped deposits, and numerous occurrences. Although several of the deposits in Ontario have been studied in detail, many others – particularly in Quebec – are less well studied. The Marbridge deposit and Cubric showing are located 20-25 km north of Malartic, Quebec. They occur in the 2714 ± 2 Ma La Motte-Vassan Formation, which includes komatiites, basalts, and minor felsic-intermediate volcanic rocks. Both have high Ni/Cu ratios (~10:1), low Pd/Ir ratios (~2:7), and other metal ratios consistent with having formed from a komatiitic magma. The mineralization at Marbridge is hosted by komatiites, but the mineralization at Cubric is hosted in a sheared 2680 ± 1.5 Ma gabbro and a sheared magnetite-facies iron formation. Marbridge Zone 1 contains typical pyrrhotite-pentlandite-chalcopyrite ± pyrite ± magnetite assemblages, whereas Marbridge Zones 2, 3, and 4, and Cubric contain pyrite-millerite-pentlandite-chalcopyrite assemblages. Marbridge Zones 2, 3, and 4 are poorly characterized, but Marbridge Zone 1 exhibits magmatic net- to semi-massive textures, and Cubric exhibits deformed semi-massive to massive textures. All exhibit broadly magmatic mantle-normalized chalcophile element patterns. Coherent base and precious metal

contents of the mineralization in the gabbro at Cubric is evidence for tectonic mobilization as a homogeneous monosulfide solid solution at temperatures over ~500ºC. Low Ir-Ru-Rh and Cr contents of the mineralization in the iron formation suggest that Ni-Cu-Pt-Pd-Au and other metals were mobilized by dissolution and reprecipitation by metamorphic-hydrothermal fluids. No source has been identified by drilling, magnetic, or electromagnetic methods within 1000m of Cubric, and S isotope signatures suggest that both the gabbro-hosted and iron formation-hosted sulfides are unlikely to have been mobilized 2-3 km from Marbridge. The results of this study confirm that Ni-Cu-Pt-Pd-Au can be mobilized significant distances both in the solid-state and by metamorphic-hydrothermal fluids and that Ir-Rh-Ru and Cr can be used to distinguish between tectonic and hydrothermal mobilization.

2 Introduction

Komatiite-associated Ni-Cu-(PGE) deposits are common in many Archean greenstone belts (e.g., Lesher and Keays 1984; Lesher 1989; Barnes 2006), including the Abitibi greenstone belt (Houlé and Lesher 2011). Although there is a consensus that they formed by partial melting of Fe ± Cu ± Ni sulfide-bearing country rocks, forming barren to weakly-mineralized Fe sulfide xenomelts that were upgraded through interaction with the komatiitic magma (e.g., Sproule et al. 2002; Lesher and Campbell 1993; Lesher et al. 2001; Lesher 2017, the relative roles of modification by magmatic diffusion, magmatic-hydrothermal fluids, metamorphic-hydrothermal fluids, and solid-state deformation in their subsequent modification and mobilization are less well understood (e.g., Barrett et al. 1977; Lesher and Keays 1984; McQueen 1987; Lesher 1989; Lesher and Keays 2002). Understanding how to recognize these processes and how they affect the dispersion and compositions of the ores is essential in developing better exploration techniques.

The purpose of this paper is to describe solid-state tectonic (mechanical) and metamorphic-hydrothermal (chemical) mobilization of Fe-Ni-Cu-(PGE) mineralization at the Cubric showing, in

the Southern Manneville fault zone in the Abitibi greenstone belt of the Superior Province, approximately 24 km north of Malartic, Quebec was discovered in 1957 (Leunur, 1959). We show that the mineralization is hosted by gabbro and silicate-oxide facies iron formation. The gabbro-hosted mineralization has high Cr, high Ni/Cu ratios, and low Pd/Ir ratios consistent with equilibration with a komatiitic magma, rather than a gabbroic magma. The iron formation-hosted mineralization has similar Ni-Cu-Pt-Pd-Au contents, but is moderately to strongly depleted in Ir-Ru-Rh and Cr. This suggests that the gabbro-hosted mineralization was tectonically mobilized from magmatically-formed mineralization as monosulfide solid solution and that the iron-formation was upgraded by metal-bearing metamorphic-hydrothermal fluids. Understanding these processes will help to better understand how they might affect deposits at other localities.

3 Research Methods

Fieldwork was conducted during June-August 2017 and May-August 2018 and included detailed mapping (1:100 and 1:50 scale) of key outcrops in the La Motte-Vassan formation, interpretation of a high resolution airborne magnetic survey to create a regional geological map, re-logging of 14 BQ diamond drill cores (10 from the Cubric Showing, 4 from the Marbridge deposit) totaling approximately 400m of drill core. Eighty samples from the La Motte Vassan formation were analyzed: fifty-four from the Cubric showing including 20 from the mineralized zone, 22 from the Cubric and Marbridge area, and 4 from the Marbridge zone 1 mineralized body.

Surface samples, ranging from 0.5-2.5 kg depending on the availability of unweathered material, were extracted from outcrops using a sledgehammer or a portable rock saw with a diamond-embedded brass saw blade, and weathered surfaces and veins were removed using a diamond-embedded stationary rock saw. Diamond drill core samples, typically 20 cm of half-BQ (3.6 cm diameter) core, were cut parallel to the split face using a stationary saw with a diamond-embedded brass blade to produce a 0.2 cm-thick x 3.6 cm-wide slab for photo-image scanning

and a chip for thin sectioning, and the remaining material was used for geochemical analysis. Saw marks were removed using a coarse diamond-embedded lap wheel, and the samples were cleaned in tap water using a plastic scrub brush, air-dried, and placed into individual plastic bags.

Sixty-five thin sections were made from the bedrock at the Cubric showing and surrounding area, including 29 from the mineralized zone, 4 from the talc-carbonate-altered ultramafic rock, and 32 from other lithologies. Four thin sections were made from bedrock at the Marbridge Zone 1 ore body. Fifteen of these samples were analyzed using the scanning electron microscope to aid in mineralogical identification and to establish mineral chemistry. All samples were examined under an optical microscope, and selected samples were examined under a scanning electron microscope to characterize their modal mineralogy and mineral chemistry. Only results from thin sections related to the mineralization will be discussed here; brief rock descriptions of the country-rock lithologies are given in **Appendix A**.

Eighty-one samples were prepared and analyzed at ALS laboratories in Sudbury. The samples were crushed using high Cr-steel Boyd jaw crusher plates (method code CRU-31), which was cleaned between samples using pink quartzite from Ethel Sand and Gravel and compressed air (method code WSH-21), and pulverized in an ESSA LM-2 tungsten carbide bowl/ring/puck mill (method code PUL-31), which was cleaned between samples using silica sand and compressed air. Al, Ba, Ca, Cr, Fe, K, Mg, Mn, Na, P, S, Si, Sr, and Ti were analyzed by inductively-coupled plasma atomic emission spectrometry (ICP-AES) (method code ME-ICP06) after fusion at 1000°C in a thermal decomposition furnace using a lithium metaborate/lithium tetraborate flux, and dissolved in 4% nitric acid and 2% hydrochloric acid. Peroxide fusion was used for samples with high sulfide contents. Ba, Ce, Cr, Cs, Dy, Er, Eu, Ga, Ge, Gd, Hf, Ho, La, Lu, Nb, Nd, Pr, Rb, Sm, Sn, Sr, Ta, Tb, Th, Tm, U, V, W, Y, Yb, and Zr were analyzed by ICP mass spectrometry (ICP-MS) (method code ME-MS81) after fusion at 1025°C in a thermal decomposition furnace using a lithium metaborate/lithium tetraborate flux

and dissolved in a mixture of nitric, hydrochloric, and hydrofluoric acids. Ag, Cd, Co, Cu, Li, Mo, Ni, Pb, Sc, and Zn were analyzed by ICP-AES (method code ME-4ACD81) after four-acid (HF-$HClO_4$-HCl-HNO_3) digestion. Au, Pt, and Pd were analyzed by ICP-AES (method codes Au-ICP21 and PGM-ICP23), after fire-assay fusion with lead oxide, sodium carbonate, borax, and silica, and dissolved in nitric acid and hydrochloric acid in a microwave oven. Ag was analyzed by flame atomic absorption spectrometry (AAS) (method code Ag-AA45) after 45-minute aqua regia (1 HNO_3: 3 HCl) digestion. Ni, Cu, Pb, and Zn in samples containing high modal abundances of sulfide were analyzed by ICP-AES (method code ME-OG62) after assay-grade 4-acid (HF-$HClO_4$-HCl-HNO_3) digestion. S and C were analyzed by infrared detection (method code ME-IR08) using Leco® inductive combustion furnace heated to approximately 1350ºC. Fl and Cl were analyzed by ion chromatography (method code ME-IC881) after potassium hydroxide (KOH) fusion and dissolved in deionized water. H_2O+ (structural water) was analyzed by infrared spectroscopy (method code OA-IR06) using a Leco® inductive combustion furnace heated to 110ºC and 1000°C. Pd, Pt, Ru, Rh, and Ir in mineralized samples and one least-altered komatiite were analyzed at the Ontario Geoscience Laboratories in the Willet Green Miller Center in Sudbury by ICP-MS (method code IMP-200) after preconcentration by NiS-fire assay with Te-coprecipitation. Lower limits of detection, precisions, and accuracies determined by analysis of duplicates and standard reference materials are reported in Appendix A. All geochemical data are reported in Appendix C.

Ten thin-section sized rock chip samples from Cubric (2 each from gabbro-hosted and iron formation hosted mineralization at surface, iron formation at depth, and unmineralized pyrite-bearing sediments) and 2 from Marbridge zone 1 were analyzed for ^{32}S and ^{34}S by stable isotope ratio mass spectrometry at Indiana University under the supervision of Prof. E.M. Ripley

A sample of the gabbro was dated by U-Pb isotope dilution-thermal ionization mass spectrometry (ID-TIMS) at the Jack Satterly Geochronological Laboratory at the University of Toronto, Canada. Detailed analytical procedures are presented in Appendix A. Four primary

prismatic euhedral zircons without core and rim textures were selected from a leucocratic pegmatitic pod within the gabbro and dated.

4 Geological Setting

4.1 Abitibi greenstone belt

The ca. 2800-2600 Ma Abitibi greenstone belt (AGB: **Fig. 1**) is one of the largest, best-preserved, best-exposed, and best-understood Archean greenstone belts in the world. It extends for several hundred km from east-central Ontario into central-western Quebec. The AGB has been recently subdivided into seven volcanic assemblages and two unconformably overlying sedimentary assemblages (Ayer et al. 2002; Thurston et al. 2008): a pre-2750 unnamed assemblage, the 2750-2735 Ma Pacaud assemblage, the 2734-2724 Ma Deloro assemblage, the 2723-2720 Ma Stoughton-Roquemaure assemblage, the 2719-2711 Ma Kidd-Munro assemblage, the 2710-2704 Ma Tisdale assemblage, the 2704-2695 Ma Blake River assemblage, the 2690-2685 Ma Porcupine assemblage, and the 2677-2670 Ma Timiskaming assemblage. The degree of metamorphism ranges from prehnite-pumpellyite to upper amphibolite facies with large areas of lower-middle greenschist facies (Jolly 1974). Most areas have experienced polyphase folding and faulting, but the strain is typically partitioned along contacts and major fault structures such as the Dester-Porcupine-Manneville fault and the Cadillac-Larder Lake fault, leaving most rocks relatively undeformed apart from a weak to moderate regional cleavage.

Komatiite-associated Ni-Cu-(PGE) deposits occur primarily in the Tisdale (e.g., Shaw Dome: Redstone-Langmuir-Hart; Bartlett Dome: Texmont; Halliday Dome: Sothman) and Kidd-Munro (e.g., Dundonald Area: Alexo, Dundeal; La Motte Township: Marbridge and Dumont) assemblages, but also in the Deloro assemblage (e.g., Bartlett Dome: Bruce Lake; Harricana-Turgeon greenstone belt: Grasset) (Houlé and Lesher 2011). Most of the Ni-Cu-(PGE) occurrences in the AGB are associated with komatiitic flows and subvolcanic sills (Houlé and

Lesher 2011), although a few are hosted by gabbroic intrusions (e.g., Montcalm: Barrie 1990). Although Al-undepleted, Al-depleted, and Ti-enriched komatiites are all present within the AGB (Sproule et al. 2002), komatiite-associated deposits are associated exclusively with Al-undepleted komatiites (Sproule et al. 2005; Houlé and Lesher 2011). They include the five different types of mineralization associated with komatiitic Ni-Cu-(PGE) deposits (Lesher and Keays 2002): Type I basal stratiform massive\net\disseminated mineralization (e.g., Alexo, Bannockburn, Langmuir), Type II internal stratabound disseminated mineralization (e.g., Dumont), Type III internal stratiform "reef"-style mineralization (e.g., Boston Creek), Type IV magmatic diffusional, magmatic-hydrothermal, or metamorphic-hydrothermal mobilized mineralization (e.g., Langmuir #2, Hart), and Type V tectonically-mobilized mineralization (e.g., Redstone and parts of most other deposits). Types are summarized in Table 1

Table 1 Summary of komatiite associated Ni-Cu-(PGE) types. Simplified from Lesher and Keays (2002).

	Type I Basal Stratiform	**Type II** Internal Stratabound	**Type III** Internal Stratiform	**Type IV** Hydrothermally or Metamorphically Mobilized	**Type V** Mechanically Mobilized
Timing	Early Magmatic	Intermediate Magmatic	Intermediate Magmatic	Late Magmatic to Syn-Metamorphic	Syn-Tectonic
External Sulfur	Yes	Yes	No	Yes (Indirect)	Yes (Indirect)
Textures	Massive, Net-textured, or Disseminated	Disseminated or "Blebby"	Disseminated	Banded within metasediments or in veins	Brecciated (durchbewegung)
Genesis	Early magma emplacement	During crystallization of Ol ± Pyx	Typically at or near the point where Plag begins crystallizing	Diffused, infiltrated, or mobilized into metasediments	Tectonically mobilized along shear zones

4.2 La Motte-Vassan formation

The 2714 ± 2 Ma La Motte-Vassan Formation is part of the Kidd-Munro volcanic assemblage (Thurston et al. 2008) and represents the oldest rocks of the Malartic Group. It occurs south of the Destor-Porcupine-Manneville Fault zone (DPMFZ) (Pilote et al. 1998) and

comprises komatiites, basalts, and minor felsic-intermediate metavolcanic rocks. Three felsic intrusions surround the formation: the ca. 2647 Ma La Motte pluton, the ca. 2681–2660 Ma Preissac pluton, and the ca. 2680–2632 Ma La Corne pluton (Carignan et al. 1993; Ducharme et al. 1997) (**Fig. 2**).

The komatiites in the La Motte-Vassan formation include thin massive and differentiated spinifex-cumulate lobe and sheet flows (e.g., Spinifex Ridge: Champagne 2004), none of which are known to be mineralized, and thick poorly-differentiated cumulate bodies, some of which are known to be mineralized (e.g., Dumont: Eckstrand 1975; Marbridge: Graterol and Naldrett 1971). All of the komatiites in the area are Al-undepleted (Champagne 2004; Sproule et al. 2005), and metal values fall in the normal range for komatiitic rocks (Houlé and Lesher 2011; Barnes et al. 2007).

The structure of the area is dominated by the DPMFZ, which is an east-to-southeast–trending polyphase deformation zone that includes two splays: The Northern and Southern Manneville fault zones (**Fig. 2**). The moderately north-dipping Northern Manneville fault separates <ca. 2694 Ma (Davis 2002) metasedimentary rocks of the La Caste formation to the south from 2720–2716 Ma (Pilote et al. 2015) mafic-dominated metavolcanic rocks of the Kinojevis Group to the north, whereas the steeply-dipping Southern Manneville fault zone separates the La Caste formation from other formations within the Malartic group (**Fig. 2**). The Marbridge deposits and Cubric showing occur along the Southern Manneville fault zone (**Fig. 2**), within strongly deformed supracrustal and plutonic rocks (Daigneault et al. 2002).

4.3 Marbridge 1-4 deposits

The Marbridge area is located 3 km northwest of the Cubric showing and 24 km north of the Town of Malartic. The Marbridge deposit contains 4 discrete zones and produced a total of 774 227 tonnes of ore with average grades of 2.28% Ni and 0.1% Cu (Graterol and Naldrett 1971); this Ni: Cu ratio is consistent with it being derived from an ultramafic magma (Houlé and Lesher,

2011). Zone 1 is the only zone with surface mineralization and is interpreted to be a large Type V (tectonically mobilized Type I) deposit (Champagne 2004; Houlé and Lesher 2011; LaFrance 2015). Zones 2-4 are interpreted to be Type I (primary magmatic) komatiite-associated deposits but are poorly characterized.

At surface, the Marbridge area contains pillow basalts and differentiated (spinifex and orthocumulate-mesocumulate) komatiites (LaFrance 2015; Giovenazzo 2000). Gabbroic and granitic dikes cut across the volcanic rocks. The latter are strongly foliated to unfoliated, but invariably have strong lineation defined by hornblende, which is oriented subparallel to the fold axes of F_2 isoclinal folds (LaFrance 2015).

Marbridge Zone 1 has a pyrrhotite-pentlandite-chalcopyrite-pyrite assemblage, and although 100m of existing drill core is preserved, the ore body was not intersected. Marbridge Zones 2, 3, and 4 do not outcrop at the surface, and there is no existing drill core for these deposits. They have a pyrite-millerite-pentlandite assemblage (Graterol and Naldrett 1971), which is different from most komatiite-associated Ni-Cu-PGE deposits (e.g., Lesher and Keays 1984; Lesher, 1989; Lesher and Keays 2002; Barnes 2006; Barnes et al. 2009), but which is similar to the observed mineralogy at Cubric. The limited data available for Zones 2, 3, and 4 hampers comparisons to Marbridge Zone 1 and Cubric.

5 Results

5.1 Cubric showing

A bedrock geological map was created using a combination of bedrock mapping and from the first vertical derivative of a drone-flown magnetic survey. The mineralization and footwall rocks are known from a hydraulically stripped outcrop and ten 25-60 m deep diamond drill cores (**Fig. 4**), all of which were relogged as part of this study. The Cubric showing exposes eight lithologies: granite, tonalite, gabbro, ultramafic rocks, actinolite schist, biotite schist, gabbro-hosted semi-massive sulfide breccia zone, and mineralized oxide facies iron formation.

The granite ranges from leucocratic to mesocratic, is coarse- to medium-grained, pink to grey on the weathered surface, and pink to white on fresh surfaces. The tonalite is uniformly mesocratic, fine- to medium-grained, brown-grey on weathered surfaces, light grey on fresh surfaces, and seems to be cross-cut by the granite. The gabbro is coarse- to medium-grained mesocratic in the center to fine-grained melanocratic along the margins, black on weathered surfaces, and black and white on fresh surfaces. It contains coarse leucocratic (pegmatitic) pods and 3-4m rafts of country rocks (komatiite, iron formation, actinolite schist, and biotite schist) near contacts. The actinolite schist is soft, with patchy magnetism, green-black on weathered surfaces, and fern to moss green on fresh surfaces. Two of the rafts within the gabbro contain one thin, continuous 2 mm thick pyrite band. The biotite schist is very soft, has a moderate to strongly foliation, is golden on weathered surfaces but jet black on fresh surfaces, and is composed mainly of medium-grained biotite. The talc-altered ultramafic rock is extremely soft, fine- to medium-grained, magnetic, white on weathered surfaces, and medium to light grey on fresh surfaces. The oxide facies iron formation is fine- to medium-grained, strongly magnetic, blackish-blue and white, and composed of alternating 0.5–1 cm-thick bands of magnetite and saccharoidal quartz. Despite the high magnetic susceptibility, the small volume of the unit makes it impossible to detect using airborne magnetics. In drill core, there is an argillite containing up to 5% pyrite and trace magnetite.

The sulfide mineralization at the Cubric showing (**Table 2**) occurs in three lithologies: 1) gabbro-hosted semi-massive sulfide breccia zone (only observed on the surface), 2) banded sulfides in magnetite-quartz iron formation (only observed on the surface), and 3) banded sulfides in silicate-sulfide iron formation (only observed at 16-17m true depth below surface). The abundance of sulfide and grades in the gabbro-hosted semi-massive sulfide breccia zone brecciated zone (1.7-12 % Ni, 0.2-1% Cu) are generally higher than in the iron formations at the surface (0.2-1.5 % Ni, 0.15-0.7% Cu) and the iron formation at depth (0.2-0.8% Ni, 0.04-0.12% Cu). The gabbro-hosted semi-massive sulfide breccia zone is rust-red on weathered surfaces

and black with a network of brecciated sulfides on fresh surfaces. Sulfides are surrounded by dark halos of chlorite. **Figure 5** contains hand sample photos comparing the mineralization textures in gabbro-hosted sulfides vs. iron formation-hosted sulfides. The mineralization in the gabbro is semi-massive and brecciated, whereas the mineralization in the iron formation comprises tapered bands of sulfides that are locally folded. **Figure 6** contains outcrop and thin section photos of the gabbro and ultramafic rocks. The outcrop photo of the gabbro shows a pegmatitic pod within the gabbro; the thin section photo shows the typical euhedral hornblende and plagioclase present throughout the outcrop in both plain polarized and crossed polarized light. The outcrop image of the ultramafic rock shows the strongly talc-carbonate altered komatiite at the bottom of the image. The thin section photos show the fine-grained talc-carbonate matrix with finely disseminated pyrrhotite, pentlandite, and coarse magnetite in cross-polarized and reflected light.

5.2 Marbridge Zone 1

Marbridge Zone 1 is exposed at the surface as a rust-red weathered rock that is dark metallic brown/brass on fresh surfaces (**Fig. 7**). It consists of semi-massive to net-textured sulfides within a serpentine-altered ultramafic host rock cut by contact-parallel, 10 cm long x 0.5 cm wide, chrysotile bands. Across the zone, from south to north, sulfide textures gradually change from semi-massive at the base of the zone to net-textured at the top of the zone. This is consistent with a northward younging direction inferred from the asymmetric zonations of differentiated spinifex-cumulate komatiite flows and pillow basalt polarities in the surrounding area (Giovenazzo 2000; this study). The mineralized zone is sandwiched between two mafic sills with chilled margins at their contacts (**Figs. 7, 8**) The mafic sills consist of 20% feldspar and 80% hornblende with average grain sizes varying from 1 mm in the center of the sills to 0.1 mm along the chilled margins of the sills. The presence of sills between the mineralized zone and surrounding volcanic rocks, and the similarity in the trend of these rocks, suggest that the

Table 2 Metal values in grab samples from the Cubric showing. All values re-calculated volatile free. Note: ME samples from surface outcrops, C08 samples from diamond drill cores.

Sample Number	Host	S wt.%	Fe wt.%	Ni wt.%	Cu wt.%	Cu ppm	Pd ppm	Pt ppm
ME-AM-17DES0146CG05	IF	12.5	49.8	0.526	0.535	531	0.129	0.081
ME-AM-18DES0279CG04	IF	13.9	50.4	1.01	0.710	430	0.276	0.074
ME-AM-18DES0279CG09	IF	9.42	45.9	0.743	0.169	167	0.028	0.039
ME-AM-18DES0279CG10	IF	8.47	46.8	0.202	0.162	405	0.063	0.017
ME-AM-18DES0279CG14	IF	7.43	13.4	1.50	0.164	197	0.249	0.088
C08-29-76'9"	IF	28.8	36.8	0.826	0.068	38.7	0.142	0.010
C08-29-81'10"	IF	25.7	27.8	0.461	0.119	93.2	0.081	0.017
C08-29A-76'2"	IF	26.8	30.4	0.293	0.040	331	0.034	0.016
C08-29B-79'0"	IF	24.5	27.5	0.264	0.084	134	0.042	0.045
C08-29B-82'2"	IF	19.5	21.5	0.527	0.070	23.9	0.106	0.012
ME-AM-17DES0146CG08	Gabbro	24.2	29.3	2.58	0.181	1326	0.451	0.211
ME-AM-17DES0146AG10	Gabbro	24.5	31.2	2.75	0.379	1517	<0.001	0.206
ME-AM-18DES0279EG15	Gabbro	26.3	33.9	2.37	0.290	1487	0.373	0.148
ME-AM-18DES0279EG16	Gabbro	60.4	40.4	12.0	0.410	3900	0.678	0.100
ME-AM-18DES0279EG18	Gabbro	12.7	17.7	2.07	0.376	864	0.313	0.119
ME-AM-18DES0279EG19	Gabbro	30.7	31.2	2.03	1.00	2620	0.334	0.224
ME-AM-18DES0279EG21	Gabbro	17.4	25.2	1.67	0.249	1261	0.203	0.153
ME-AM-18DES0279EG22	Gabbro	22.4	28.7	2.50	0.247	1334	0.229	0.163
ME-AM-18DES0279EG23	Gabbro	29.4	32.1	5.05	0.202	1895	0.386	0.143

sulfides were not tectonically mobilized as previously suggested by Giovenazzo (2000) and LaFrance (2015). Instead, it appears that the sulfides formed in an ultramafic body and became disconnected from their host rocks by the emplacement of mafic sills parallel to stratigraphy (**Fig. 8**). Outcrops of komatiite with spinifex textures are observed only 30 m away from the mineralized zone.

5.3 Structural geology

Most structures in the Marbridge and Cubric areas are associated with movement along the Southern Manneville fault zone. The D_1 event is expressed as layer-parallel faults that superpose various volcanic domains (Daigneault et al. 2004; Desrochers and Hubert 1996). In the Cubric-Marbridge area, these D_1 structures are overprinted by the D_2 thrusting event along the DPMFZ. The principal S_2 foliation is a strong penetrative cleavage that generally strikes northwest, but can vary locally by as much as 45°. The S_2 cleavage is defined by the strong preferred orientation of calcite and magnetite in komatiites, a weak fabric defined by amphiboles in gabbro, parallel quartz-magnetite-sulfide bands in iron formation, a weak fabric defined by biotite in granite, and a strong fabric defined by mica and actinolite in schists. It is axial planar to isoclinal upright F_2 folds (**Fig. 9**) that strike parallel to the regional structural trend (**Fig. 10A**). A non-penetrative, north-south trending, steeply-dipping S_3 cleavage is axial planar to open F_3 folds (**Fig. 10B**) that overprint the isoclinal F_2 folds on both outcrop-scale and map-scale, as interpreted from the high-resolution aeromagnetic map (**Fig. 3**). At Cubric, both the iron formation and the gabbro are deformed by the D_2 event, which suggests that mobilization for sulfides into these lithologies would must be pre-D_2 or syn-D_2.

5.4 Petrography

The gabbro is composed of fine-grained plagioclase (30–50%, An_{13-16}) and 50–70% medium- to coarse-grained euhedral magnesiohornblende ($Ca_{1.8}Al_{0.5}Fe_{1.6}Mg_{2.65}Si_7O_{22}(OH)_2$). The former is most likely a metamorphically-modified igneous phase, whereas the latter is either

a modified igneous phase (less likely, given the lack of other hydrous igneous phases) or a metamorphic phase that replaced igneous pyroxene during regional amphibolite facies metamorphism.

The ultramafic rock consists of 90% talc, calcite, and dolomite with ~10% fine (<1 mm) disseminated magnetite, pyrrhotite, and pentlandite preferentially localized along S_2 foliation planes. The oxide-facies iron formation is composed of alternating 0.5–1 cm-thick bands of magnetite (50-80%), sulfides (10-40%; pyrite > pentlandite ~ millerite > chalcopyrite), and saccharoidal quartz (10-30%) **(Fig. 11)**. Chalcopyrite is closely associated with pyrite and occurs as irregular, weakly polygonal grains inside larger pyrite grains and along pyrite grain boundaries. The gabbro-hosted semi-massive sulfide breccia zone contains 30-80% sulfide (pyrite > millerite ~ pentlandite > chalcopyrite ~ violarite >>> pyrrhotite >> galena ~ sphalerite).

The sulfides fill fractures or form irregular connected patches that are surrounded by fine-grained untwined plagioclase (An_{13-16}) and chlorite, inferred to have replaced hornblende**.** Pyrite, chalcopyrite, and pentlandite are weakly polygonal with foam textures. The relationship between chalcopyrite and pyrite varies: in some areas, both phases are intergrown and polyhedral, but in other areas - sometimes in the same polished thin section - chalcopyrite and pyrite form a ragged mixture with irregular- to amoeboidal-shaped chalcopyrite within pyrite grains, possibly representing a replacement texture.

Marbridge Zone 1 is net-textured to semi-massive and contains 20-60% sulfide (typically ~50% pyrrhotite, ~25% pentlandite, ~20% magnetite, ~5% chalcopyrite) and 40-80% radiating acicular serpentine (probably antigorite). None of the three samples examined in this study are brecciated.

5.5 Lithogeochemistry

Major elements from all igneous lithologies from the Cubric surrounding area were plotted against Mg to aid in their classification (**Fig. 13**). However, only lithologies relevant to mineralization will be discussed.

The gabbro contains high abundances of Al-Ti-K-heavy rare earth elements (HREE) (**Figs. 13** and **14**), moderate abundances of Si-Ca-Mn, and low abundances of Mg relative to the ultramafic rocks in the La Motte-Vassan formation. It varies in composition across the outcrop as a result of varying proportions of hornblende and plagioclase. It is enriched in highly incompatible lithophile elements (HILE) relative to moderately incompatible lithophile elements (MILE) with negative Nb-Ta ± Ti anomalies (**Fig. 14)**.

The ultramafic rock has a high abundance of Mg and Ca with low Si, Al, Ti, and HILE-MILE. They are orthocumulate komatiites with 25-30% MgO, which are not good candidates for generating Ni-Cu-(PGE) mineralization, which is typically associated with basal mesocumulate-adcumulate komatiites with higher MgO values (see discussion by Arndt et al. 2008; Lesher 1989; Lesher and Keays 2002). All known komatiites in the La Motte-Vassan formation are Al-undepleted (Sproule et al. 2002) (**Fig. 15)**, similar to the majority of komatiites in the Kidd-Munro and Tisdale volcanic assemblages, including those at the Alexo mine and Pyke Hill (Puchtel et al. 2004), Marbridge deposit (LaFrance 2015), Spinifex Ridge (Champagne 2004), and Bannockburn C-Zone (Taranovic et al. 2012). Most of the komatiite rocks from the Cubric area are slightly depleted in HILE relative to MILE; however, two samples (ME-AM19-DES0279BG11 and ME-AM19-DES0279BG12) are enriched in HILE relative to MILE, suggesting some degree of crustal contamination **(Fig. 16)** (see discussion by Lesher et al. 2001; Sproule et al. 2002). These compositions and the mineralogy are consistent with it being a talc-carbonated non-cumulate Al-undepleted komatiite (see Lesher 1989; Arndt et al. 2008).

The gabbro-hosted semi-massive sulfide breccia zone is enriched in Fe-Na-Cu-Pb-Pd-Pt-Co and depleted in Si-K-Ti relative to the unmineralized gabbro. The depletions in major elements can be attributed to dilution by sulfide, so the whole-rock data were re-calculated to 100% silicates, resulting in a composition similar to the least-mineralized gabbro.

The sulfide-rich iron formation is enriched in Fe, Au, and S, and depleted in Si, Cr, Mo, relative to the least mineralized IF. The depletions in major elements can be attributed to dilution by sulfide, so the whole-rock data were also re-calculated to 100% silicates, resulting in a composition similar to the least-mineralized iron formation.

5.6 Sulfide Chemistry

The mineralized zone at Cubric has high Ni-Cu-Co-Pd concentrations that increase systematically from south to north as with the increase in sulfide modal abundances. There is a strong positive correlation between S and Ni, Co, Cr, Ir, Pt, and Pd, suggesting that these metals are hosted in sulfide phases. Zn shows no correlation with S content and is similar in concentration within both the gabbro-hosted semi-massive sulfide breccia zone and unmineralized gabbro, suggesting that the sulfide mineralization contains negligible Zn. Pb values in both the iron formation and the gabbro-hosted semi-massive sulfide breccia zone are very low, which is consistent with the sulfides having formed in an ultramafic magma (**Fig. 17**). Surface samples of the quartz-magnetite iron formations have lower S content and metal concentrations (7-12% S, 0.2-1.5% Ni, and 0.16-0.7% Cu) than those of the gabbro-hosted semi-massive sulfide breccia zone brecciated zone (11-23% S, 1.6-12% Ni, and 0.18-1% Cu). Pyrite contents increase with depth while maintaining similar metal concentrations (20-29% S, 0.2-0.8 %Ni, 0.7-0.12% Cu) relative to the S in the iron formation at the surface.

At depth, the mineralized iron formation contains variable amounts of pyrite, which likely explains the increase in S while maintaining the same metal values; however, the bulk sulfides still have a high Ni: Cu ratio suggesting they were derived from an ultramafic magma. There are

moderate to strong correlations between Fe-Ni-Co-Cr-Zn-Au-Ir-Pt-Pd and S (**Fig. 17)**, indicating that these elements are housed in or associated with sulfides, whereas Cu-As-Mo-Pb, all of which are also chalcophile, have weak correlations with S, suggesting later modification.

The abundances of S-Fe-Ni in mineralized samples from Cubric and Marbridge Zones 1-3-4 are plotted on a S-Fe-Ni phase diagram at temperatures of 100-135 °C (**Fig. 18)**. The Cubric mineralized samples plot in the pyrite-pyrrhotite-pentlandite field, which is consistent with an originally magmatic composition, but contain millerite instead of pentlandite, suggesting that pentlandite was oxidized to millerite. Marbridge Zone 1 samples also plot in the pyrite-pyrrhotite-pentlandite field, which matches their observed pyrrhotite-pentlandite-chalcopyrite-pyrite mineral assemblage. Marbridge Zones 3 and 4 plot in the pyrite-pentlandite-millerite field (Graterol and Naldrett 1971).

5.7 Metals in 100% Sulfides

In order to compare samples containing different abundances of sulfides, the metal tenors (metal abundances in 100% sulfides) of the Cubric and Marbridge samples were calculated assuming that all of the Cu is in stoichiometric chalcopyrite, that all of the Ni is in pentlandite with an average formula of $Fe_4Ni_5S_8$, and that the remaining S is in stoichiometric pyrite. Metal tenors (metals in 100% sulfides) in the disseminated sulfides in the ultramafic rock at Cubric are higher than those in sulfides in the iron formation and semi-massive brecciated mineralization. Ni_{100}, Co_{100}, Pd_{100}, and Pt_{100} are plotted against Cu_{100} in **Figure 19**. There is little to no correlation between these metals and Cu.

Metal tenors were normalized to the primitive mantle and compared to data from Kambalda (**Fig. 20**), the type-example of komatiite associated Ni-Cu-PGE deposits (Lesher 1989; Lesher and Keays 2002)**.** In general, the pattern of the gabbro-hosted semi-massive sulfide breccia zone is similar to the range of Kambalda Type I mineralization, which suggests the sulfides formed in an ultramafic magma **(Fig. 20)**, but are slightly enriched in Ir-Rh-Ru. The

mineralization at the Marbridge zone 1 is geochemically similar to the gabbro-hosted semi-massive sulfide breccia zone and Cubric.

The metal tenors in the oxide facies iron formation are similar to Kambalda Type I mineralization in terms of Ag, Bi, S, Te, Se, As, Au, Pd, Cu, Ni, Co, Fe, and Zn, but are slightly enriched in Fe-Cu and strongly depleted in Rh-Ru-Ir and Cr relative to Kambalda Type I mineralization **(Fig. 20)**. The depletion of IPGE and Cr is more similar to Kambalda Type IV magmatically-hydrothermally mobilized mineralization.

Base and precious metals tenors are plotted against Cu_{100} (**Fig 19**) to determine if the changes in tenor are related to the crystallization of MSS, which would produce wide variations in Cu_{100} (Naldrett 2004), or to variations in magma: sulfide ratio, which would produce positive correlations between all $Metal_{100}$ values (Naldrett 2004). Metal tenors scatter widely but have low Cu_{100} contents (**Fig. 19**), indicating that the variations in tenor do not result from MSS fractionation.

5.8 Geochronology

Three of the four analyzed zircons are slightly discordant, and only one is strongly discordant. A crystallization age of the rock is given by the upper intercept on Concordia of a regression line or Discordia line going through all four zircons and yielded an age of 2680.1 ± 1.5 Ma (**Fig. 21**). This age is younger than the ca. 2714 age of the La Motte – Vassan formation.

5.9 Sulfur Isotopes

$\delta^{34}S$ values range +3.6 to +3.2 per mil for net- and semi-massive textured samples from Marbridge Zone 1, +2.2 per mil for gabbro-hosted sulfides from Cubric, and -2.9 to +0.07 per mil for iron formation-hosted sulfides and komatiites from Cubric (**Fig. 22**).

The S isotopic compositions of the net- and semi-massive sulfides at Marbridge are significantly heavier (3.6-3.9 ‰ $\delta^{34}S$) than mantle-derived sulfides (0.1 ± 0.5 ‰ $\delta^{34}S$: Sakai et

al. 1984), consistent with derivation from a crustal source (e.g., Ripley 1981; Lesher and Groves 1986; Lesher 2017). The S isotope compositions of the gabbro-hosted sulfides at Cubric (2.2‰ $\delta^{34}S$) are lighter than the net- and semi-massive sulfides at Marbridge Zone 1, so are unlikely to be derived from the same source, and the iron formation-hosted sulfides at Cubric are lighter and more variable (+0.1 to -2.9 ‰ $\delta^{34}S$), suggesting derivation from a mixture of different sources.

6 Discussion

The key issues to be discussed are: 1) the original sulfide composition prior to mobilization and alteration, 2) the degree of metal fractionation in the sulfides during mobilization events, 3) the degree of post-mobilization alteration, and 4) the implications of these factors for the genesis of the mineralization at the Cubric showing and implications for exploration in the Abitibi Greenstone Belt.

6.1 Original Sulfide Chemistry

Although most of the Ni-Cu-PGE deposits in the AGB are associated with komatiites (Gross 2009), some with gabbros (e.g., Montcalm: Barrie 1990). The former are chemically distinguished from the latter by their higher Ni/Cu and lower Pd/Ir ratios (e.g., Barnes and Naldrett 1985; Naldrett 2004; Barnes et al. 2007). These ratios can be modified by fractional crystallization of MSS (see reviews by Naldrett 2004 and Barnes and Lightfoot 2005), tectonic mobilization of chalcopyrite/ISS relative to pyrrhotite-pentlandite/MSS (e.g., Barrett et al. 1977; McQueen 1981; McQueen et al. 1986; see below), or metamorphic-hydrothermal modification (e.g., Lesher and Keays 1984; Lesher and Keays 2002; Mukwakwami et al. 2014). Type I komatiite-associated Ni-Cu-PGE deposits are typically enriched in Ag > Bi > S > Te > Se > As > Sb > Pb > Mo > Au > Pd > Rh > Ni > Ir > Os > Co > Fe > Zn, Re > Cr (Lesher and Keays

2002)[1]. Types II and III are not semi-massive to massive sulfides, so they were unlikely to be the source. Relative to this sequence, Cubric gabbro-hosted sulfides are slightly enriched in Rh-Ru-Ir and depleted in Au and Te, whereas Cubric iron formation-hosted sulfides are slightly enriched in Fe and Cu and significantly depleted in Ir, Ru, Rh, and Cr; however, both are similar to the Type I range of other elements.

The broad similarities in the mantle-normalized metal patterns of the Cubric sulfides to other Type I komatiite-associated deposits (**Fig. 20**), the paucity of sulfides in the Cubric gabbro outside of the shear zone, the presence of disseminated Fe-Ni-Cu sulfides in the Cubric komatiite, the abundance of komatiite in the LaMotte – Vassan formation, and the proximity of the komatiite-associated Marbridge deposits suggest that the metals in the gabbro-hosted sulfides at Cubric were originally derived from a komatiitic magma rather than a gabbroic magma.

Similarly, although iron formations can contain significant amounts of Cu-Zn-Pb-Au-Ag-Sb-Ni (as well as Hg-B-Sn-W), they typically do not contain significant amounts of PGEs, Co, or Cr (Gross 2009), which are present in the iron formation at Cubric. So, it is more likely that the metals in the iron formation-hosted sulfides were derived from a komatiite source and mobilized into the iron formation rather than as a result of primary sedimentary deposition.

6.2 Tectonic Mobilization

The degree of metal fractionation in magmatic Fe-Ni-Cu sulfides during tectonic mobilization (type V) depends on composition, pressure, and temperature, which determines which phases are present (sulfide melt, MSS + sulfide melt, or Po-Pn-Ccp), how much Ni and Cu can dissolve in MSS, and mineral ductilities. The ductility of minerals depends on internal controls such as crystallography and mineral composition and external controls such as temperature, differential stress, lithostatic pressure, fluid pressure, and strain rate. If

[1] Ag was plotted incorrectly in Lesher and Keays (2002) because of an error in units (ppb vs ppm).

deformation occurred between 700 and 1200°C, then Au-PPGE-Cu-Zn-Pb-Ag-enriched residual sulfide melt may be mobilized relative to lPGE-Cr-enriched MSS (**Fig 23 A**). If deformation occurred between 500 and 850°C, then except in very Cu-rich systems, sulfides will mobilize as a homogeneous *MSS* phase and will have relatively consistent metal ratios (**Fig 23 B**) (Barrett et al., 1977). If deformation occurred below 500°C, then Cu-Zn±Au±PGE±Mo±Te±Bi enriched chalcopyrite may be mechanically mobilized relative to Ni-rich pentlandite and Fe-rich pyrrhotite (**Fig. 23 C**).

Although experimental studies suggest that pyrrhotite should be more ductile than chalcopyrite at temperatures between 100 °C and >500°C (Kelly and Clark 1975), chalcopyrite appears to be more ductile than pyrrhotite in natural examples because it commonly fills pressure shadows around brecciated clasts in deformed pyrrhotite- chalcopyrite massive sulfide lenses and is injected in fractures in the wall rocks of those lenses (McQueen 1981). Additionally, at low P, the chalcopyrite's brittle-ductile transition is at a lower temperature than pyrrhotite (Marshall and Gilligan 1987). The higher strain rates in laboratory experiments may explain this difference in the rheological behavior of pyrrhotite and chalcopyrite and relates to the larger problem of extrapolating experimental results to natural deformation (Paterson 1987). The relative rheology and ductility of sulfide minerals increase from pyrite, pentlandite, pyrrhotite, to chalcopyrite (Cox 1987; Marshall and Gilligan 1987).

There is no significant fractionation of Cu-PPGE, which are concentrated in lSS and chalcopyrite, from Co-lPGE, which are concentrated in pyrrhotite in the gabbro-hosted mineralization at Cubric. Together with the relatively low abundances of Cu in komatiite-associated mineralization (e.g., Barnes and Naldrett 1985; Lesher and Keays 2002; this study) suggests that mobilization occurred as sulfide melt or a homogenous *MSS* containing Co-lPGE and Cu-PPGE. The fabrics in the gabbro-hosted mineralization combined with the gabbro being ca. 34 Ma younger than the komatiites of the La Motte-Vassan formation, deformation and mobilization would have occurred in the solid-state during post-magmatic metamorphism.

One iron formation sample (ME-AM-18DES0279CG14) was collected along the same shear zone as the gabbro-hosted mineralization and is located less than 1m away from the gabbro hosted mineralization. This sample contains normal lPGE values and has a sulfide chemistry, which more closely resembles the gabbro-hosted sulfides. This sample is evidence for the shear zone mobilizing sulfides across multiple lithologies.

6.3 Magmatic Diffusion

Type lV mineralized metasediments at Langmuir (greenschist facies), Kambalda (lower amphibolite facies), and Thompson (upper amphibolite faces) occur only adjacent to (within 30-50 m: (e.g., Green and Naldrett 1981; Paterson et al. 1984; Bleeker 1990) magmatic mineralization at a range of metamorphic grades and have been interpreted to have formed during high-temperature magmatic diffusion (Lesher and Keays 1984; Lesher and Keays 2002). This occurs as the much higher abundances of metals in the magmatic mineralization and much lower concentrations of metals in the sulfide-bearing iron formation sought to reduce their concentrations to a common level. This may have occurred via solid-state lattice diffusion (slower: see Crank 1979) or by grain-boundary diffusion (more rapid: see Sippel and Foster 1963).

Although there are few complete geochemical datasets for this type of mineralization, mineralized metasediments at Kambalda (Paterson et al. 1984) are enriched in Te-Se-Zn-Ag and depleted in lr-Cr relative to adjacent magmatic mineralization, mineralized metasediments at Langmuir (Green and Naldrett 1981) are enriched in Cu and depleted in lr-Rh-Os-Ru-Co relative to adjacent magmatic mineralization, and mineralized metasediments at Thompson Bleeker (1990) are enriched in Pb-Zn and depleted in Cr-Ni-Co-Cu relative to adjacent magmatic mineralization (Lesher and Keays 1984; Bleeker 1990; Lesher and Keays 2002).

A similar depletion pattern of lr > Ru > Rh > Cr is observed in Cubric iron formation-hosted sulfides, but not the gabbro-hosted sulfides. lf this represents diffusion adjacent to Type I

mineralization, then the mineralized iron formation must have been later rafted into the gabbro. We cannot preclude this possibility, but we have no evidence for this other than the broad geochemical similarity to Type IV mineralization at Kambalda, Langmuir, and Thompson.

6.4 Mobilization in Metamorphic-Hydrothermal Fluids

Type IV quartz-pyrrhotite-pentlandite ± chalcopyrite ± pyrite ± sphalerite ± violarite ± magnetite veins at Kambalda transgress adjacent basalts and exhibit hydrothermal textures (Lesher and Keays 1984). They are enriched in Se and depleted in Ir > Cr > Cu ~ Pd > Zn relative to elements of similar compatibility (Lesher and Keays 2002). Quartz – albite – carbonate – chalcopyrite ± pyrrhotite ± pentlandite veins at the Donaldson deposit in Nunavik are enriched in As > Sb > Pd > Pt > Cu and depleted in Ir > Os > Ru > Rh > Bi > Te (Dillon-Leitch et al. 1986). No Cr-Zn data are reported. Similar signatures are observed in quartz – calcite – sulfide veins at Garson mine in Sudbury, which are also depleted in Ir > Pt > Rh > Au > Cr > Pd relative to average contact ore (Mukwakwami et al. 2014). Shear zone-hosted sulfide-rich veins at the Otway prospect in Western Australia are depleted in Ir > Cu > Fe > Pd (Keays et al. 1982), but no Pt, Rh, Ru, Zn, or Cr data are reported. The abundance of other reported metals at these occurrences are similar to the abundances in Kambalda Type I deposits, suggesting that they originated from a Type I source and the depleted elements were not mobilized (probably Ir, possibly Pd) or not deposited (probably Fe and Cu) under the particular hydrothermal conditions that characterized that system. Fractionation in hydrothermally mobilized systems varies with metal solubility: IPGE's and Cr have low solubilities, so will be left behind in the residual sulfide body, and depletions in these elements are characteristic of Type IV mobilization (**Fig 23 D**).

The depletion pattern of Ir > Ru > Rh > Cr in Cubric iron formation-hosted sulfides is also broadly similar to hydrothermally-mobilized mineralization at Donaldson West, Kambalda, Sudbury, and Otway. A key is the saccharoidal quartz bands in the mineralized iron formation.

We cannot preclude them representing metamorphosed boudinaged sedimentary cherty bands, but they are not present in all parts of the iron formation, so they are more likely to be quartz veins that have been transposed into the foliation. The differences in mobilities of different metals compared to the other deposits likely reflects differences in the compositions of the fluids and the ligands available to transport metals. The precipitation mechanism was the most likely reaction of metal-bearing fluids with oxides and sulfides in the iron formation.

6.5 Sulfide Alteration

The pyrite-millerite-magnetite-chalcopyrite-violarite mineral assemblage in the Cubric showing does not match the pyrrhotite-pentlandite-chalcopyrite ± pyrite assemblage of most komatiite-associated Ni-Cu-(PGE) deposits or the whole-rock chemistry, but has been described in deposits that have undergone oxidation and/or sulfidation (e.g., Green and Naldrett 1981; Nickel et al. 1974; Tenailleau et al. 2006; Barnes et al. 2009). There are many possible reactions that could have produced the observed mineral assemblages, including:

$$Fe_{1-x}S\ (Po) + (1 - 2x)\ H_2S\ (aq) = (1 - x)FeS_2\ (Py) + (1 - 2x)H_2\ (g) \quad [1]$$

$$4\ FeS\ (Po) + 2O_2 = Fe_3O_4\ (Mag) + FeS_2\ (Py) + S_2\ (g) \quad [2]$$

$$FeS\ (Po) + Fe_4Ni_5S_8\ (Pn) + 2O_2 = Fe_3O_4\ (Mag) + 2FeS_2\ (Py) + 5NiS\ (Ml) \quad [3]$$

$$Fe_4Ni_5S_8\ (Pn) + 2.75O_2 + 5.5\ H_2S\ (aq) = 2.25FeNi_2S_4\ (Vl) + 2.25FeS_2\ (Py) + 5.5\ H_2O \quad [4]$$

Reaction 1 produces pyrite by sulfidation of pyrrhotite, but cannot explain the presence of magnetite and millerite at Cubric. Reaction 2 produces equal amounts of pyrite and magnetite by oxidation of pyrrhotite, but pyrite is much more abundant than magnetite at Cubric, and this reaction cannot explain the presence of millerite. Reaction 3 produces magnetite, pyrite, and millerite by oxidation of pyrrhotite and pentlandite at moderate temperatures up to 350°C, which is consistent with the observed mineralogy (Barnes et al. 2009). If the amount of Pn exceeded the amount of Po, Po would be the limiting reagent, and this could explain why there is still Pn, but no Po present at Cubric, but all but the highest-grade komatiite-associated deposits contain

more pyrrhotite than pentlandite (Cowden et al. 1986; Ross and Keays 1979; Lesher and Campbell 1993). Cubric and Marbridge Zones 2, 3, and 4 contained more pyrite than pyrrhotite than at Marbridge Zone 1 (Naldrett and Gasparrini 1971), but phase relationships in the Fe-S system limit the amount of S that can dissolve in sulfide melt (see review by Naldrett 2004). Reaction 4 predicts the conversion of some pentlandite to violarite and pyrite under mild near-surface hydrothermal conditions or in the presence of meteoric water (e.g., Tenailleau et al. 2006; Nickel et al. 1974). Reaction 4 requires an input of S, which is consistent with the trend toward S in **Figure 20**. Since none of these reactions perfectly predict the observed mineralogy, a combination of all four reactions, therefore, seems most likely.

6.6 Geological History and Implications for the Distribution of Ni-Cu-PGE Mineralization and exploration in the La Motte-Vassan Formation and Other Parts of the Abitibi Greenstone Belt

Komatiite-associated Ni-Cu-PGE mineralization normally appears to form when a sulfide-under saturated komatiitic flow or sill (heat and metal source) incorporates S from country rocks (see reviews by Lesher 1989; Lesher and Keays 2002; Lesher 2017; Lesher 2019). If the amount of magma is large relative to the amount of S in the country rocks, the magma may dissolve most or all of the S (Lesher and Burnham, 2001), which may then exsolve during crystallization of olivine in more-or-less cotectic proportions (e.g., Duke 1986; Barnes et al. 2007). If the amount of magma is small relative to the amount of S in the country rocks, then the miscible silicate component will dissolve, but the immiscible sulfide component will form a sulfide xenomelt (Lesher and Campbell 1993; Lesher et al. 2001; Lesher 2017). If the komatiitic flow or sill is not channelized, it will be unable to partially melt the footwall rocks (as in the sheet-flow facies in the Kambalda and Raglan areas: Lesher 1989; Lesher 2007). If the komatiitic flow or sill is channelized but does not access S-rich country rocks, it will also be unmineralized (see discussion by Lesher 2019).

The distribution of komatiitic rocks in the La Motte-Vassan Formation is imperfectly known, but the presence of Type I mineralization at Marbridge; Type IV (mobilized from Type I) in the Cubric iron formation and Type V (mobilized Type I) in the Cubric gabbro; three uncategorized Ni-Cu showings with limited data (La Motte-Leblanc, Caminco-Nickel, and Quebec Molly); and Type II mineralization at Dumont indicates that there is potential for the discovery of additional komatiite-associated Ni-Cu-PGE mineralization in the La Motte-Vassan Formation and other areas of the Abitibi greenstone belt where komatiitic magmas have channelized and encountered S-bearing sedimentary or volcanic rocks.

The sulfides at Cubric are interpreted to have been originally associated with a komatiite and tectonically mobilized into the 2680.1 ± 1.5 Ma gabbro and metamorphic-hydrothermally mobilized into the iron formation. The ultramafic rock at the south end of the outcrop is an orthocumulate komatiite with 27-30% MgO, which is not a good candidate for generating Type I mineralization, which is typically associated with basal mesocumulate-adcumulate komatiites (see discussion by Arndt et al. 2008; Lesher 1989; Lesher and Keays 2002). The komatiites 20m to the north contain similar (~25-30%) MgO values as at the Cubric showing.

The distance of mobilization is not known because no source has been identified. Type V komatiite-associated mineralization in the Rocky's Reward deposit (De Vitry et al. 1998) has been mobilized 2 km from the Perseverance deposit, so it reasonable to consider that the gabbro-hosted mineralization may have been mobilized from the Marbridge district. The S isotope ratios for Cubric gabbro-hosted mineralization are intermediate between Marbridge Zone 1, and magmatic S. S isotopes may fractionate at low-intermediate temperatures (e.g., Ohmoto, 1986), so we cannot distinguish between fractionation during mobilization or derivation from isotopically different sources. Similarly, the S isotopes in the iron formation are much lighter than the gabbro-hosted sulfides, but we cannot distinguish between fractionation during mobilization or derivation from isotopically different sources. A provisional model for the two

stages of mobilization (metamorphic-hydrothermal and metamorphic-tectonic) is shown in **Figure 24**.

7 Conclusions

1) The mineralization at the Cubric showing has been mobilized from a Type I komatiite associated Ni-Cu-PGE deposit into an iron formation and a hornblende gabbro.
2) The mineralization in the iron formation is depleted in Ir > Ru > Rh > Cr and is interpreted to have been transported by metamorphic-hydrothermal fluids. This occurred prior to the emplacement of the 2680.1 ± 1.5 Ma gabbro.
3) The mineralization in the hornblende gabbro is geochemically similar to Kambalda Type I mineralization and is interpreted to have been tectonically mobilized as a single-phase MSS after the emplacement of the 2680.1 ± 1.5 Ma gabbro.
4) The pyrite - millerite - pentlandite - chalcopyrite - violarite mineralogy is attributed to incorporate pyrite-rich sulfides at the magmatic stage and/or oxidation and sulfidation during metamorphism.
5) It is technically possible that both types of mineralization were mobilized from the Marbridge area, but it may also have been mobilized from an unexposed or eroded Type I deposit.

8 Acknowledgments

Funding was provided by the Canada First Research Excellence Fund. We are grateful to Pierre Pilote (Ministère de l'Énergie et des Ressources Naturelles du Québec) and Réal Daigneault (UQAC) for information and discussions about the regional and local geology; to Michael Houlé (GSC) for discussions and additional samples from the Cubric mineralized zone; to Globex Mining Enterprises Inc., Quebec Precious Metals Corporation, and Sphinx Enterprises Ltd. for providing access to the Cubric Ni showing and the Marbridge deposit site, drill core, and company data; to Global UAV Technologies Ltd. for providing the drone magnetic survey; and to Luc Roy, Naomi Welt, Sam Battey, Kevin Kotylak, Michelle (Mouche) Jacques, and Jeremy Rivest (MERC/Metal Earth) for field assistance and discussions. This is Metal Earth publication number MERC-ME-2020-039

9 Figures

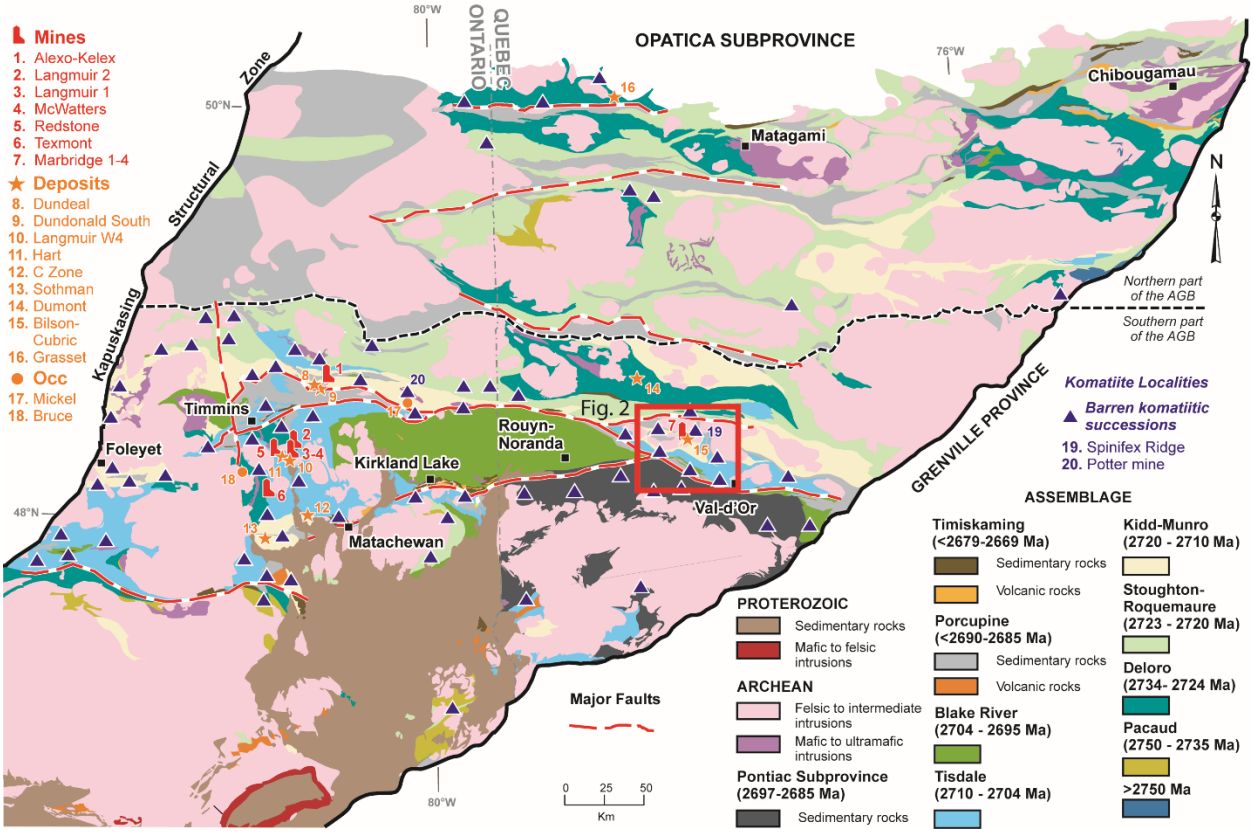

Figure 1 Simplified geological map of the Abitibi greenstone belt (after Houlé et al. 2017) showing the area of Figure 2 (red box) and the locations of the Marbridge deposit (location 7) and the Cubric showing (location 15). Occ = occurrences

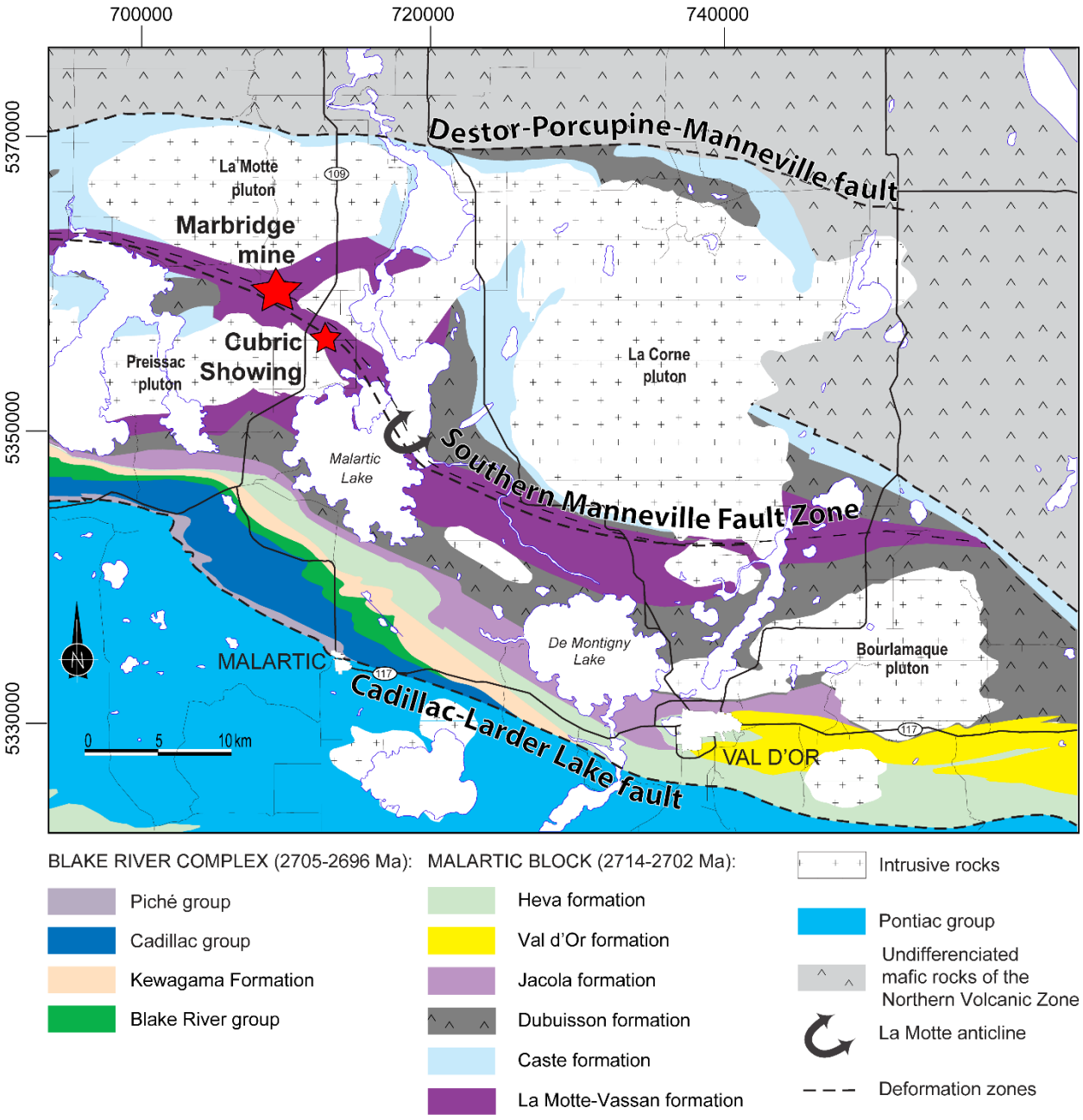

Figure 2 Simplified geological map of the southern middle portion of the Amos-Malartic Transect (modified from Mueller et al., 2008) showing the locations of the Marbridge deposit and Cubric Showing

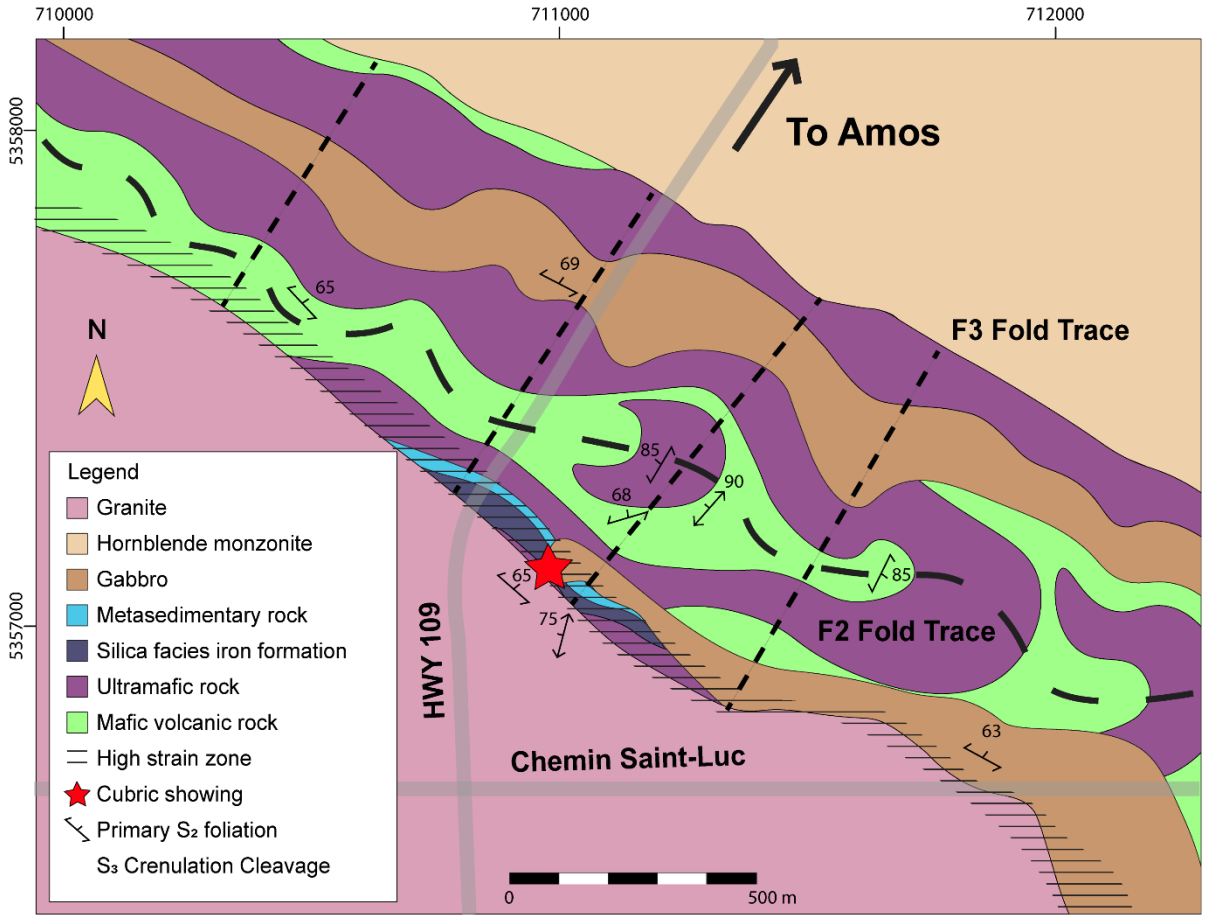

Figure 3 Geological map of the Cubric area, created using a combination of bedrock mapping and airborne magnetics

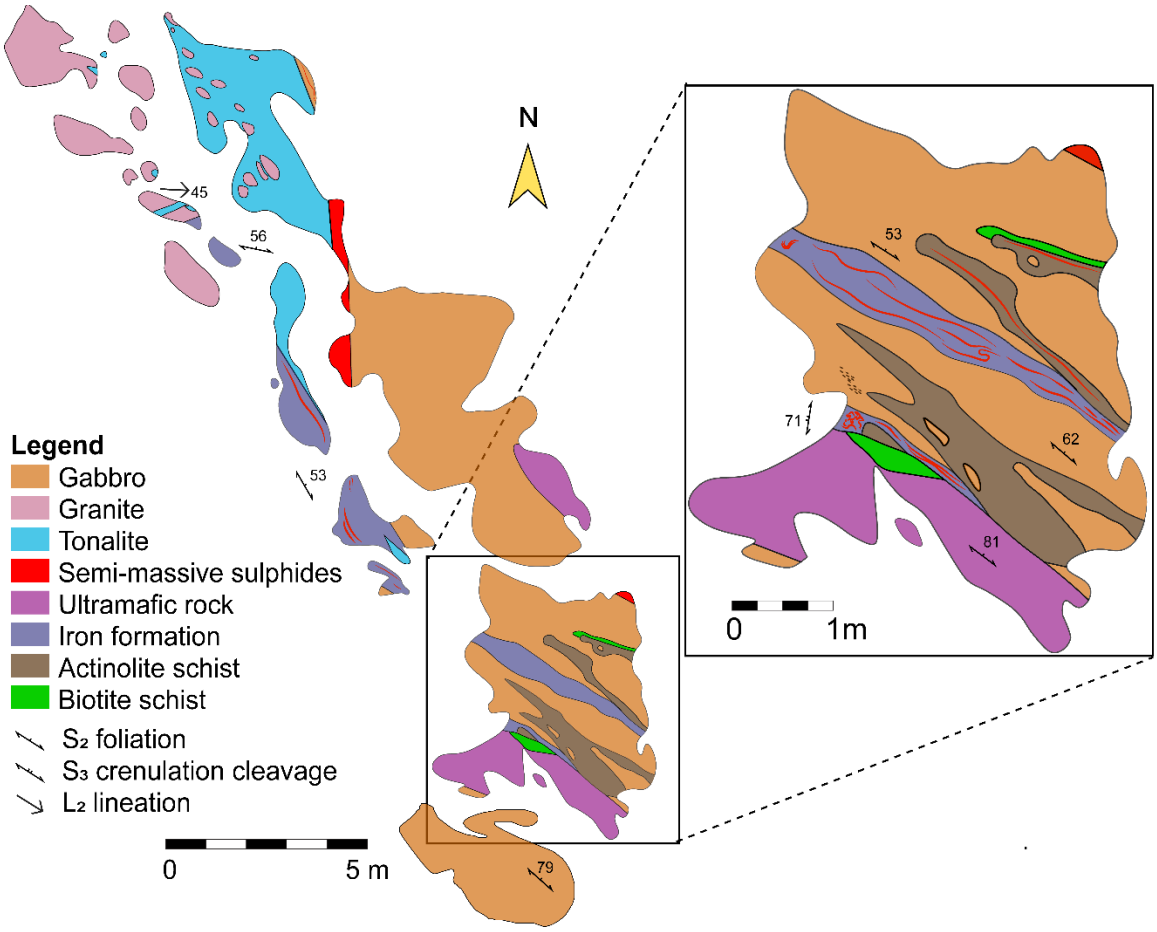

Figure 4 Outcrop-scale map of the Cubric showing, including an enlargement of the southern part of the outcrop

Figure 5 Photographs of sulfide textures as the Cubric showing. A) and B) gabbro-hosted semi-massive Fe-Ni-(Cu) sulfide breccia zone in chlorite-altered gabbro. C) and D) banded Fe-(Cu)-(Ni) mineralization in silicate-magnetite facies iron formation.

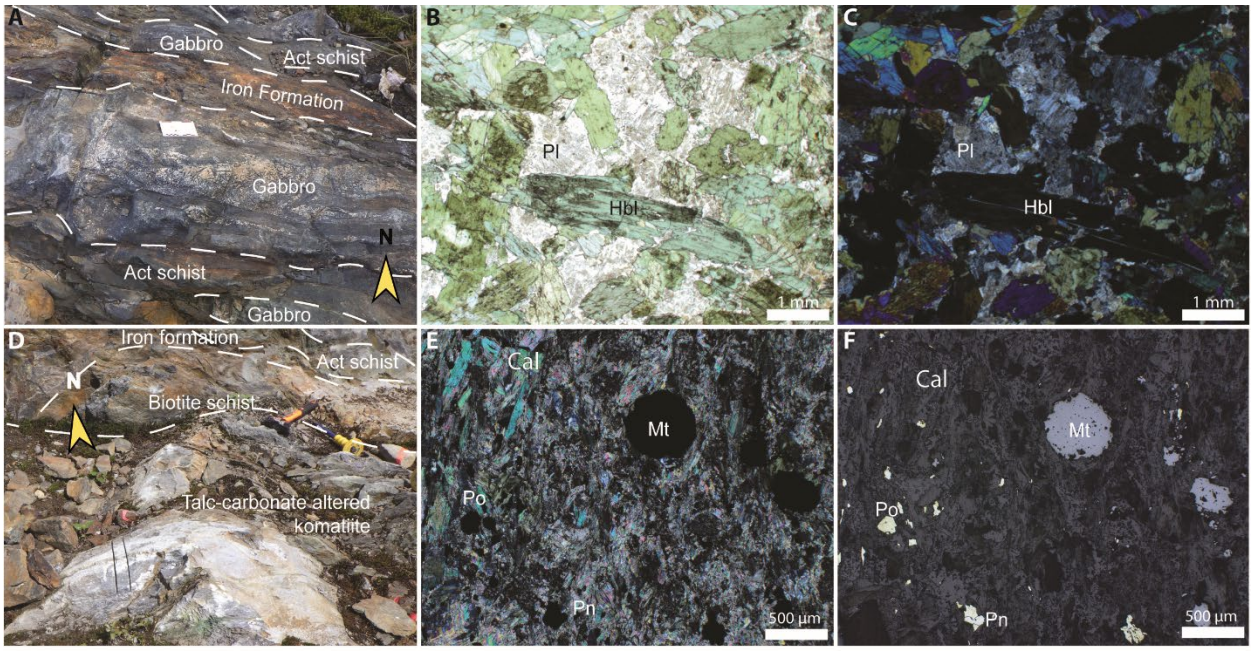

Figure 6 Photographs and photomicrographs of gabbro host and country rocks at the Cubric showing. A) Gabbro containing a pegmatitic pod (center of the photo). B) Gabbro (sample ME-AM19-DES0279AG07B) in plane-polarized light. C) The same area in crossed polarized light. D) Talc-altered ultramafic rock. E) Talc-altered ultramafic rock (sample ME-AM18-DES0279BG01B) in crossed polarized light. F) The same area in reflected light.

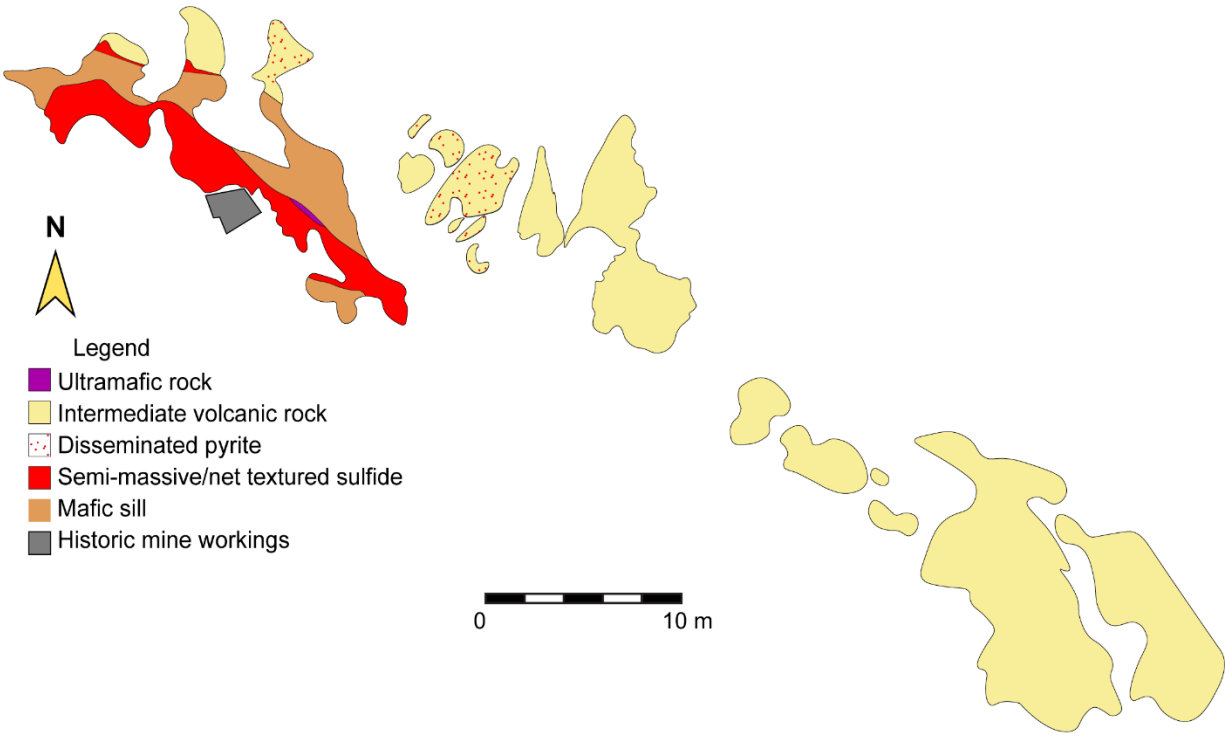

Figure 7 Outcrop-scale map of Marbridge Zone 1 showing mafic sills running parallel to the mineralized zone. Modified from LaFrance (2015) to include the sills and update the lithologies based on new geochemical data

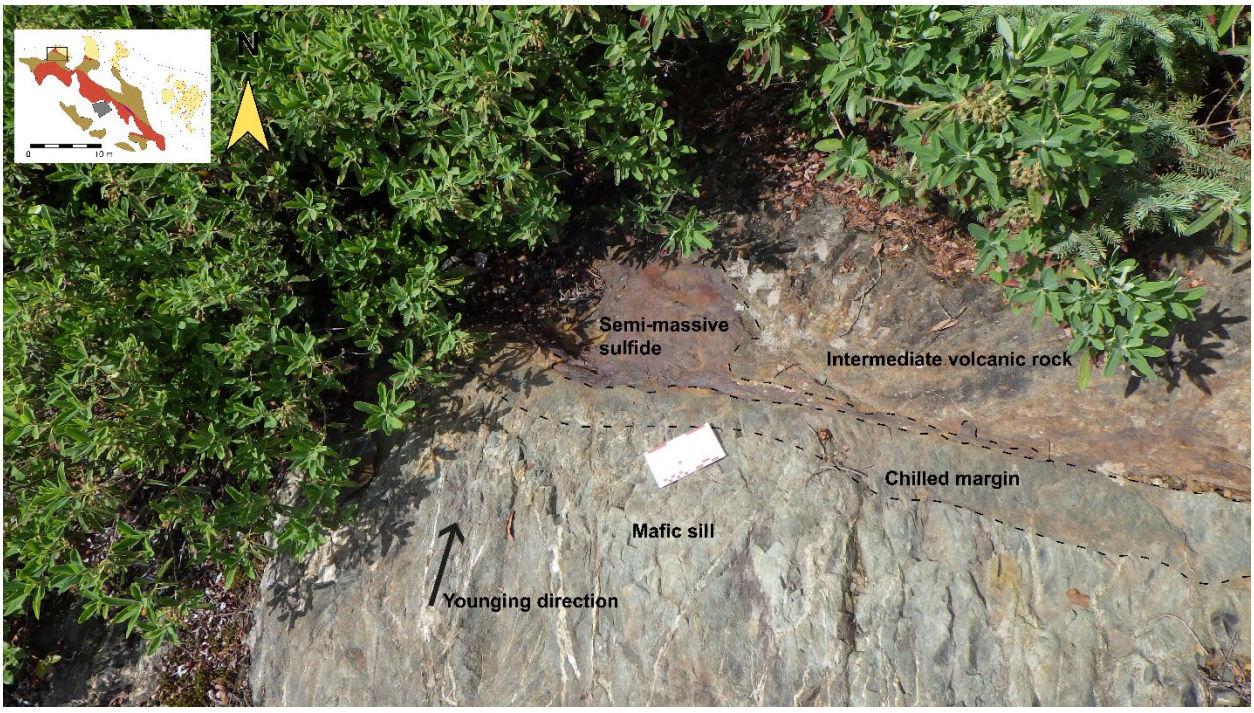

Figure 8 Photo of Marbridge mineralized Zone 1 mineralized zone transgressed by a mafic sill with a thin chilled margin. Scale card is 8.5 cm

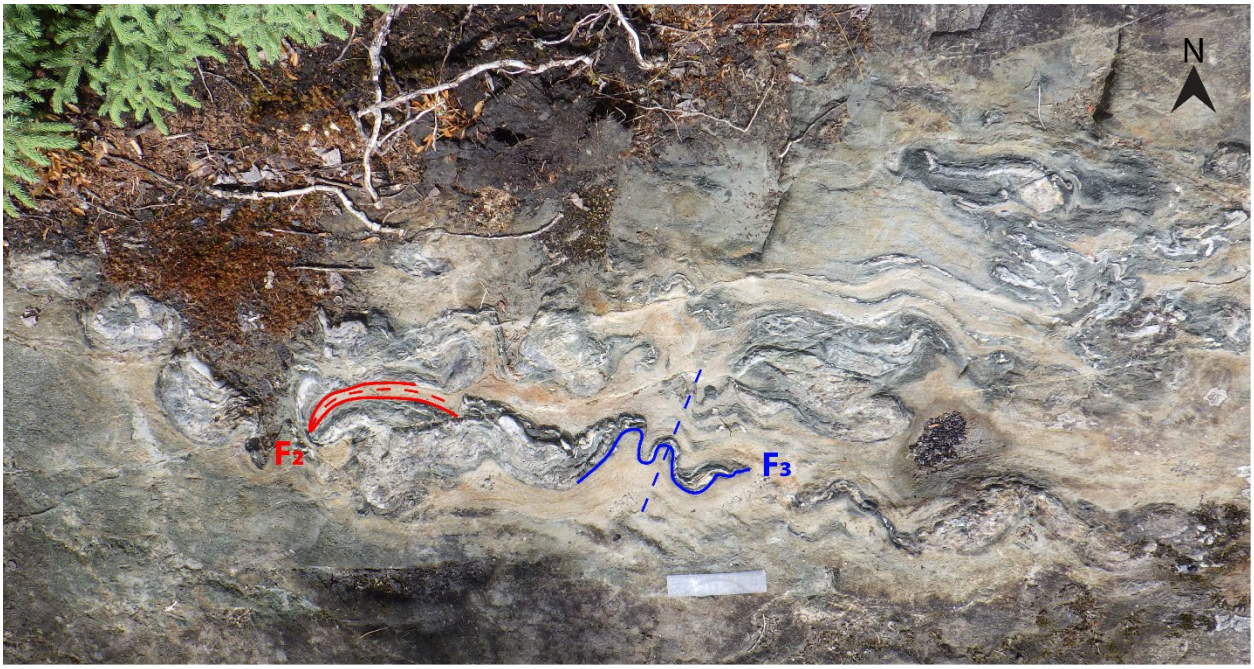

Figure 9 A D_2-D_3 interference fold pattern in the La Motte - Vassan formation near the Cubric showing. Scale card is 15 cm long

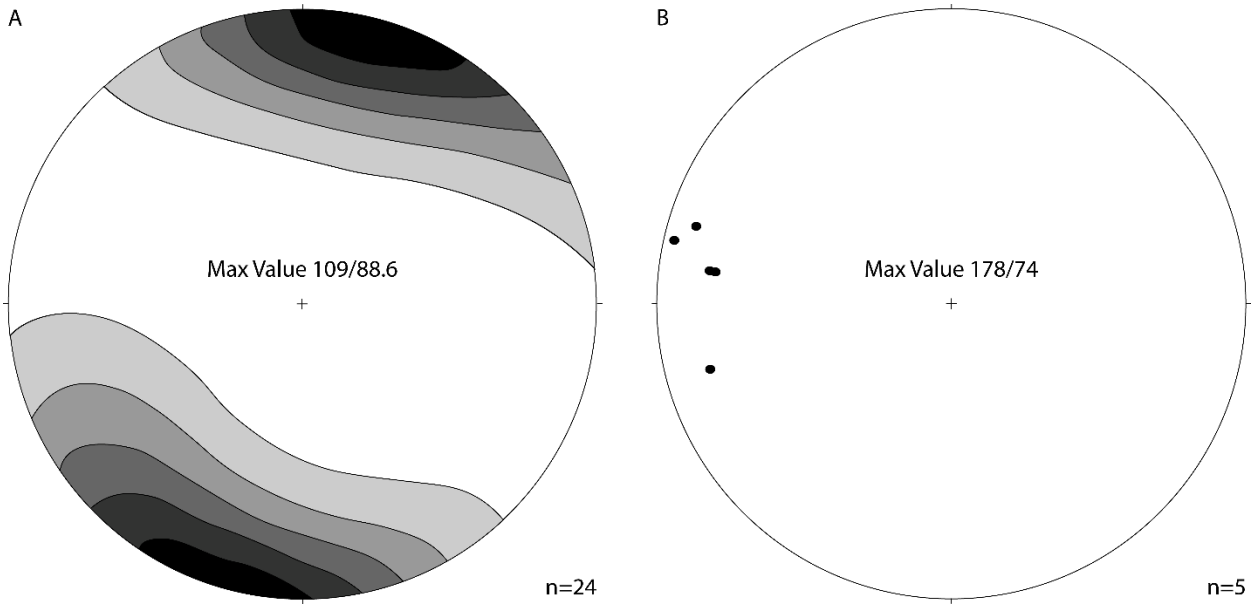

Figure 10 Lower hemisphere (Schmidt projection) stereonets showing the distribution of foliation in the Cubric area. A) Contoured distribution of poles to the S2 foliation; black is high density, and white is low density. B) Poles to the S3 cleavage

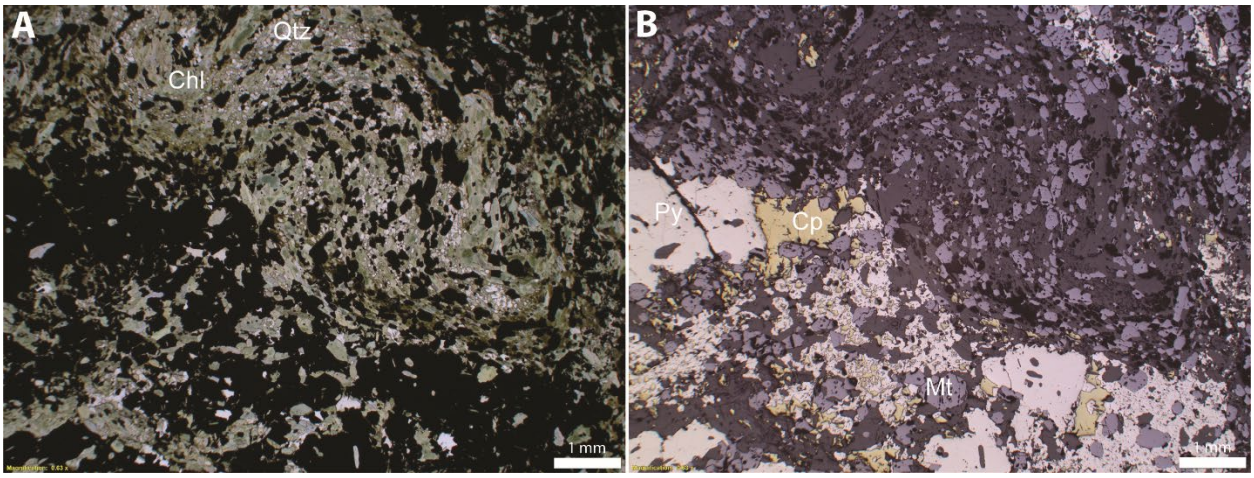

Figure 11 Photomicrographs of deformed iron formation (sample ME-AM-18DES279CG10) in A) plane-polarized transmitted light and B) plane-polarized reflected light, showing folded magnetite-silicate bands and sulfide-rich pyrite-magnetite-chalcopyrite bands. Millerite and pentlandite occur along the margins of pyrite grains. Chalcopyrite occurs along the margins and in the cores of pyrite grains. There are minor chalcopyrite, pyrite, and pentlandite grains in the magnetite-silicate layers.

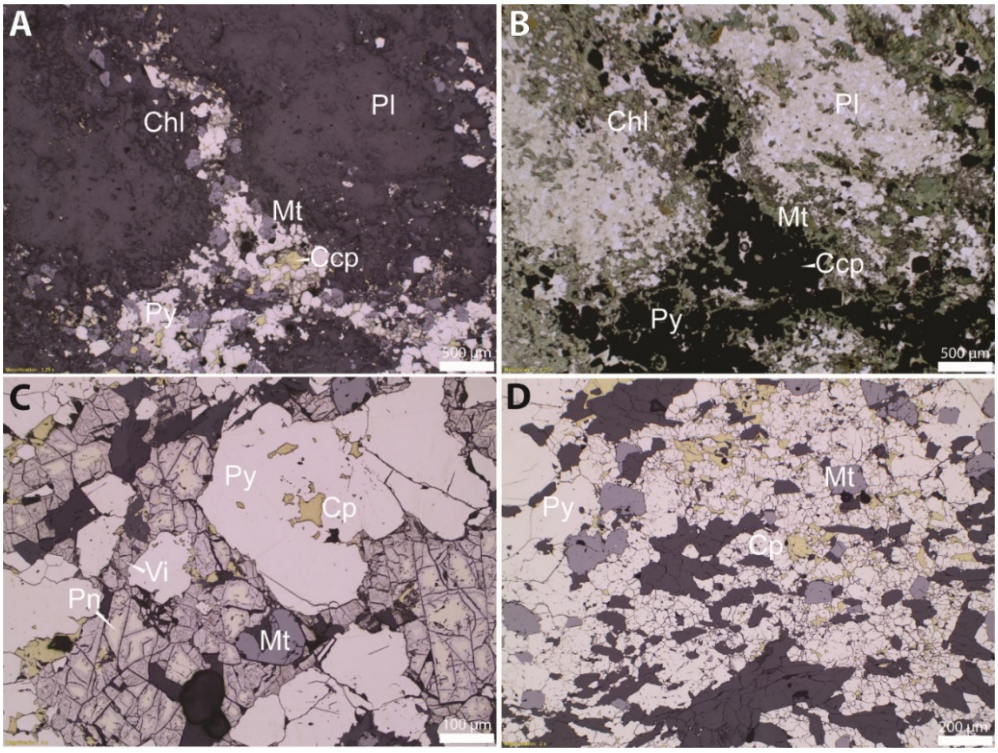

Figure 12 Photomicrographs of the gabbro-hosted semi-massive sulfide breccia zone. Sample ME-AM18-DES0279EG22 in A) reflected light and B) plane-polarized light showing chlorite concentrated around sulfides. Sample ME-AM18-DESEG23. A gabbro in reflected light showing weathering of pentlandite to violarite and chalcopyrite within pyrite. D) gabbro-hosted semi-massive sulfide breccia zone sample ME-AM18-DES279EG04B in reflected light showing sharp boundaries, polygonal shapes, and 120º grain boundaries between chalcopyrite and pyrite.

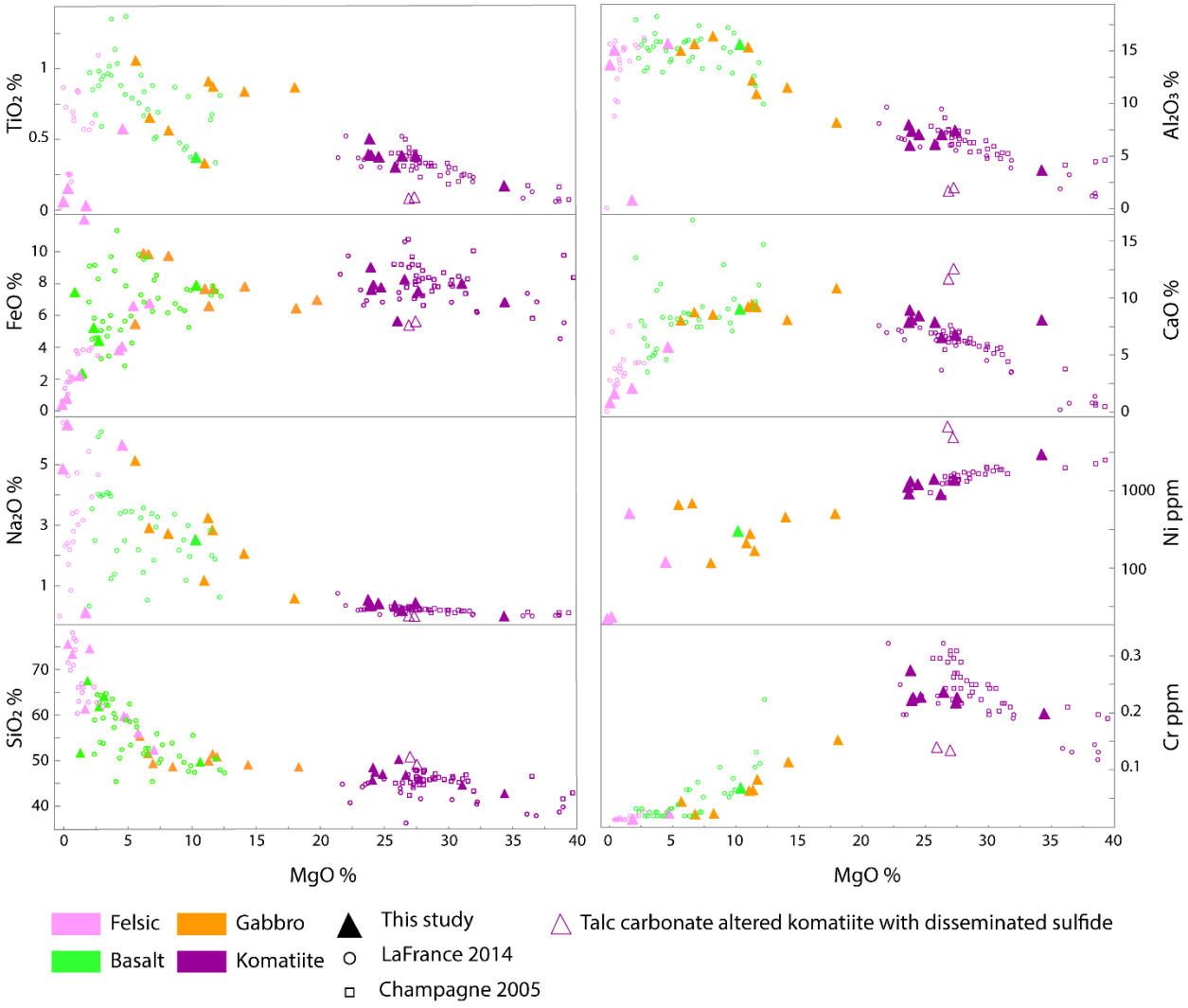

Figure 13 MgO vs. major oxide/element (SiO_2, TiO_2, Al_2O_3, Fe_2O_3, CaO, Na_2O, Cr_2O_3, Ni) plots for all barren lithologies in the La Motte-Vassan formation. All data recalculated volatile free. Data is located in Appendix C.

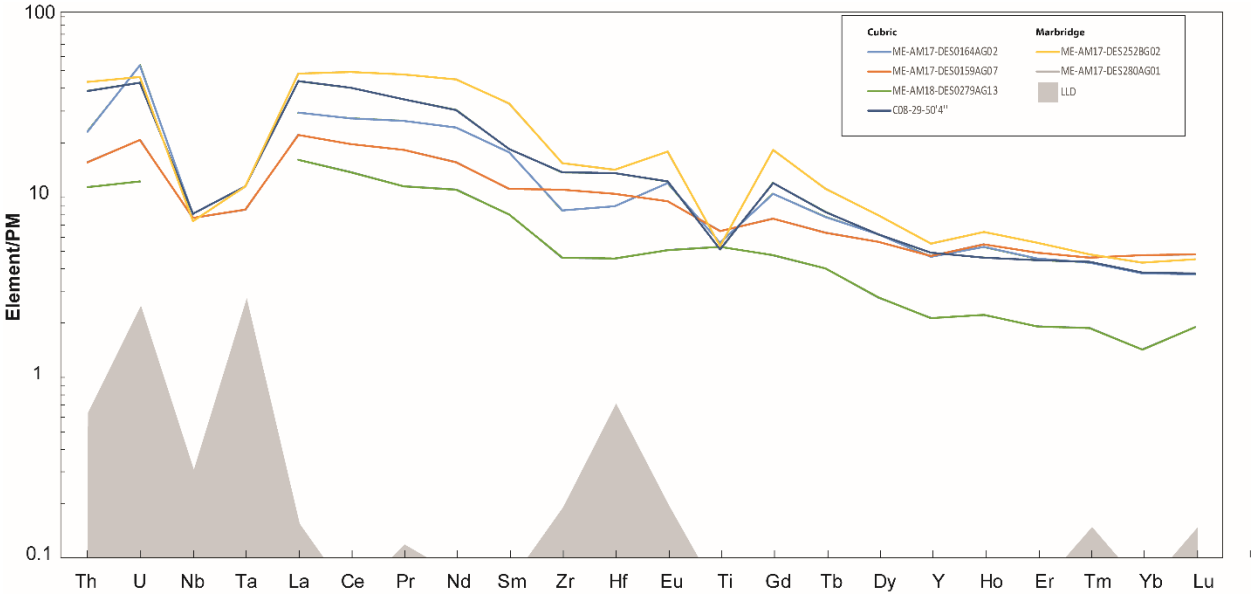

Figure 14 Primitive mantle-normalized (McDonough and Sun, 1995) extended trace element diagram for the unmineralized gabbro in the Cubric outcrop. Lower limits of detection (LLDs) are outlined but apply only to samples analyzed in this study.

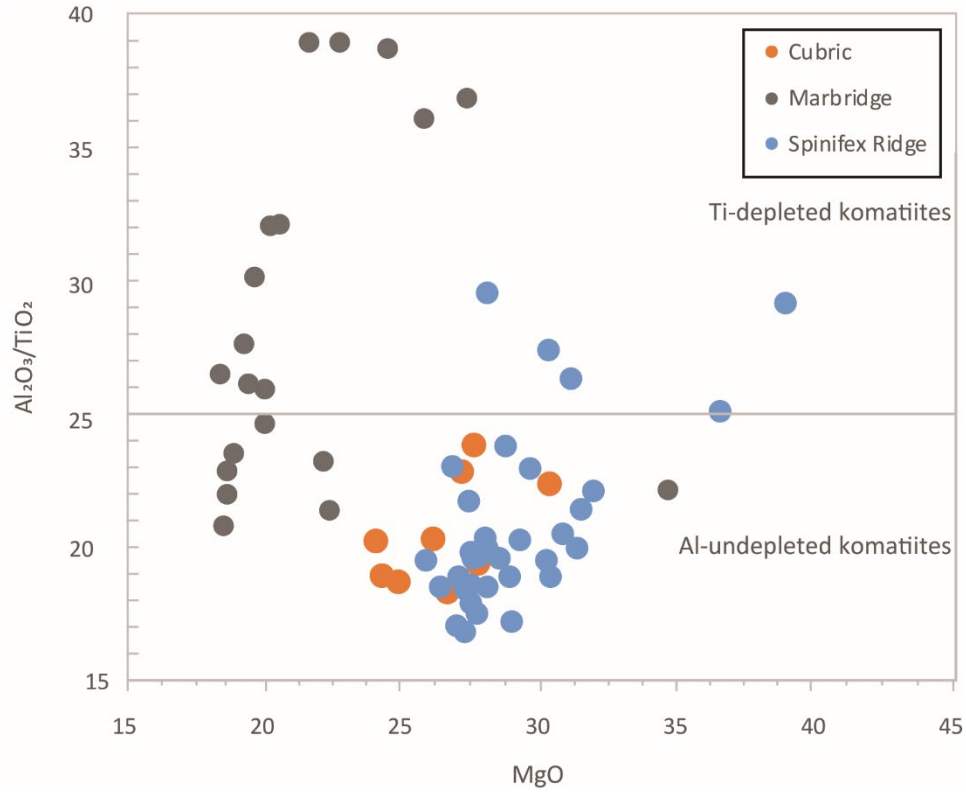

Figure 15 MgO vs. Al_2O_3/TiO_2 plot of komatiite rocks from the La Motte-Vassan formation. The komatiites are Al-undepleted. All data recalculated volatile free to 100%. Spinifex Ridge data from Champagne (2005); Marbridge data from Lafrance (2014); Cubric data from this study.

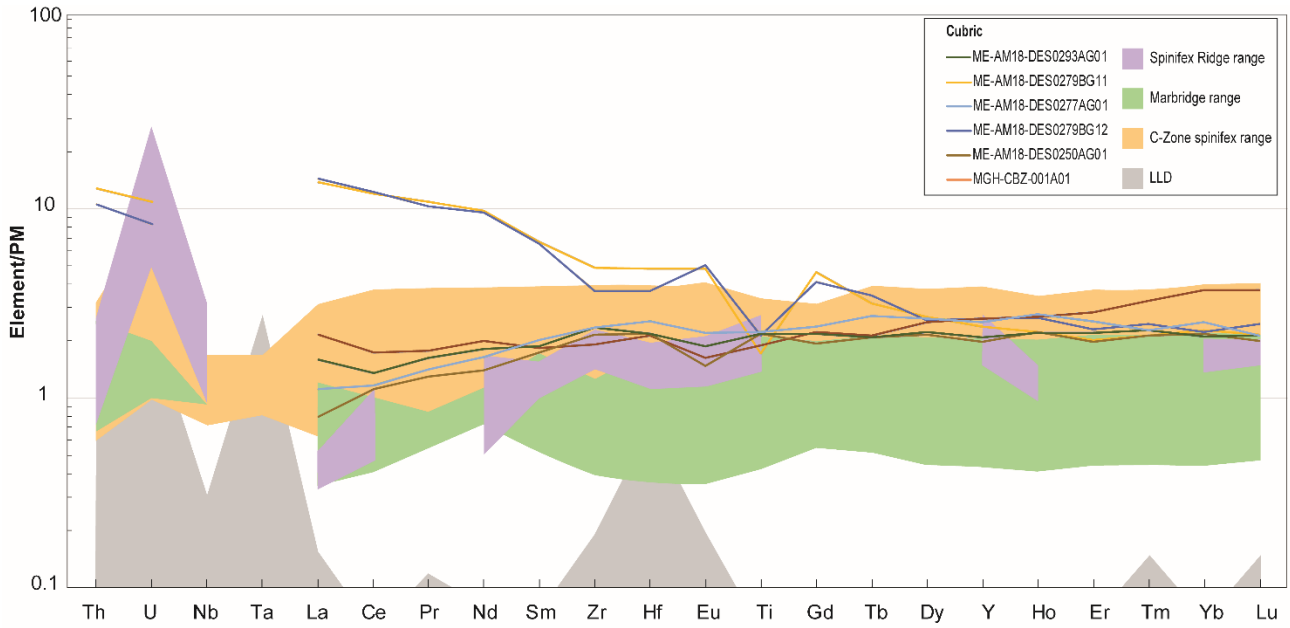

Figure 16 Primitive mantle-normalized (McDonough and Sun, 1995) extended trace element diagram for the komatiite rocks in the La Motte-Vassan formation. Cubric komatiites are talc-carbonate altered and contain trace-1% disseminated sulfide. Ranges for Spinifex Ridge and Marbridge komatiites are plotted for comparison. LLD is outlined but applies only to samples collected for this study.

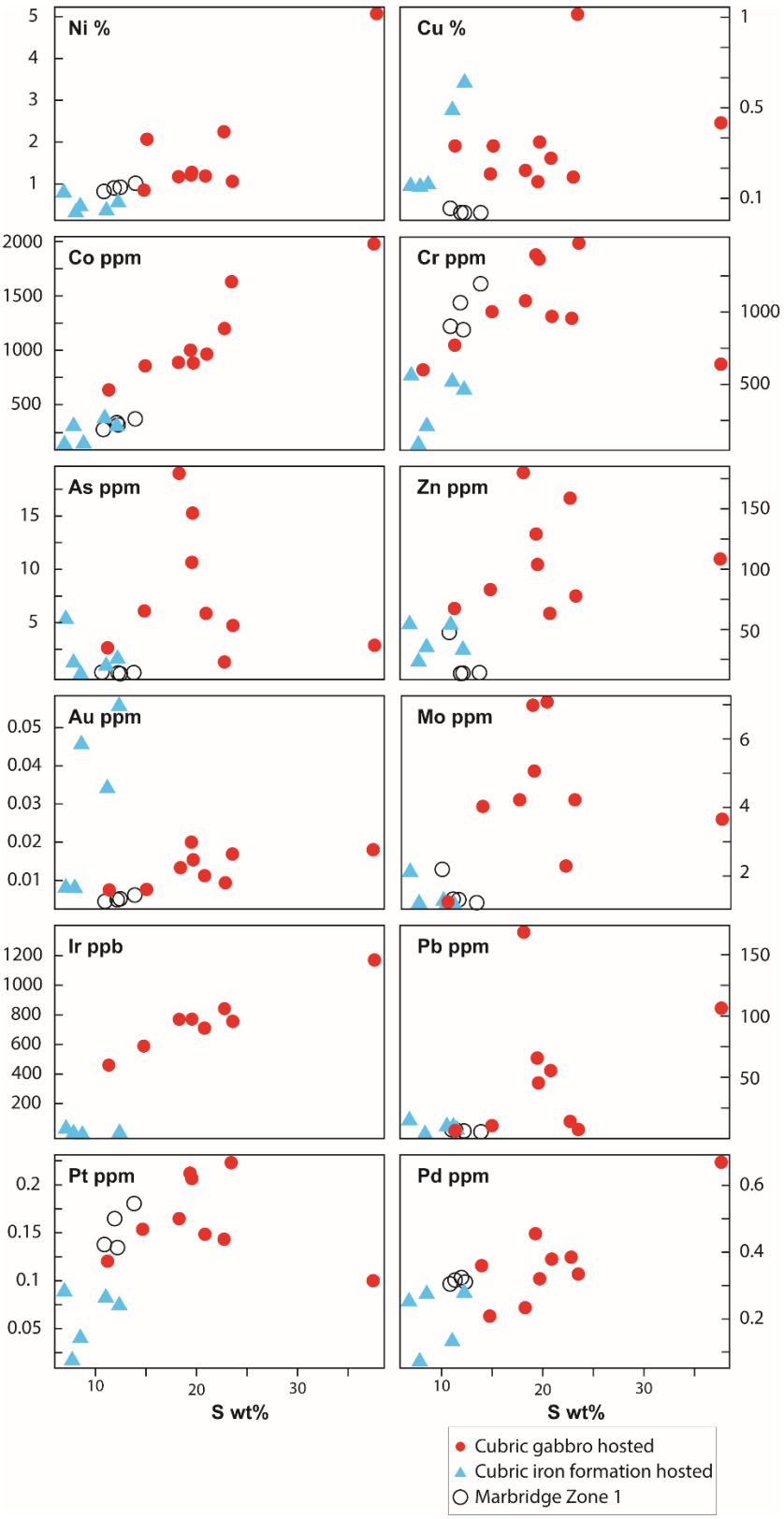

Figure 17 Metals vs. S in the sulfide-bearing rocks (iron formation and brecciated gabbro) at the Cubric showing and Marbridge Zone 1.

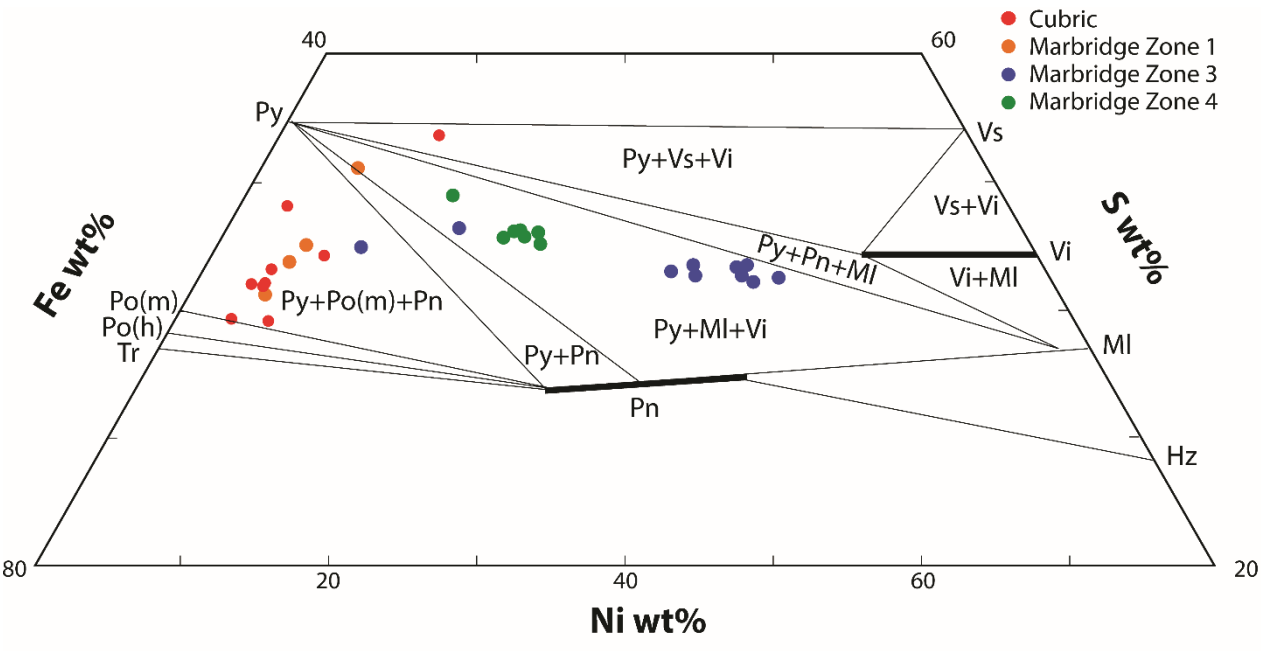

Figure 18 S-Fe-Ni plot showing the compositions of Cubric sulfides and mineral assemblages at 100-135°C (from Naldrett, 2004). Data for Marbridge Zone 3 and 4 from Graterol and Naldrett (1971). Fe corrected for Fe in silicate and magnetite.

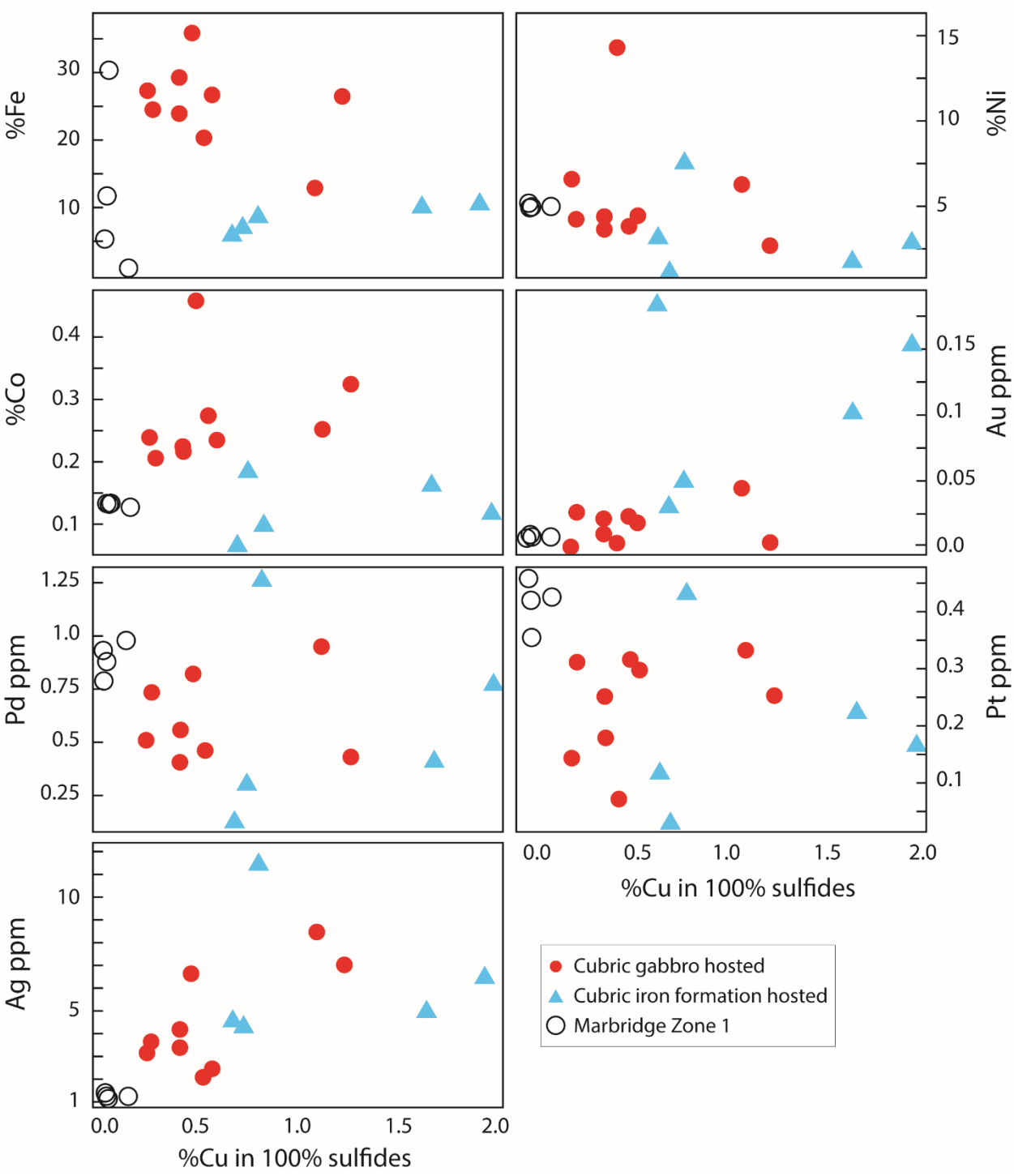

Figure 19 Base and precious metals in 100% sulfides vs. Cu in 100% sulfides in the sulfide-bearing rocks (iron formation and brecciated gabbro) at the Cubric showing and Marbridge Zone 1.

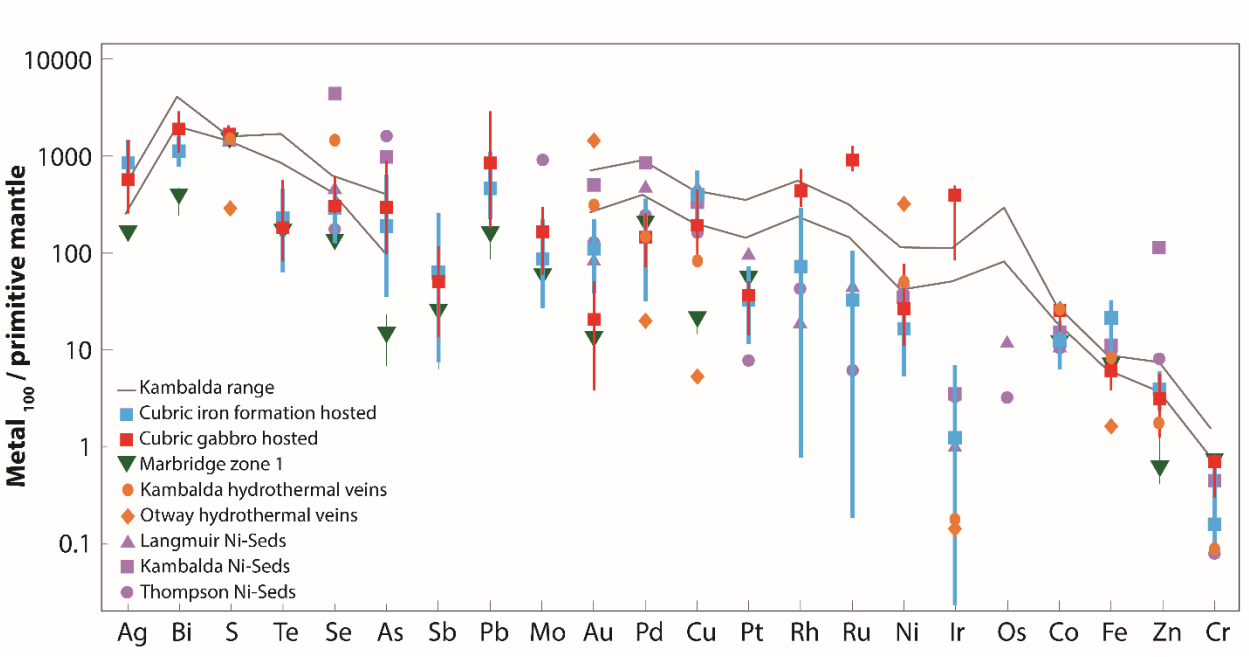

Figure 20 Metals in 100% sulfide normalized to the primitive mantle (McDonald and Sun, 1995) and plotted in increasing order of compatibility from left to right. Kambalda Type I mineralization and Kambalda, Langmuir, and Thompson Type IV mineralization are plotted for comparison (Lesher and Keays, 2002). The sulfides in Cubric iron formation are depleted in Ir, similar to Type IV mineralization. Brecciated sulfides in Cubric gabbro are similar to Type I mineralization but are slightly enriched in lPGE. The average values for each lithology are plotted with the blue and red lines showing the ranges for each element.

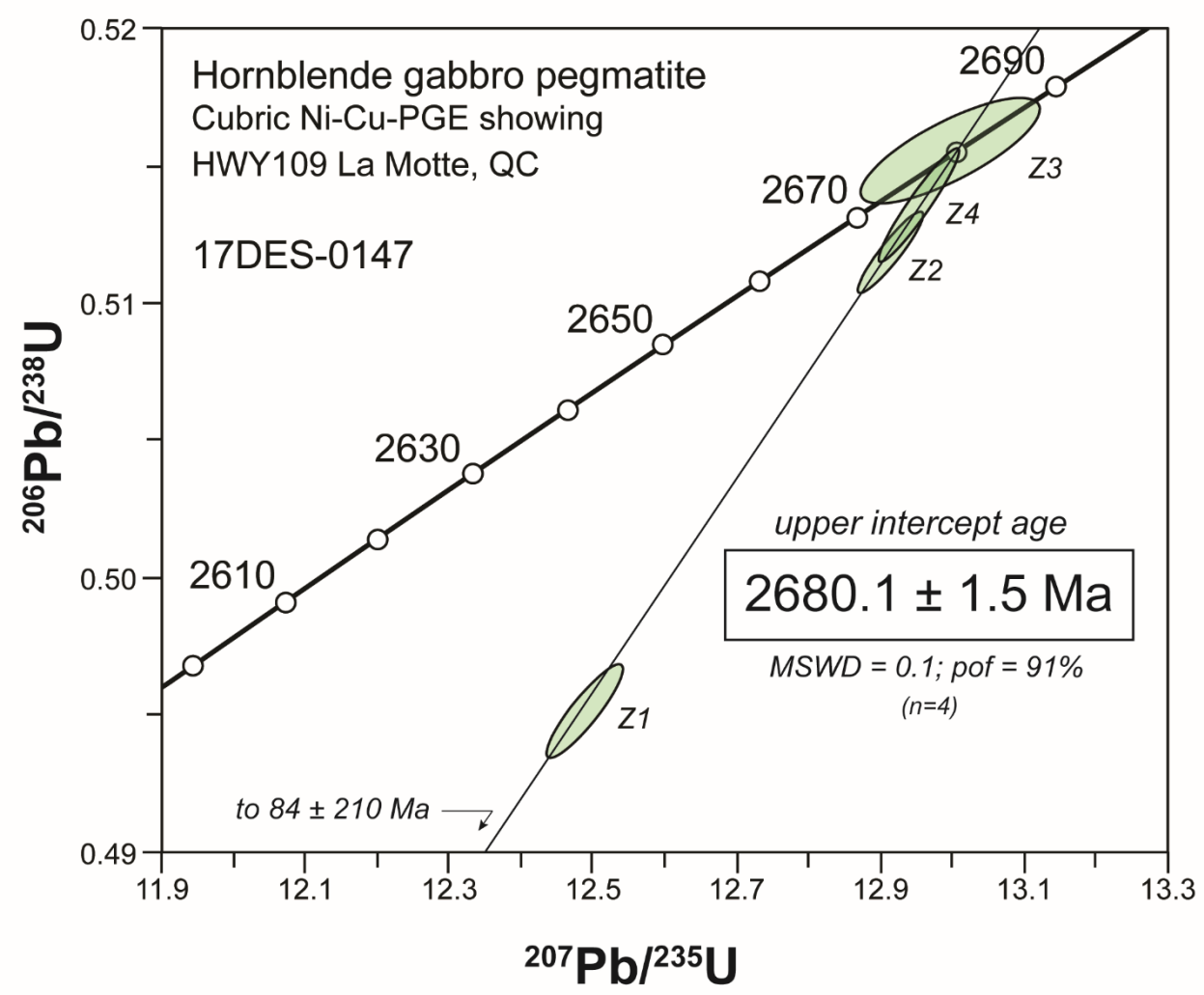

Figure 21 $^{206}Pb/^{238}U$ vs. $^{207}Pb/^{235}U$ Concordia plot showing ID-TIMS analyses of single zircons extracted from gabbro (sample ME-AM17-DES0147AG08) at the Cubric showing. The 2680.1 ± 1.5 Ma age constrains the maximum timing of deformation and mobilization of sulfides.

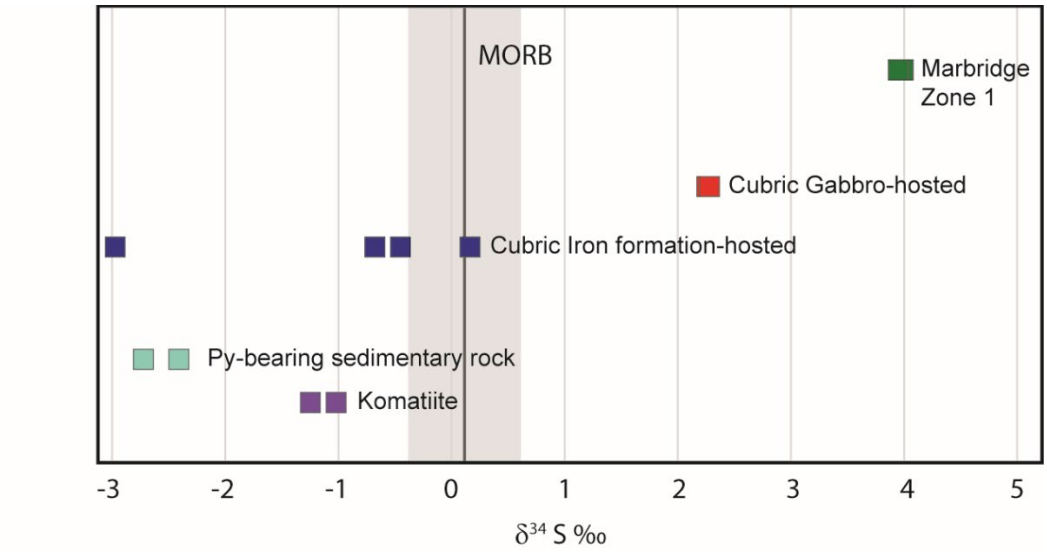

Figure 22 δ^{34}S ‰ data for sulfide-bearing lithologies in the Marbridge and Cubric areas, including 1) isotopically lighter Cubric komatiite, mineralized Cubric facies iron formation, and barren pyrite-bearing argillite; 2) intermediate Cubric gabbro-hosted mineralization; and 3) isotopically heavier Marbridge Zone 1 net-textured mineralization.

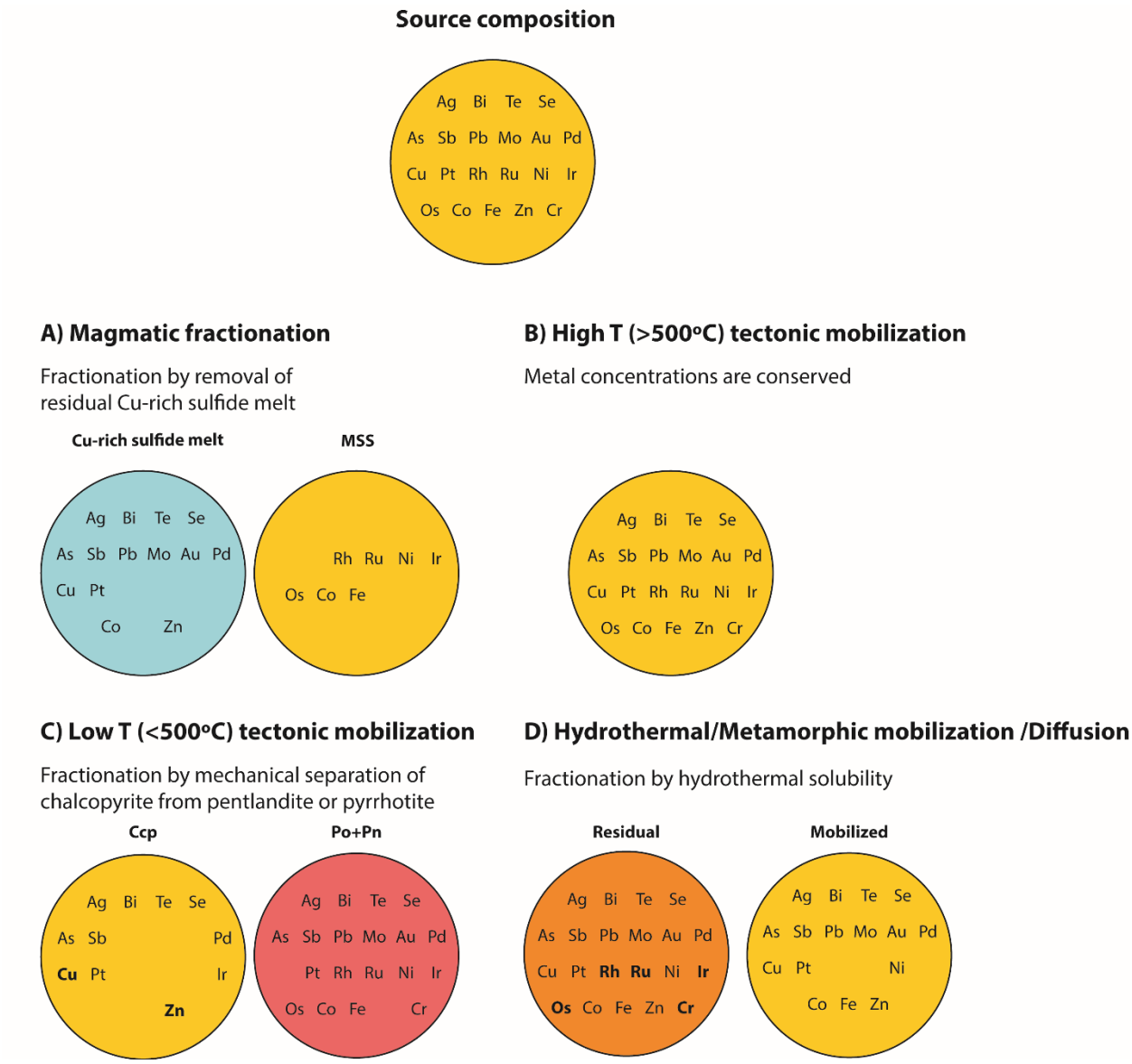

Figure 23 Summary of how metal fractionation/mobilization processes may change sulfide metal proportions. A) Segregation of Cr-Ni-Cu-IPGE-Zn-Mo-Bi-Te-Sb-Co-Fe-As-Se-rich MSS and Ag-Pb-Zn-Au-PPGE-rich residual sulfide liquid. B) Hydrothermal mobilization, leaving a Cr-IPGE-rich residue and, depending on ligands and temperature gradient, producing a precipitate that may be zoned with respect to Fe-Au-Pd-Pt-Zn-Cu. C) Low-T (<500°C) tectonic mobilization resulting in the mechanical separation of more ductile Zn ± Pb-bearing Ccp from less ductile Po-Pn-PGMs. D) High-T (>500°C) tectonic mobilization where most elements are housed in MSS.

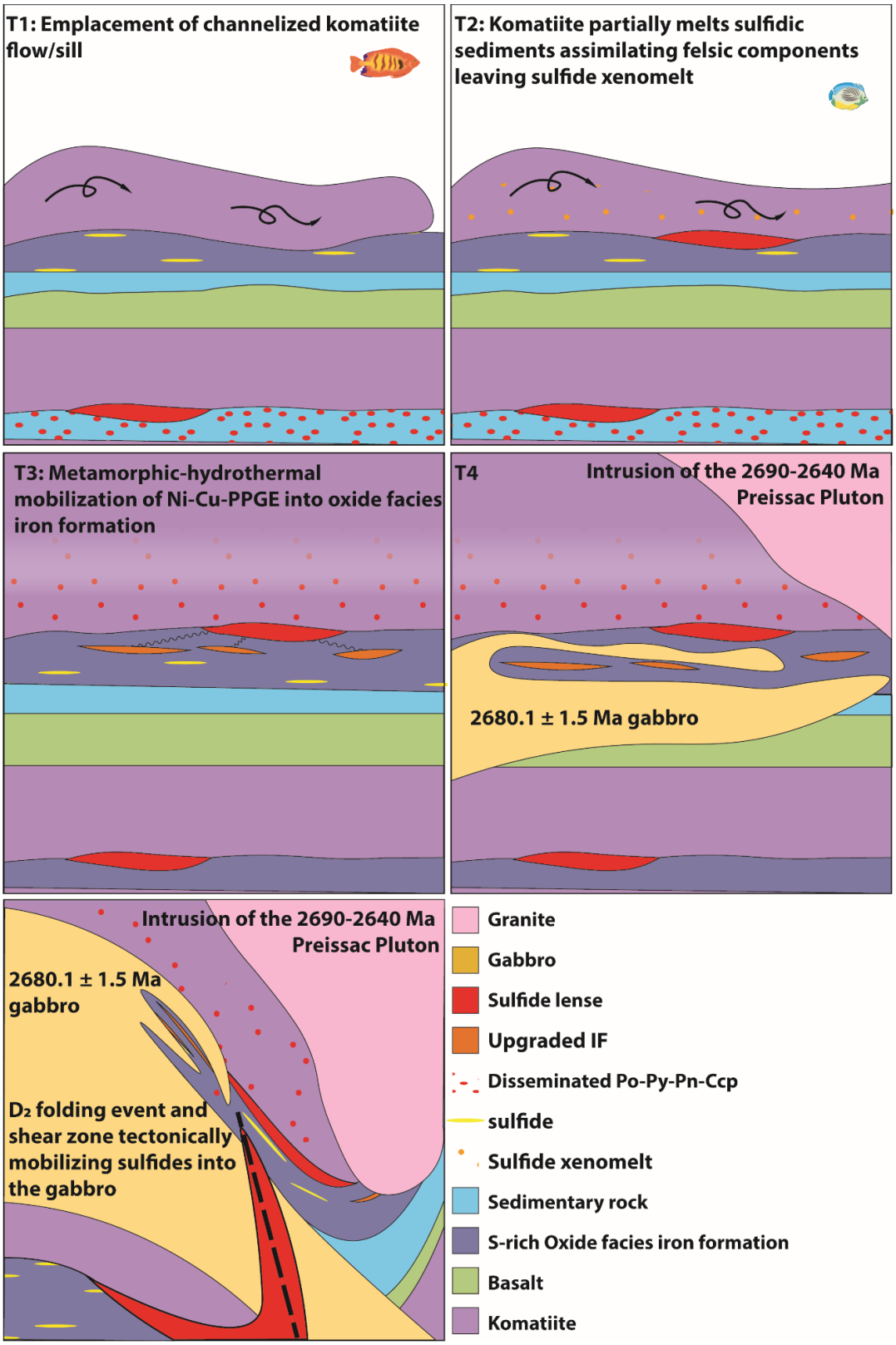

Figure 24 Schematic model for the formation and mobilization of the Ni-(Cu)-(PGE) mineralization at the Cubric showing.

10 References

Arndt N, Lesher CM, Barnes SJ (2008) Komatiite. Cambridge University Press, New York.

Ayer J, Amelin Y, Corfu F, Kamo S, Ketchum J, Kwok K, Trowell N (2002) Evolution of the southern Abitibi greenstone belt based on U-Pb geochronology; autochthonous volcanic construction followed by plutonism, regional deformation, and sedimentation. Precambrian Research 115:63-95. doi: 10.1016/S0301-9268(02)00006-2.

Barnes S-J, Naldrett AJ (1985) The fractionation of the platinum-group elements at the Alexo Komatiite, Abitibi greenstone belt, northern Ontario. The Canadian Mineralogist 23, Part 2:165–183.

Barnes S-J, Lightfoot PC (2005) Formation of magmatic nickel sulfide deposits and processes affecting their copper and platinum group element contents. Society of Economic Geologists, Littleton, CO, United States. One Hundredth Anniversary Volume:143-178

Barnes SJ (2006) Komatiite-hosted nickel sulfide deposits; geology, geochemistry, and genesis. Society of Economic Geologists (US) 13:51-97.

Barnes SJ, Lesher CM, Sproule RA (2007) Geochemistry of komatiites in the Eastern Goldfields Superterrane, Western Australia and the Abitibi greenstone belt, Canada, and implications for the distribution of associated Ni-Cu-PGE deposits. Applied Earth Science 116:167-187. doi: 10.1179/174327507X271996.

Barnes SJ, Lesher CM, Burnham OM, Fiorentini ML (2009) Komatiite magmas and nickel sulfide deposits; a comparison of variably endowed terranes. Geochimica et Cosmochimica Acta 73:755–780.

Barrett FM, Binns RA, Groves DI, Marston RJ, McQueen KG (1977) Structural history and metamorphic modification of Archean volcanic-type nickel deposits, Yilgarn Block, Western Australia. Economic Geology and the Bulletin of the Society of Economic Geologists 72:1195-1223. doi: 10.2113/gsecongeo.72.7.1195.

Barrie CP (1990) Petrogenesis and tectonic evolution of the Kamiskotia and Montcalm gabbroic complexes and adjacent granitoid-greenstone belt terrane, western Abitibi Subprovince, Ontario, Canada. Precambrian Research 50:173-199.

Bleeker W (1990) Genesis and evolution of the Thompson Ni ore body, Manitoba. Geological Association of Canada, Waterloo, ON, Canada, Waterloo Ontario Canada, pp 1-246.

Carignan J, Gariepy C, Machado N, Rive M (1993) Pb isotopic geochemistry of granitoids and gneisses from the late Archean Pontiac and Abitibi subprovinces of Canada. Chemical Geology 106:299-316. doi: 10.1016/0009-2541(93)90033-F.

Champagne C (2004) Physical volcanology and geochemistry of the komatiites of Spinifex Ridge, La Motte-Vassan Formation, Abitibi. Universite du Quebec a Montreal, Montreal Quebec, pp 1-155.

Cowden A, Donaldson MJ, Naldrett AJ, Campbell IH (1986) Platinum-group elements and gold in the komatiite-hosted Fe-Ni-Cu sulfide deposits at Kambalda, Western Australia. Economic Geology 81:1226-1235.

Cox SF (1987) Flow mechanisms in sulphide minerals. Ore Geology Reviews 2:133-171.

Crank J (1979) The Mathematics of Diffusion. Clarendon Press, Bristol, England.

Daigneault R, Mueller WU, Chown EH (2002) Oblique Archean subduction; accretion and exhumation of an oceanic arc during dextral transpression, Southern volcanic zone, Abitibi Subprovince, Canada. Precambrian Research 115:261-290. doi: 10.1016/S0301-9268(02)00012-8.

Daigneault R, Mueller WU, Chown EH (2004) Abitibi greenstone belt plate tectonics; the diachronous history of arc development, accretion and collision. Developments in Precambrian Geology 12:88-103.

Davis DW (2002) U-Pb geochronology of Archean metasedimentary rocks in the Pontiac and Abitibi subprovinces, Quebec, constraints on timing, provenance and regional tectonics. Precambrian Research 115:97-117. doi: 10.1016/S0301-9268(02)00007-4.

De Vitry C, Libby JW, Langworthy PJ (1998) Rocky's Reward nickel deposit. Monograph Series - Australasian Institute of Mining and Metallurgy 22:315-319.

Desrochers J-P, Hubert C (1996) Structural evolution and early accretion of the Archean Malartic composite block, southern Abitibi greenstone belt, Quebec, Canada. Canadian Journal of Earth Sciences = Revue Canadienne des Sciences de la Terre 33:1556-1569. doi: 10.1139/e96-118.

Dillon-Leitch HCH, Watkinson DH, Coats CJA (1986) Distribution of platinum-group elements in the Donaldson West Deposit, Cape Smith Belt, Quebec. Economic Geology and the Bulletin of the Society of Economic Geologists 81:1147-1158. doi: 10.2113/gsecongeo.81.5.1147.

Ducharme Y, Stevenson RK, Machado N (1997) Sm-Nd geochemistry and U-Pb geochronology of the Preissac and Lamotte leucogranites, Abitibi Subprovince. Canadian Journal of Earth Sciences = Revue Canadienne des Sciences de la Terre 34:1059-1071. doi: 10.1139/e17-086.

Duke JM (1986) Petrology and economic geology of the Dumont Sill; an Archean intrusion of komatiitic affinity in northwestern Quebec. Geological Survey of Canada, Ottawa, ON, Canada.

Eckstrand OR (1975) The Dumont serpentinite; a model for control of nickeliferous opaque mineral assemblages by alteration reactions in ultramafic rocks. Economic Geology and the Bulletin of the Society of Economic Geologists 70:183-201. doi: 10.2113/gsecongeo.70.1.183.

Giovenazzo D (2000) Mineralisations Nickeliferes Dans Le Secteur La Motte-Vassan : La Mine Marbridge Geologie de la region de Val d'Or, Sous-province de l'Abitibi -Volcanologie physique et evolution metallogenique. Falconbridge Limited, pp 73-80.

Graterol M, Naldrett AJ (1971) Mineralogy of the Marbridge No. 3 No. 4 nickel-iron sulfide deposits; with some comments on low temperature equilibration in the Fe-Ni-S system. Economic Geology and the Bulletin of the Society of Economic Geologists 66:886-900. doi: 10.2113/gsecongeo.66.6.886.

Green AH, Naldrett AJ (1981) The Langmuir volcanic peridotite-associated nickel deposits: Canadian equivalents of the Western Australian occurrences. Economic Geology and the Bulletin of the Society of Economic Geologists 76:1503-1523.

Gross GA (2009) Iron formation in Canada, genesis and geochemistry Open-File Report - Geological Survey of Canada. Geological Survey of Canada, Calgary, AB, Canada, pp 164.

Houlé M, Lesher C (2011) Komatiite-associated Ni-Cu-(PGE) mineralization in the Abitibi greensone belt, Ontario. Reviews in Economic Geology 17:89-121.

Houlé MG, Lesher CM, Préfontaine S (2017) Physical Volcanology of Komatiites and Ni-Cu-(PGE) Deposits of the Southern Abitibi Greenstone Belt. Economic Geology and the Bulletin of the Society of Economic Geologists 19:103–132.

Jolly WT (1974) Regional metamorphic zonation as an aid in study of Archean terrains; Abitibi region, Ontario. The Canadian Mineralogist 12, Part 7:499-508.

Keays RR, Nickel EH, Groves DI, McGoldrick PJ (1982) Iridium and palladium as discriminants of volcanic-exhalative, hydrothermal, and magmatic nickel sulfide mineralization. Economic Geology and the Bulletin of the Society of Economic Geologists 77:1535-1547. doi: 10.2113/gsecongeo.77.6.1535.

Kelly WC, Clark BR (1975) Sulfide deformation studies; III, Experimental deformation of chalcopyrite to 2,000 bars and 500 degrees C. Economic Geology and the Bulletin of the Society of Economic Geologists 70:431-453. doi: 10.2113/gsecongeo.70.3.431.

LaFrance V (2015) Caractérisation de Lêenvironnement Géologique de la Mine Marbridge, Abitibi, Québec Sciences de la Terre. L'Université du Québec à Chicoutimi, Chicoutimi Quebec, pp 1-147.

Lesher CM, Keays RR (1984) Metamorphically and hydrothermally mobilized Fe-Ni-Cu sulphides at Kambalda, Western Australia. Inst. Min. and Metall., London, United Kingdom.

Lesher CM, Groves DI (1986) Controls on the formation of komatiite-associated nickel-copper sulfide deposits. Society for Geology Applied to Mineral Deposits 4:43-62.

Lesher CM (1989) Komatiite-associated nickel sulfide deposits. Reviews in Economic Geology 4:45-101.

Lesher CM, Campbell IH (1993) Geochemical and fluid dynamic modeling of compositional variations in Archean komatiite-hosted nickel sulfide ores in Western Australia. Economic Geology and the Bulletin of the Society of Economic Geologists 88:804-816. doi: 10.2113/gsecongeo.88.4.804.

Lesher CM, Burnham OM, Keays RR, Barnes SJ, Hulbert L (2001) Trace-element geochemistry and petrogenesis of barren and ore-associated komatiites. Canadian Mineralogist 39:673-696. doi: 10.2113/gscanmin.39.2.673.

Lesher CM, Keays RR (2002) Komatiite-associated Ni-Cu-(PGE) deposits; geology, mineralogy, geochemistry, and genesis. Canadian Institute of Mining and Metallurgy 54:579-617.

Lesher CM (2007) Ni-Cu-(PGE) deposits in the Raglan area, Cape Smith Belt, New Quebec. Geological Association of Canada Mineral Deposits Division 5:351-386.

Lesher CM (2017) Roles of xenomelts, xenoliths, xenocrysts, xenovolatiles, residues, and skarns in the genesis, transport, and localization of magmatic Fe-Ni-Cu-PGE sulfides and chromite. Ore Geology Reviews 90:465-484. doi: 10.1016/j.oregeorev.2017.08.008.

Lesher CM (2019) Up, down, or sideways: Emplacement of magmatic FeNiCuPGE sulfide melts in large igneous provinces. Canadian Journal of Earth Sciences 56:756-773. doi: 10.1139/cjes-2018-0177.

Leuner WR (1959) Preliminary report on the west half of the La Motte Township Abitibi East Electoral district. Open-File Report – Energy et Ressources Naturelles Quebec. Energy et Ressources Naturelles Quebec, Val D'or Quebec, Canada. pp 8.

Marshall B, Gilligan LB (1987) An introduction to remobilization; information from ore-body geometry and experimental considerations. Ore Geology Reviews 2:87-131. doi: 10.1016/0169-1368(87)90025-4.

McQueen KG (1981) The nature and metamorphic history of the Wannaway nickel deposit, Western Australia. Economic Geology and the Bulletin of the Society of Economic Geologists 76:1444-1468.

McQueen KG, Brown MC, Taylor G (1986) Low pressure type metamorphism and tectonic evolution in the southeastern Lachlan fold belt. Abstracts - Geological Society of Australia 15:1-136.

McQueen KG (1987) Deformation and Remobilization in some Western Australian Nickel Ores. Ore Geology Reviews 2:269-286. doi: 10.1016/0169-1368(87)90032-1.

Mukwakwami J, Lesher CM, Lafrance B (2014) Geochemistry of deformed and hydrothermally mobilized magmatic Ni-Cu-PGE ores at the garson mine, Sudbury. Economic Geology and the Bulletin of the Society of Economic Geologists 109:367-386. doi: 10.2113/econgeo.109.2.367.

Naldrett AJ, Gasparrini EL (1971) Archaean nickel sulphide deposits in Canada; their classification, geological setting and genesis with some suggestions as to exploration. Geological Society of Australia 3:201-225.

Naldrett AJ (2004) The genesis of magmatic Ni-Cu sulphide deposits; what we know and what we don't know. Transactions - Institution of Mining and Metallurgy Section B: Applied Earth Science 113:153-154. doi: 10.1179/037174504225005546.

Nickel EH, Ross JR, Thornber MR (1974) The Supergene Alteration of Pyrrhotite-Pentlandite Ore at Kambalda, Western Australia. Economic Geology and the Bulletin of the Society of Economic Geologists 69:93-107. doi: 10.2113/gsecongeo.69.1.93.

Paterson HL, Donaldson MJ, Smith RN, Lenard MF, Gresham JJ, Boyack DJ, Keays RR (1984) Nickeliferous sediments and sediment-associated nickel ores at Kambalda, Western Australia In: Buchanan DL, Jones MJ (eds) Sulphide deposits in mafic and ultramafic rocks. Inst. Min. and Metall., London, United Kingdom, pp 81-94.

Paterson MS (1987) Problems in the extrapolation of laboratory rheological data. Tectonophysics 133:33-43.

Pilote P, Moorhead J, Mueller W, Canada Agd, Canada GAo, Canada Amd, Canada MAo, Québec Apdgedgd, hydrogéologues Aid, canadienne Ug (1998) Développement d'un arc volcanique, le région de Val d'Or, ceinture de l'Abitibi - volcanologie physique et évolution métallogénique: guide d'excursion A2, 14-17 mai 1998. Association géologique du Canada/Association minéralogique du Canada.

Pilote P, Daigneault R, David J, McNicoll V (2015) Revised geology, U-Pb dating and new interpretations of the relationships between the Malartic Louvicourt - Piche - Cadillac Groups and the larder Lake-Cadillac Fault Zone, Abitibi Subprovince, Quebec. 38:1-135.

Puchtel IS, Humayun M, Campbell AJ, Sproule RA, Lesher CM (2004) Platinum group element geochemistry of komatiites from the Alexo and Pyke Hill areas, Ontario, Canada. Geochimica et Cosmochimica Acta 68:1361-1383. doi: 10.1016/j.gca.2003.09.013.

Ripley EM (1986) Application of stable isotopic studies to problems of magmatic sulfide ore genesis with special reference to the Duluth Complex, Minnesota. Society for Geology Applied to Mineral Deposits 4:25-42.

Ross JR, Keays RR (1979) Precious metals in volcanic-type nickel sulfide deposits in Western Australia; I, Relationship with the composition of the ores and their host rocks. The Canadian Mineralogist 17, Part 2:417-435.

Sakai H, Des Marais DJ, Ueda A, Moore JG (1984) Concentrations and isotope ratios of carbon, nitrogen and sulfur in ocean-floor basalts. Geochimica et Cosmochimica Acta 48:2433-2441. doi: 10.1016/0016-7037(84)90295-3.

Sippel RF, Foster MR (1963) Grain boundary and diffusion metasomatism. Journal of Geology 71:251-255.

Sproule RA, Lesher CM, Ayer JA, Thurston PC, Herzberg CT (2002) Spatial and temporal variations in the geochemistry of komatiites and komatiitic basalts in the Abitibi greenstone belt. Precambrian Research 115:153-186. doi: 10.1016/S0301-9268(02)00009-8.

Sproule RA, Lesher CM, Houlé MG, Keays RR, Ayer JA, Thurston PC (2005) Chalcophile element geochemistry and metallogenesis of komatiitic rocks in the Abitibi greenstone belt, Canada. Economic Geology and the Bulletin of the Society of Economic Geologists 100:1169-1190. doi: 10.2113/gsecongeo.100.6.1169.

Taranovic V, Lesher CM, Houlé MG, Bedard JH (2012) Physical volcanology and genesis of komatiite-associated Ni-Cu-(PGE) mineralization in the C zone, Bannockburn Township, Ontario. Economic Geology and the Bulletin of the Society of Economic Geologists 107:835-857. doi: 10.2113/econgeo.107.5.835.

Tenailleau C, Pring A, Etschmann B, Brugger J, Grguric B, Putnis A (2006) Transformation of pentlandite to violarite under mild hydrothermal conditions. American Mineralogist 91:706-709. doi: 10.2138/am.2006.2131.

Thurston PC, Ayer JA, Goutier J, Hamilton MA (2008) Depositional gaps in Abitibi greenstone belt stratigraphy; a key to exploration for syngenetic mineralization. Economic Geology and the Bulletin of the Society of Economic Geologists 103:1097-1134. doi: 10.2113/gsecongeo.103.6.1097.

11 Appendix A Supplementary Data

11.1 Isotope Dilution Thermal Ionization Mass Spectrometry

The description below of the methodology used for dating the Gabbro is from Dr. Mike Hamilton, a geochronologist at the Jack Satterly Lab, University of Toronto.

Rocks were crushed using a jaw crusher and then underwent grinding using a disk mill. Initial separation of heavy minerals was carried out by passing the heavy concentrate over a shaking, riffled water (Wilfley™) table multiple times. Further processing employed density separations with methylene iodide and paramagnetic separations with a Frantz isodynamic separator. Final sample selection was achieved by handpicking in alcohol under a binocular microscope, choosing the freshest, least cracked, core-and inclusion-free grains of zircon.

Analytical methods involved isotope dilution thermal ionization mass spectrometry (ID-TIMS) following chemical abrasion (CA, modified after Mattinson, 2005). Zircon grains that underwent CA treatment were annealed in quartz crucibles at 900°C for 2 days. This removes much, although not all, of the radiation damage induced by decay of U and Th contained in the mineral, rendering least altered zircon more inert to chemical attack. The annealed grains were subsequently leached in approximately 0.10 ml of concentrated hydrofluoric (HF) acid for up to several hours in Teflon vessels at 200°C. Altered parts of the crystals, which contain isotopically disturbed Pb, dissolve more rapidly than annealed, unaltered crystal domains for low to moderate levels of radiation damage. Attack is variable, depending on the uranium concentration of the grains and the consequent degree of radiation damage. Chemical abrasion has the advantage of penetrative removal of alteration domains where Pb-loss has occurred, and generally improves concordance.

Weights of mineral fractions chosen for ID-TIMS analysis were estimated from scaled digital photomicrographs, using the density of zircon. Estimated weights should be accurate to about ±20%. This affects only U and Pb concentrations, not age information, which depends only on 68 isotope ratio measurements. Samples were washed briefly in 7N HNO3 prior to dissolution. A mixed 205Pb-235U isotopic spike was adde9d to the dissolution capsules during sample loading. Zircon grains were dissolved using concentrated HF in Teflon bombs at 200°C for 3-4 days, then dried and re-dissolved in 3N HCl overnight to ensure complete dissolution and equilibration with the spike (Krogh, 1973). U and Pb were isolated using 50 microliter anion exchange columns using HCl elutions, dried down, and then loaded onto outgassed rhenium filaments with silica gel (Gerstenberger and Haase, 1997).

Pb and UO2 were analyzed on a VG354 mass spectrometer using a Daly collector in pulse counting mode. The mass discrimination correction for this detector was constant at 0.07%/AMU. Thermal mass discrimination corrections are 0.10%/AMU for Pb and U. Dead time of the Daly system was 16 ns for Pb during the analytical period, monitored using the SRM982 Pb standard.

Mass spectrometer data was reduced using in-house software (UtilAge program) coded by D. Davis. All common Pb was assigned to procedural blank. Initial Pb from geological sources above 1 picogram was corrected using the Pb evolution model of Stacey and Kramers (1975). Plotting of Concordia curves and averaging of age results were carried out using the Isoplot 3.71 Add-In for MS Excel, of Ludwig (2009). The age calculated is based on a regression using

a modified version of the York (1969) algorithm, in which points are weighted proportional to the inverse of the square of the assigned errors, incorporating error correlations (see Ludwig, 2009); uncertainties in the U decay constants are not considered. Probabilities of fit would be expected to be 50% on average for random data with correctly chosen analytical errors. All age errors and error ellipses are given at the 2 sigma or 95% level of confidence.

11.2 Background lithology descriptions

The granite is coarse- to medium-grained, and composed of quartz (5-60%), plagioclase (30-50%, An), and K-feldspar (0-35%, microcline). Minor amounts of biotite define a weak foliation.

The tonalite is fine- to medium-grained, and composed of quartz (30%), and untwined plagioclase (60%, An) that exhibit 120° annealed grain junctions, and minor (<2-3%) chlorite.

The actinolite schist consists of medium-to coarse-grained acicular actinolite (50-80%, $Ca_{1.9}Fe_{0.4}Mg_{4.3}Si_8O_{22}(OH)_2$), 30-50% fine-grained quartz, and trace magnetite.

The biotite schist is composed of 60% biotite, 20% muscovite, 20% quartz, and trace amounts of zircon. Zircons are prismatic but metamict and are surrounded narrow dark pleochroic halos, presumably attributable to radiation damage. Quartz grains show undulose extinction.

The argillite is composed of 75-80% quartz 20-25% amphibole, up to 5% pyrite, and trace biotite, magnetite, zircon, and garnet. Quartz grains exhibit weak 120° annealed grain junctions.

12 Appendix B Summary of Field Work Publications

12.1 2017 Summary of Field Work

Lithological and structural setting of the Cubric nickel showing, Southern Manneville fault, southern Abitibi Subprovince, Quebec

Danielle Shirriff, Xiaohui Zhou and Bruno Lafrance

Mineral Exploration Research Centre, Harquail School of Earth Sciences, Laurentian University, Sudbury, Ontario, P3E 2C6

INTRODUCTION

The Abitibi greenstone belt is known for its numerous gold and copper-zinc mineral deposits. Less-known nickel mineralization is hosted in supracrustal rocks of the La Motte–Vassan formation of the Malartic group. This includes the past-producing Marbridge deposit, which was mined in the 1960s, and four other nickel showings, including the Cubric, Ataman, Cominco and La Motte–Leblanc nickel showings (Jolin, 2015). The genesis of nickel mineralization at the Cubric nickel showing is poorly understood due to its geological complexity, especially since it is hosted in a high-strain zone along the Southern Manneville fault. In the summer of 2017, a M.Sc. thesis mapping project on the Cubric nickel showing was initiated as part of the Malartic-transect mapping program of a Metal Earth initiative. The goal of this thesis project is to study the stratigraphic and structural setting of nickel mineralization at the Cubric nickel showing to see how it compares with that in the Marbridge mine area.

REGIONAL GEOLOGY

The Cubric–Marbridge area is located in La Motte Township, about 3 km northwest of the village of La Motte, Quebec (Figure 1). The supracrustal rocks of the La Motte–Vassan formation consist predominantly of komatiite, basalt and minor felsic volcaniclastic rocks, which are intruded by gabbroic and granitic dykes. The komatiite shows steam vents and spinifex texture, and the basalt exhibits pillow structures, which suggest extrusion of the lava under water (Champagne, 2004; Lafrance, 2015). The felsic volcaniclastic rocks yielded a $^{207}Pb/^{206}Pb$ zircon age of 2714 ±2 Ma (Pilote et al., 1998). The supracrustal rocks are intruded by three major plutons: the ca. 2642 Ma La Motte pluton, the ca. 2681–2660 Ma Preissac pluton and the ca. 2680–2642 Ma La Corne pluton (Carignan et al. 1991; Ducharme et al. 1997). The La Motte–Vassan formation underwent several deformation events.

METHODS

Regional mapping was done on the La Motte–Vassan formation at 1:5000 scale. Three outcrops were mapped in detail at the 1:50 scale: the Cubric nickel showing, a stripped outcrop along strike of the Marbridge mine horizon and a roadcut outcrop along strike of the Cubric nickel showing. In total, 52 samples were collected for petrographic and whole-rock major- and trace-element geochemical analysis. Two samples were collected for U-Pb zircon geochronology to constrain the absolute timing of mineralization and remobilization of the ore.

ROCK UNITS AT THE CUBRIC NICKEL SHOWING

From south to north, the Cubric nickel showing consists of gabbro, komatiite, banded iron formation with cherty beds, late mafic dykes, mafic to intermediate metavolcanic rocks and granite. The gabbro typically displays fine-grained chilled margins and pegmatite centres. At the northern end of the outcrop, the gabbro contains xenoliths of metavolcanic clasts. It consists of 30–50% plagioclase, and 50–70% hornblende and pyroxene. The komatiite is talc altered and magnetic (~50 × 10^{-3} siemens per metre [S/m]). The banded iron formation consists of alternating magnetite and chert beds 0.5–1 cm thick with saccharoid texture. In contrast to the komatiite, it is extremely magnetic (2000 × 10^{-3} S/m). The late mafic dykes have a distinct dark green weathering colour and consist of black, medium-grained acicular amphibole. The mafic to intermediate metavolcanic rocks are fine grained and grey to brown on fresh surfaces. A late granite crosscuts the banded iron formation and metavolcanic rocks (Figure 2a).

MINERALIZATION

Mineralization is present in the banded iron formation and along its contact with the gabbro (Figure 2b). It consists of pyrite, chalcopyrite and pentlandite. In the banded iron formation, the sulphides occur as layers parallel to isoclinally folded bedding planes. Sulphides occur as disseminations in the late mafic dykes, and as anastomosing stringer sulphide veins at the contact between the banded iron formation and gabbro. A massive sulphide pod, roughly 10–20 cm in diameter, is present within the gabbro, which otherwise is unmineralized except along its contact with the banded iron formation.

In 2007, Exploration Bull's Eye and Services Géologiques T-Rex Inc. completed a drilling program consisting of ten holes on the Cubric nickel showing and the surrounding area. Assays from the core and surface samples returned values of up to 5.33 wt. % Ni, 1.47 wt. % Cu, 1.5 ppm platinum-group elements, 33 ppb Au and 4 ppb Ag (Stoch 2000; Théberge, 2008).

STRUCTURAL GEOLOGY AND DEFORMATION HISTORY

Four generations of structures are present at the Cubric nickel showing. Early D_1 structures are represented by foliated fragments of metavolcanic rocks within the gabbro (Figure 3a). Later D_2 structures are represented by isoclinal upright folds plunging moderately (~35º) to the north. The folds have an axial planar cleavage striking northwest and dipping moderately (~50–70º) to the northeast (Figure 3b). The cleavage affects all rock types and is the most pronounced and penetrative structure observed on outcrops. Late upright, northeast-plunging S-folds, with a northwest-striking steeply-dipping crenulation cleavage, overprint the penetrative cleavage, which is displaced in a dextral sense along the crenulation cleavage (Figure 3c). Some S-C fabrics, indicative of dextral shearing, are observed on outcrops but their relationship to the S-folds and the crenulation cleavage is not known (Figure 3d).

DISCUSSION AND CONCLUSION

Early mineralization at the Cubric nickel showing is expressed as a large pod or clast within the gabbro intrusion, which suggests that it predates the emplacement of the gabbro. The mineralization was then remobilized during deformation, as it occurs as deformed stringers along the sheared contact between the banded iron formation and gabbro. Thus, the mineralization was likely initially associated with komatiite at its contact with the banded iron formation, then dissected and displaced during the emplacement of the gabbro, and later remobilized during deformation of the gabbro and its host metavolcanic rocks. Future exploration and drilling programs should therefore focus on the northern contact of the gabbro, and along the contact between the gabbro and sheared banded iron formation.

FUTURE WORK

Petrographic and lithogeochemical analysis, and U-Pb dating will be done on selected samples to characterize the tectonic setting of the rocks hosting nickel mineralization, and to determine the timing

and style of sulphide remobilization. Fieldwork will be done next summer on the other three nickel showings: Ataman, Cominco and La Motte–Leblanc. Comparisons between all four nickel showings will be made to better understand the genesis of nickel mineralization and remobilization in the La Motte–Vassan formation within the Southern Manneville fault.

ACKNOWLEDGMENTS

The authors would like to thank Globex Mining Enterprises Inc. and Sphinx Resources Ltd. for allowing them access to both the Cubric nickel showing and Marbridge mine, and for sharing their data. The authors would also like to thank Pierre Pilote and Réal Daigneault for suggesting this project.

Harquail School of Earth Sciences, Mineral Exploration Research Centre contribution MERC-ME2017-008.

REFERENCES

Arndt, N.T. 1994. Archean komatiites; Archean Crustal Evolution, v. 11, p. 11–44.

Champagne, C. 2004. Volcanologie physique et géochimie des komatiites de Spinifex Ridge, formation de La Motte–Vassan, Abitibi; M.Sc. thesis, Department of Earth Sciences, Université du Québec à Chicoutimi.

Carignan, J., Gariépy, C., Machado, N. and Rive, M. 1991. Pb isotopic geochemistry of granitoids and gneisses from the late Archean Pontiac and Abitibi Subprovinces of Canada; Chemical Geology, v. 106, no. 4, p. 299–315.

Ducharme, Y., Stevenson, R.K. and Machado, N. 1997. Sm–Nd geochemistry and U–Pb geochronology of the Preissac and Lamotte leucogranites, Abitibi Subprovince; Canadian Journal of Earth Sciences, v. 34, no. 8, p. 1059–1071.

Imreh, L. 1984. Sillon de La Motte–Vassan et son avant-pays méridional: synthèse volcanologique lithostratigraphique et gîtologique; Ministère de l'Énergie et des Ressources, Québec.

Jolin, D. 2015. Globex Mineral and Royalty Properties LaMotte Township. La Motte (Quebec); Globex Mining Enterprises Inc., Rouyn-Noranda, Quebec.

Lafrance, V. 2015. Caractérisation de l'environnement géologique de la mine Marbridge, Abitibi, Québec; M.Sc. thesis, Department of Earth Sciences, Université du Québec à Chicoutimi.

Mueller, W.U., Daigneault, R., Gaboury, D. and Pearson, V. 2008. Field Trip A9 20-25th May 2008, s.l. GAC/MAC-Quebec.

Pilote, P. Moorhead, J. and Mueller, W. 1998. Développement d'un arc volcanique, la région de Val-d'Or: ceinture de l'Abitibi -Volcanologie physique et évolution métallogénique; Association géologique du Canada–Association minéralogique du Canada, Réunion annuelle, Québec 1998, Guide d'excursion A2.

Stoch, J. 2000. Globex finds platinum-palladium-rhodium-cobalt values on La Motte township Nickle Property Quebec., Rouyn-Noranda; Globex Mining Enterprises Inc., press release.

Théberge, J., 2008. Project La Motte Rapport : Travaux 2007-2008, Rouyn-Noranda: Ressources naturelles et Faune, Quebec.

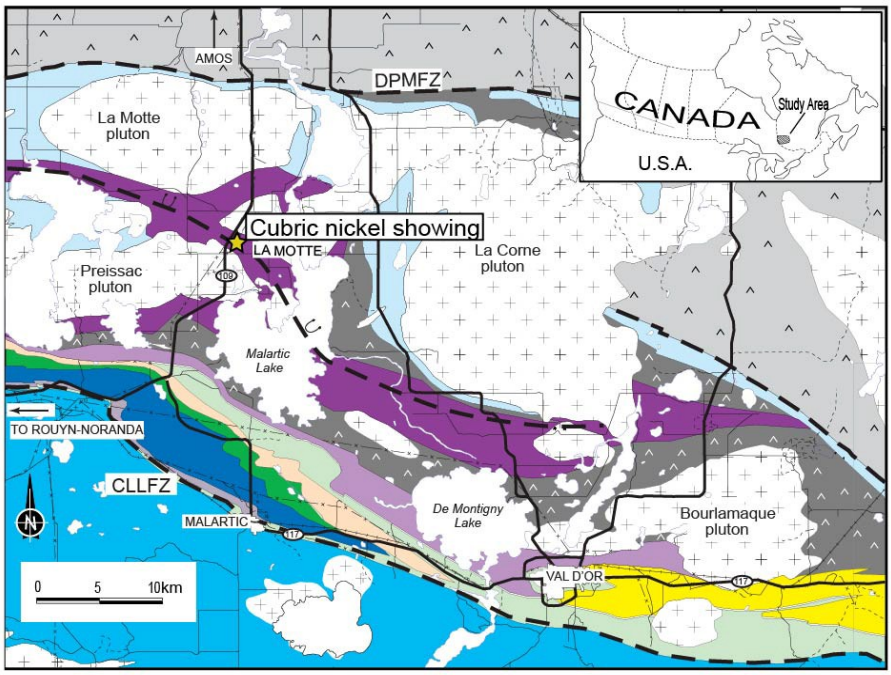

Intrusive rocks
Undifferenciated mafic volcanic rocks of the NVZ
Pontiac group: turbidites

BLAKE RIVER CALDERA COMPLEX (2705-2696 Ma):

Piche group: greywacke, conglomerate, minor volcaniclastic rocks; ultramafic slivers
Cadillac group:greywacke, argillite, conglomerate
Kewagama Formation: greywacke, conglomerate, minor volcaniclastic rocks
Blake river group: mafic and felsic flows, minor volcaniclastic rocks
La motte anticline
Deformation zones
Cadillac-Larder Lake Fault Zone (CLLFZ)
Destor-Porcupine-Manneville Fault Zone (DPMFZ)

MALARTIC BLOCK (2714-2702 Ma):

Heva formation: basalt flows and breccias, minor volcaniclastic rocks
Val d'Or formation: andesitic volcaniclastic rocks, basalt flows and breccias
Jacola formation: basalt flows and breccias, minor komatiites
Dubuisson formation: basalts, minor komatiites
Caste formation: turbidites
La Motte-Vassan formation: komatiites, minor basalts, volcaniclastic rocks

Figure 1. Simplified geology of the Malartic-transect area, southern Abitibi Subprovince; the location of the Cubric outcrop is indicated (modified from Mueller et al., 2008).

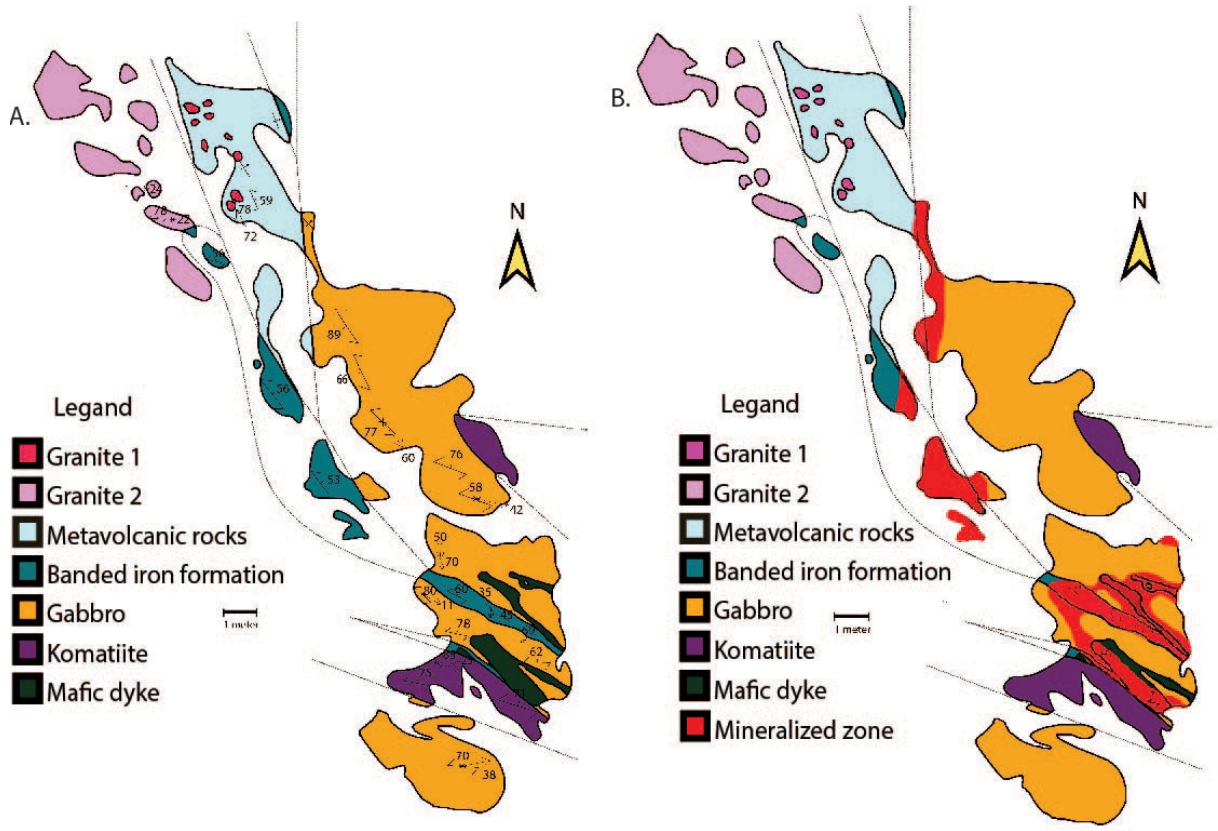

Figure 2. Outcrop map of the Cubric nickel showing, southern Abitibi Subprovince: **a)** rock types and their structural measurements from the outcrop; **b)** distribution of the ore body through the outcrop.

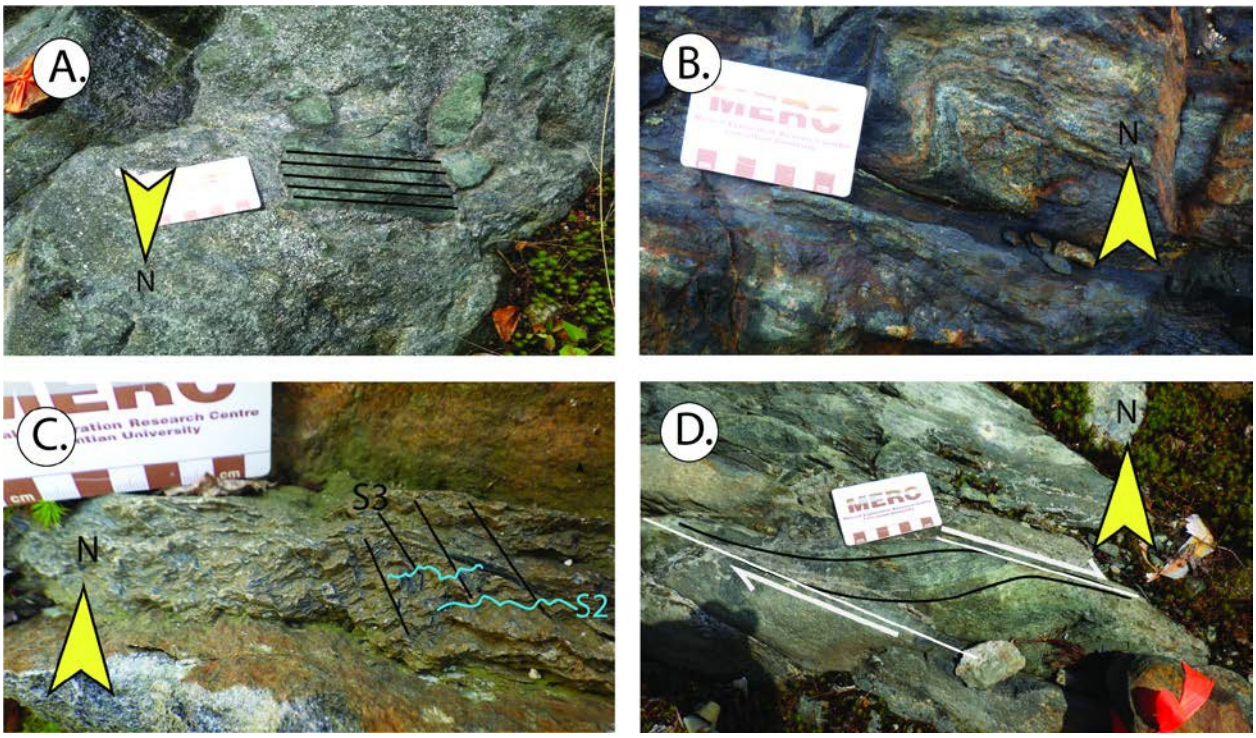

Figure 3. Field photographs of deformation structures at the Cubric nickel showing, southern Abitibi Subprovince: **a)** gabbro with foliated metavolcanic xenoliths and foliation indicated by solid black lines; **b)** S-shaped F_2 folds in banded iron formation; **c)** S_3 crenulation cleavage at the southern end of an outcrop, with S_2 and S_3 foliations traced in blue and black, respectively (note slight dextral offset along the S_3 foliation); **d)** S-C fabrics in ultramafic rocks, with shear line traced and direction of movement indicated. Scale card is 9 cm in length.

12.2 2018 Summary of Field Work

Lithological and structural setting of the Cubric Ni-Cu-(PGE) showing, southern Abitibi Subprovince, Quebec

D. Shirriff, C.M. Lesher, B. Lafrance and X. Zhou

Mineral Exploration Research Centre, Harquail School of Earth Sciences, Goodman School of Mines, Laurentian University, Sudbury, Ontario, P3E 2C6

INTRODUCTION

The Amos–Malartic transect is one of several metal-endowed geological-geophysical traverses in the Abitibi greenstone belt being studied as part of the Metal Earth project. The transect intersects the Malartic group in the southern Abitibi greenstone belt. The 2714 ±2 Ma (Pilote, et al., 1998) La Motte–Vassan formation represents the oldest rocks of the Malartic group, consisting of komatiite, basalt and felsic-intermediate volcanic rocks. The La Motte–Vassan formation hosts several Ni-Cu-(PGE) occurrences, including the historic Marbridge mine, which produced 702 224 tonnes of ore grading 2.28% Ni and 0.1% Cu (Sphinx Resources Ltd., 2015), and the Cubric showing, located 3 km east of the mine. The genesis of the mineralization at the Cubric showing is poorly understood due to its structural complexity. The goal of this project is to better constrain the geological controls on Ni-Cu-(PGE) mineralization in the La Motte–Vassan formation to assist in understanding metal endowment along the Amos–Malartic transect. The area surrounding the showing was mapped using a combination of bedrock mapping, core logging and data from an airborne magnetic survey.

REGIONAL GEOLOGY

The Cubric–Marbridge area is located in La Motte Township, about 3 km west of the village of La Motte, Quebec (Figure 1). The supracrustal rocks of the La Motte–Vassan formation consist of komatiite, basalt and sedimentary rocks as well as a lesser quantity of felsic volcaniclastic rocks, which are intruded by gabbroic and granitic dikes (Imreh, 1984). The felsic volcaniclastic rocks within the La Motte–Vassan formation yielded a Pb/U zircon age of 2714 ±2 Ma (Pilote et al., 1998). These supracrustal rocks are surrounded by three major intrusions: the ca. 2647 Ma La Motte pluton, the ca. 2681–ca. 2660 Ma Preissac pluton and the ca. 2680–ca. 2632 Ma La Corne pluton (Carignan et al. 1991; Ducharme et al. 1997). The ages of the La Motte and Preissac plutons were determined using Pb/U monzonite geochronology, whereas the age of the La Corne pluton was determined using Pb/U zircon geochronology (Carignan et al. 1991; Machado et al. 1991 Ducharme et al. 1997). The Cubric–Malartic area occurs along the southern limb of the La Motte anticline (Imreh, 1984) within the Southern Manneville deformation zone, a splay of the regional Porcupine–Destor–Manneville fault (Daigneault et al., 2002).

METHODS

In the summer of 2018, the geological setting of the Cubric showing was determined; fifteen stations in a 4 km^2 area around the showing were mapped. The outcrop–scale map of the Cubric showing from the previous field season was modified (Figure 2) as new information became available, and an additional map and sketch (Figures 3, 4) at the outcrop scale were completed in the Cubric area to help relate the outcrops to the regional map pattern. A high-resolution drone magnetic survey completed in April 2018 became an

important tool in the development of the geological map. The first horizontal derivative was used to map the contacts of several units where outcrop was lacking, and a regional fold pattern was identified using this method. In February 2018, some 105 m of drill core from the Marbridge site provided by Sphinx Resources Ltd was re-logged, sampled and compared to samples from the Cubric area. In August 2018, Globex Mining Enterprises Inc. provided access to over 300 m of drill core, which were also re-logged and sampled this summer.

ROCK UNITS AT THE CUBRIC NICKEL SHOWING

There are eight different rock units at the Cubric showing: granite, intermediate intrusive rocks, semi-massive sulphides, iron formation, hornblende gabbro, ultramafic rocks, amphibole schist and biotite schist (Figure 2). The granite at the northwestern end of the outcrop is mineralogically similar to the Preissac pluton and is located in proximity to it. The intermediate intrusive rocks are fine to medium grained, appear grey to brown on fresh surfaces and are extremely hard; they are interpreted as a roof pendant between the La Corne pluton and the Preissac pluton. The iron formation consists of alternating massive magnetite-sulphide bands with occasional interbedded chert (0.5–1 cm thick) with saccharoidal texture. At the Cubric showing, the bedding of the iron formation runs parallel to the early foliation. Although small in volume, the iron formation is extremely magnetic. By far the most abundant rock type at the Cubric showing is a hornblende gabbro, which consists of 30–50% plagioclase and 50–70% hornblende. Grain sizes within the hornblende gabbro vary across the unit from leucocratic pegmatitic-textured pods near the contacts with supracrustal rocks to mesocratic coarse–medium grained in the centre to fine-grained melanocratic near the mineralized body. One of these leucocratic pods yielded a $^{207}Pb/^{235}U$ zircon age of 2680.5 ±1.5 Ma. This age is consistent with the early felsic phase of the La Corne pluton (Carignan et al. 1991; Ducharme et al. 1997). The ultramafic rock is talc-carbonate altered with small (<1 mm) magnetite bands. The amphibole schist is distinctly dark green and consists of medium-to coarse-grained acicular amphibole. This unit is typically 15–20 cm thick and non-uniform in mineralogy with thin, continuous sulphide bands 2 mm thick running parallel to foliation. This schist unit has distinct ends indicating it may be rafts within the hornblende gabbro rather than a late intrusive body. The biotite schist found in contact with the amphibole schist is black, very soft and is composed almost exclusively of medium-grained biotite.

MINERALIZATION

At the Cubric showing, there are two very distinct sulphide textures: within the hornblende gabbro, sulphides are semi massive and brecciated, whereas within the silicate-facies iron formation, sulphides and amphibole schist occur in folded bands parallel to the primary foliation. Mineralization consists of pyrite-pyrrhotite-magnetite-chalcopyrite±pentlandite±violarite, with grades up to 2.5% Ni and 0.2% Cu at the surface. A high-grade mineralized body was not observed in drill core and is interpreted as not extending at depth.

STRUCTURAL GEOLOGY AND DEFORMATION HISTORY

In addition to grid mapping and core logging, a magnetic survey was used to interpret the geology within a 4 km^2 area around the Cubric showing (Figure 5). Potential evidence for a S_1 cleavage can be observed in a 20 cm xenolith within the hornblende gabbro (Figure 6). Xenoliths of this mineralogical and textural type are observed up to 6 km away within the hornblende gabbro phase of the La Corne pluton but only at the Cubric showing is a xenolith with internal foliation present. A thin section will be made to determine if this is an igneous or tectonic fabric. For consistency within this report, it will be assumed to be a tectonic foliation and other deformation events follow in sequence. The northwest-striking, steeply dipping foliation is the principal S_2 cleavage observed throughout the La Motte–Vassan formation. The mineral lineation on this cleavage plunges moderately to the east. The S_2 cleavage is axial planar to northwest-striking, upright, isoclinal to tight, regional folds in this area. The D_2 deformation relating to these structures is a northeast-southwest shortening event. These folds are overprinted by a late northwest-southeast D_3 shortening event, which produced northeast-striking open folds. This interpretation is based on aeromagnetic

data and is validated by outcrop-scale observations. An outcrop shows an isoclinally folded east-striking quartz vein overprinted by late tight to open northeast-striking folds (Figure 5). The north-northeast–striking sub-vertical crenulation cleavage is axial planar to the late northeast-striking folds.

DISCUSSION AND CONCLUSION

The mineralization at the Cubric showing is located within the iron formation and the hornblende gabbro. The $^{207}Pb/^{235}U$ zircon age of 2680.5 ±1.5 Ma for the gabbro establishes a maximum age for mobilization and constrains the timing of the D_2 and D_3 deformation events. However, there is a discrepancy in the mineralogy and geochemistry of the Cubric showing as the trace amounts of pentlandite present cannot account for the 2.5% Ni. Two hypotheses have been considered to explain the Ni enrichment: 1) mobilization from a komatiite-hosted deposit during deformation and modification by metamorphic hydrothermal fluids or 2) precipitation from a hydrothermal fluid. Whole-rock geochemistry and assay data show that mineralization at the Cubric showing has a high Ni/Cu ratio consistent with a komatiitic origin and occurs close to an ultramafic body. However, the most abundant sulphide mineral is pyrite, which is commonly associated with hydrothermal activity. Moreover, the pyrite crystals are associated with hydrothermal-alteration minerals such as biotite and chlorite. Unfortunately, evidence for both hypotheses is circumstantial and must be tested using more robust methods to determine genesis. One such method involves using trace-metal geochemistry including iridium and chromium, which are virtually insoluble in hydrothermal fluids but are commonly found in magmatic systems (Lesher and Keays, 2002). Studying these elements will prove useful in attempting to resolve these hypotheses. Scanning electron microscopy will be conducted on Ni-bearing minerals to reveal mineral phase and potential overprinting textures on the microscopic scale. If the system is determined to be magmatic, the relative mobilities of the entire suite of base and precious metals during deformation and metamorphism will be established.

ACKNOWLEDGMENTS

The authors would like to thank Globex Mining Enterprises Inc. and Quebec Precious Metals Corporation for allowing them access to both the Cubric Ni showing and Marbridge mine sites, as well as drill core samples and other company data. P. Pilote (Ministère de l'Énergie et des Ressources naturelles du Québec) and R. Daigneault (Université du Québec à Chicoutimi) are thanked for helping develop this research project. The help given by the Metal Earth project staff and Malartic transect undergraduate field assistants, L. Roy, N. Welt, S. Battey, K. Kotylak, M. Jacques, and J. Rivest, was especially appreciated.

Harquail School of Earth Sciences, Mineral Exploration Research Centre contribution MERC-ME-2018-062

REFERENCES

Carignan, J., Gariépy, C., Machado, N. and Rive, M. 1993. Pb isotopic geochemistry of granitoids and gneisses from the late Archean Pontiac and Abitibi subprovinces of Canada; Chemical Geology, v. 106, p. 299–315.

Daigneault, R., Mueller, W. and Chown, E. 2002. Oblique Archean subduction: accretion and exhumation of an oceanic arc during dextral transpression, Southern Volcanic Zone, Abitibi Subprovince Canada; Precambrian Research, v. 115, p. 261–290.

Ducharme, Y., Stevenson, R. and Machado, N. 1997. Sm–Nd geochemistry and U–Pb geochronology of the Preissac and Lamotte leucogranites, Abitibi Subprovince; Canadian Journal of Earth Sciences, v. 34, no. 8, p. 1059–1071.

Imreh, L. 1984. Sillon de La Motte–Vassan et son avant-pays méridional: synthèse volcanologique lithostratigraphique et gîtologique; Ministère de l'Énergie et des Ressources du Québec, Direction générale de l'exploration géologique et minérale, MM82-4, 72 p., 2 maps.

Lesher, C. and Keays, R. 2002. Komatiite-associated Ni-Cu-PGE deposits: geology, mineralogy, geochemistry and genesis; *in* The Geology, Geochemistry Mineralogy and Mineral Beneficiation of Platinum Group Elements; L. Cabri (ed.); Canadian Institute of Mining and Metallurgy, v. 54, p. 579–617.

Machado, N., Gariépy, C., Philippe, S., David, J., 1991 Géochronologie U-Pb du territoire québécois : Fosses du Labrador et de l'Ungava et sous-Province de Pontiac; Ministère de l'Énergie et des Ressources du Québec, MB 91-07, 50 p.

Mueller, W., Daigneault, R., Gaboury, D. and Pearson, V. 2008. Effusive and explosive subaqueous volcanism in the Abitibi greenstone belt: ocean floor and subaqueous caldera volcanism: Geological Association of Canada–Mineralogical Association of Canada, Joint Annual Meeting, Quebec, 20–25 May 2008, Guidebook to Field Trip A1, 85 p.

Pilote, P., Moorhead, J. and Mueller, W. 1998a. Développement d'un arc volcanique, la région de Val-d'Or, ceinture de l'Abitibi–volcanologie physique et évolution métallogénique; Geological Association of Canada–Mineralogical Association of Canada, Joint Annual Meeting, Québec 1998, Fieldtrip guidebook A2, 104 p.

Shirriff, D., Zhou, X. and Lafrance, B. 2017. Lithological and structural setting of the Cubric nickel showing, Southern Manneville fault, southern Abitibi Subprovince, Quebec; Mineral Exploration Research Centre, Laurentian University, Sudbury, Ontario, 6 p.

Sphinx Resources Ltd. 2015. Sphinx acquires Marbridge high-grade nickel-copper mine project from Royal Nickel Corporation; news release, June 2, 2015, https://sphinxresources.ca/sphinx-acquires-marbridge-high-grade-nickel-copper-mine-project-from-royal-nickel-corporation/ [accessed September 10, 2018]

FIGURES

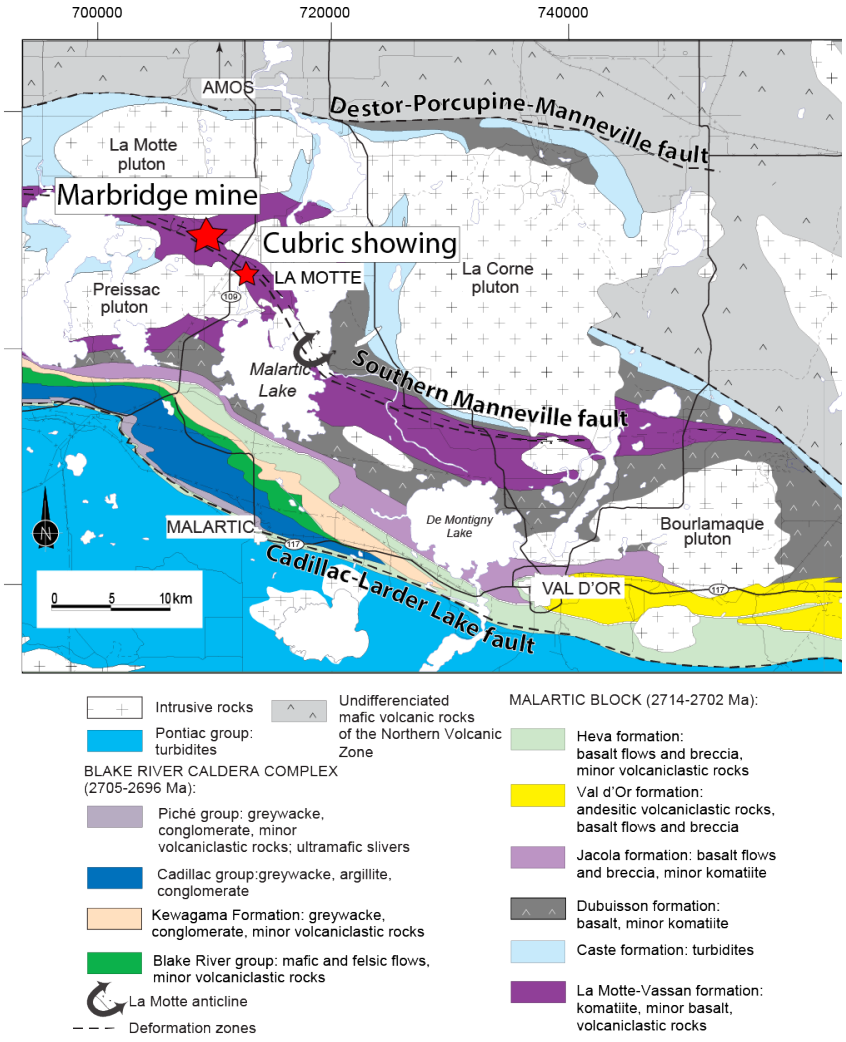

Figure 1. Simplified geology of the Malartic transect area, southern Abitibi Subprovince, with location of the Cubric outcrop. Figure *modified from* Mueller et al. (2008).

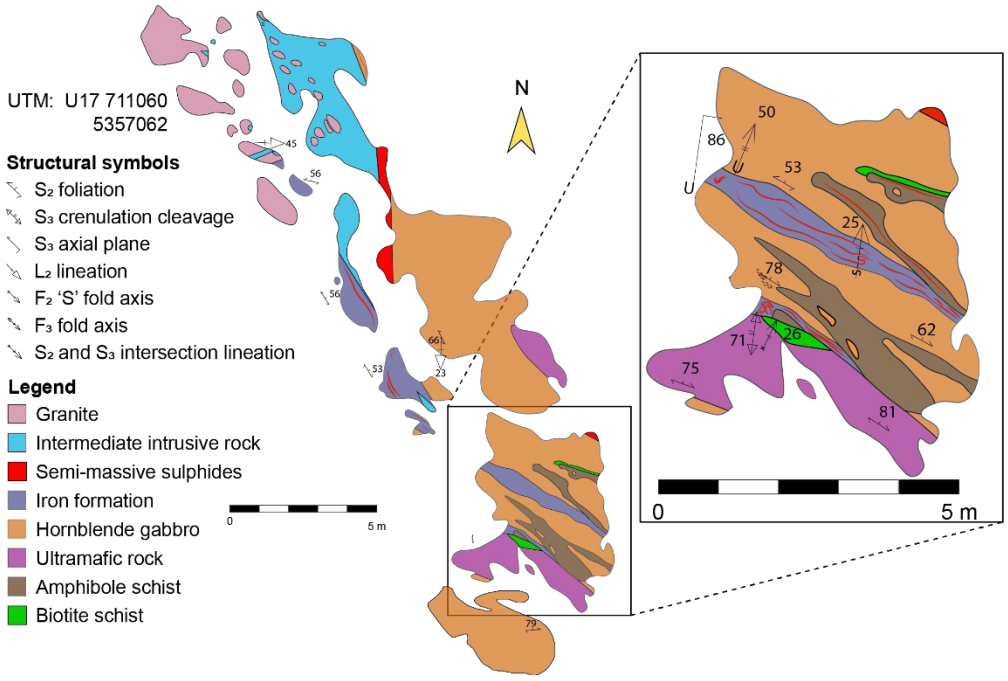

Figure 2. Outcrop map of the Cubric Ni showing, southern Abitibi Subprovince (inset of area with more detailed mapping). Figure *modified from* Shirriff, et al. (2017).

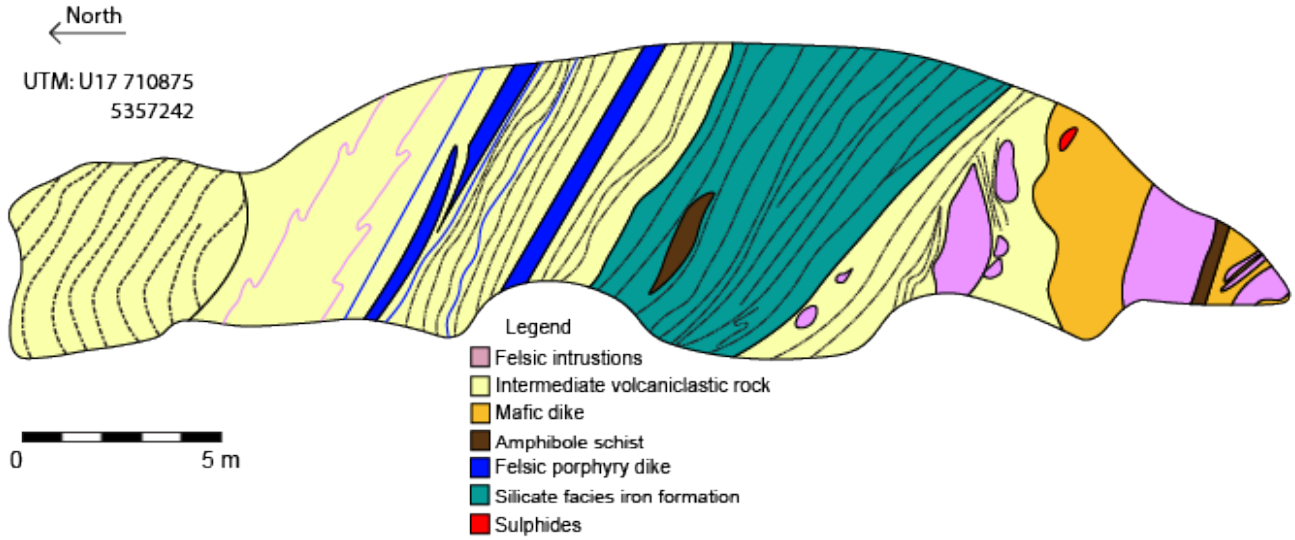

Figure 3. Road-cut outcrop map along strike of the Cubric showing; vertical section faces west.

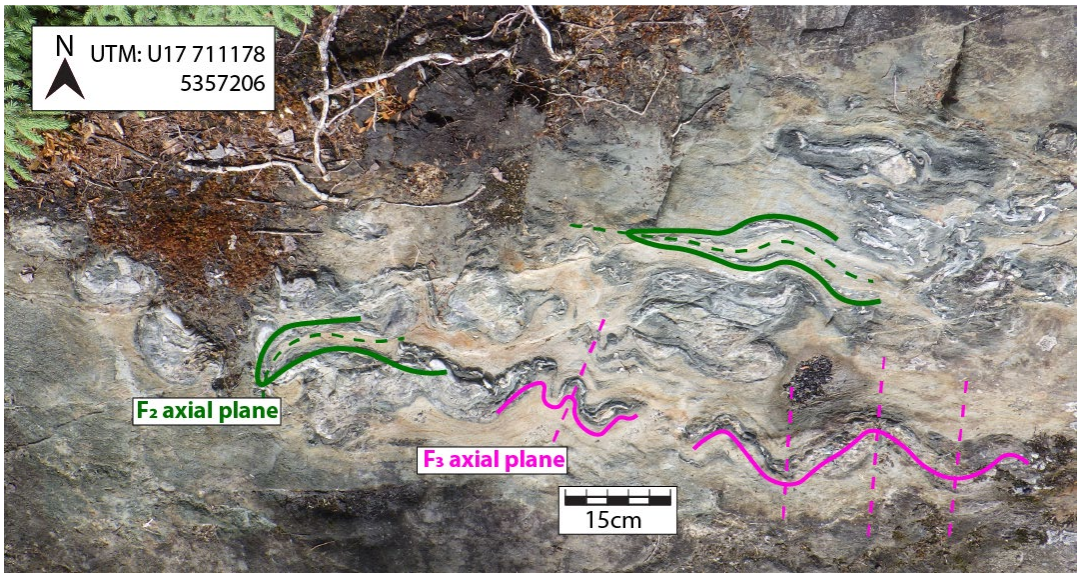

Figure 4. Field photograph showing a F_2 and F_3 fold interference pattern. Isoclinally F_2-folded quartz veins are overprinted by F_3 folds. The F_2 fold trace is indicated in green, with the axial plane as a green dashed line; the F_3 fold trace is indicated in pink with a pink dashed line as the axial plane.

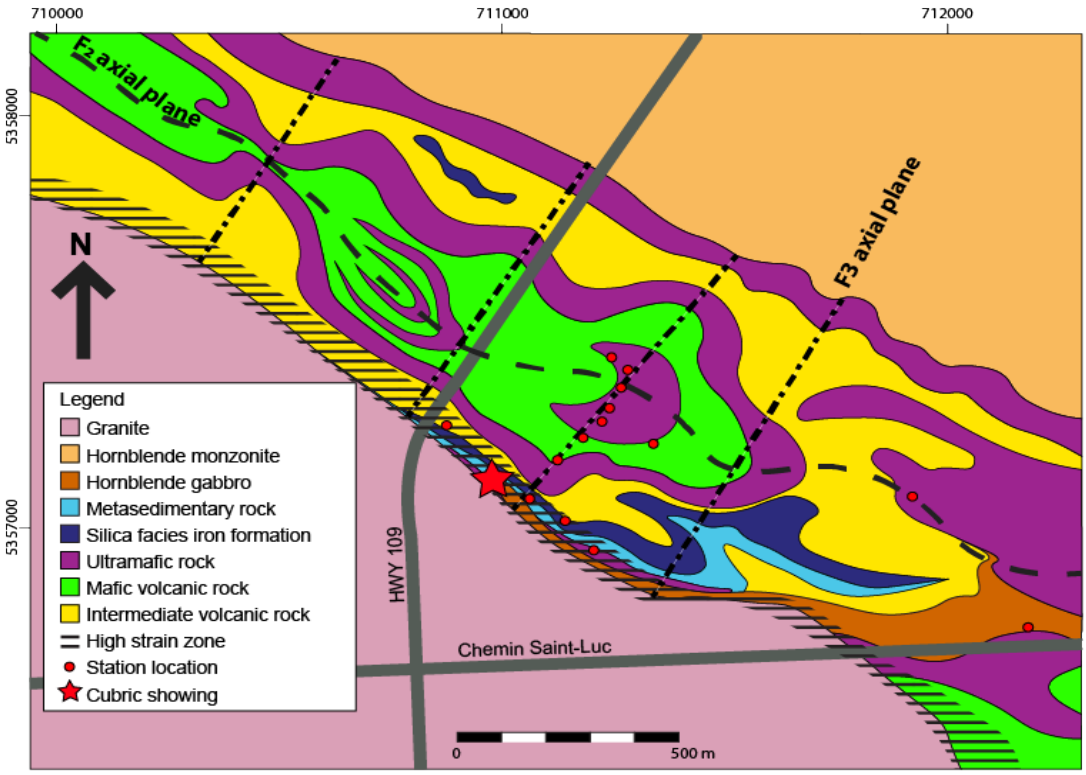

Figure 5. Aeromagnetic map interpretation of the Cubric surrounding area, showing location of. F_2 and F_3 fold traces.

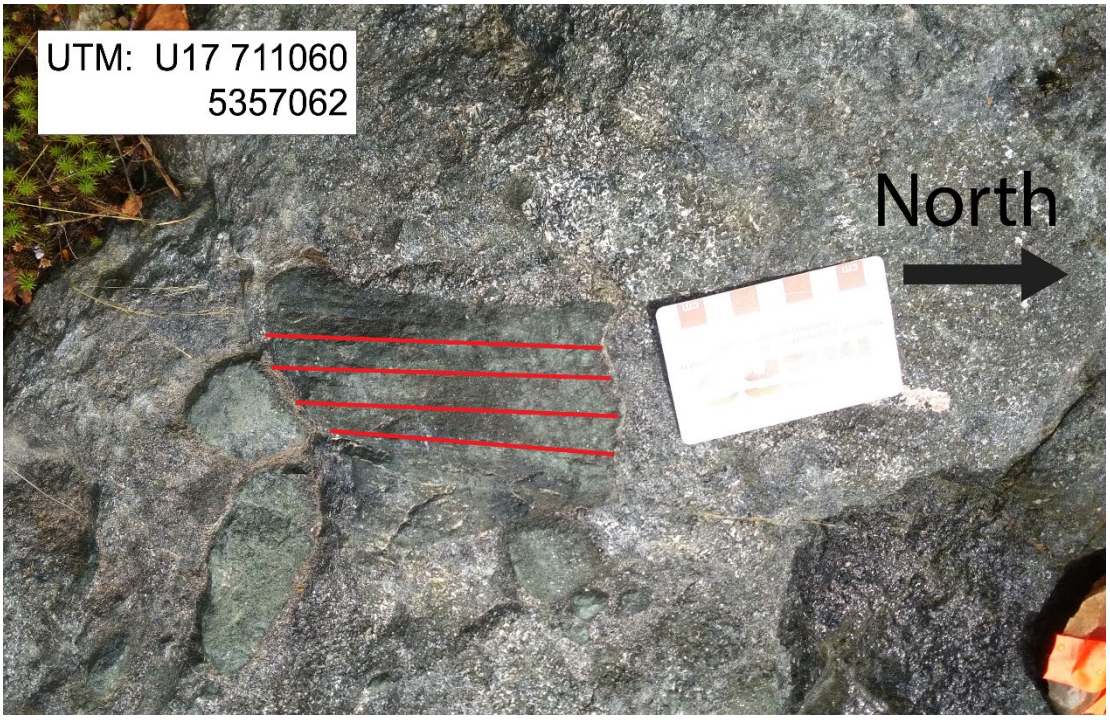

Figure 6. Field photograph showing xenolith with an S_1 cleavage possibly indicating an early deformation event.